External Peer Review of the Draft Report on Model Development for Assessing California Methyl Bromide Ambient Air Concentrations

Submitted to:

Loren Hall
Office of Civil Rights
U.S. Environmental Protection Agency
1200 Pennsylvania Avenue, NW
Washington, DC 20460

Submitted by:

Eastern Research Group, Inc.
110 Hartwell Avenue
Lexington, Massachusetts 02421-3136

July 12, 2005

Printed on Recycled Paper

QUALITY NARRATIVE STATEMENT

ERG selected reviewers according to selection criteria provided by EPA. EPA confirmed that the scientific credentials of the reviewers proposed by ERG fulfilled EPA's selection criteria. Reviewers conducted the review according to a charge prepared by EPA and instructions prepared by ERG. ERG checked the reviewers' written comments to ensure that each reviewer had provided a substantial response to each charge question (or that the reviewer had indicated that any question[s] not responded to was outside the reviewer's area of expertise). Since this is an independent external review, ERG did not edit the reviewers' comments in any way, but rather transmitted them unaltered to EPA.

Table of Contents

REVIEW COMMENTS OF

Paul Bartlett, Ph.D.
Principal Modeler and Research Associate (on sabbatical)
Center for the Biology of Natural Systems
Queens College, City University of New York
Flushing, NY
917-756-8191
paulwoodsbartlett@hotmail.com

Reviewer: Paul Bartlett
paulwoodsbartlett@hotmail.com
917 756-8191

June 28, 2005, Revised July 6, 2005

External Peer Review: ***Model Development for Assessing California Methyl Bromide Ambient Concentrations***

Charge Questions

This external peer review is the next step in the document review process. As an external peer reviewer, please read the entire document and consider the accuracy of the content, as well as the soundness of the interpretation of the findings presented. Prepare a written response to each of the following six charge questions/statements. Feel free to make legible notations in the page margins and return all annotated pages with your written comments.

1. Does the document, Model Development for Assessing California Methyl Bromide Ambient Concentrations, provide a clear and adequate description of the goals and methods EPA used to develop and review alternative exposure models? What additional information, if any, is critically needed to complete the documentation?

The performance criteria for the application of the model need to be more clearly outlined and distinguished so that the advantages and limitations of the model can be more readily evaluated for the desired application, and the potential results of model application more easily interpreted according to the demands of the application. The performance criteria are different for different application objectives and goals. They should be understandable to the lay person and the expert.

I will present here what I presume to be the goals of the study that need to be clarified, from my reading of the documents and from my correspondence with ERG and conference call with the representatives of EPA and its contractor.

Goal.

The document identifies the goal of this model to characterize the ambient air concentration of school receptors throughout California in such a way that differences between receptors can be distinguished, for target durations of exposure. These receptors will be in locations different than the receptors for which monitoring data was used to construct the model.

The evaluation of the model is concerned with how well the model will predict, what levels, will it predict, and what degree of uncertainty to locations not monitored to construct the model.

Target Application Receptors.

In order to evaluate the proposed model and methods of the model, we need to know how well the model is likely to perform to the target application receptors. For this evaluation, the target application receptors need to be characterized. This is missing from the document. The similarities and differences from the conditions of the monitored receptors used to construct the model need to be better known to evaluate the ability to apply the model outside the three counties used to develop the model. In most modeling constructs, the model performance is least certain when applied to conditions outside the range that was used to construct the model from empirical data. This is especially true of regression models. Regression models excel at interpolation, but work poorly in extrapolation. Regression models also are not very effective at characterizing conditions at the distribution tails, unless very large sample sizes are used.

Presumably the target receptors include additional school receptors within the three counties monitored, but include much more receptors outside those counties. The characteristics of the source-to-receptor relationships of the target application receptors need to be better known to evaluate the potential efficacy of the proposed model. It would be useful for the application receptors to be mapped in conjunction with MeBr typical use patterns. Relevant information to be characterized includes the distribution of intensity of use, the variation in source to receptor distance, differences of conditions affecting emission and atmospheric transport (eg soil, soil moisture, irrigation, meteorological and topological conditions).

Soil and meteorological conditions. My understanding from the conference call is that the three counties monitored represent a wide range of soil conditions and meteorological conditions and that the differences tend to average out. It was also stated in the call that the range of conditions are inclusive of the counties to be applied. This needs to be stated and documented.

Soil moisture. Soil moisture is regarded to be a significant factor for emission rates. It was stated in the conference call that MeBr is generally applied to irrigated fields, so that soil moisture is not likely to be an issue for emission, as there is no significant variance. Since MeBr is applied prior to planting, this needs to be better established and documented. Furthermore, in some uses of fumigants, irrigation is sometimes applied after fumigant application to seal the soil surface in order to reduce the rapid loss of the fumigant to atmospheric emission. Whether or not this practice is used, or may be used with MeBr should be documented.

Air Concentration and Exposure Duration.

The document outlined three types of exposure of interest: short term to long term. The model appears to target subchronic (7-8 weeks) for final application of results, but leaves it open to apply it to other periods of duration. It acknowledges in the text that short tem daily exposure is most difficult to model with the highest range of uncertainty. To what extent the model is intended for other periods than subchronic needs to be better expressed. It is not demonstrated that this model would be useful for longer periods.

Prediction of general exposure over time, or specific actual period.

Whether the model performance for a specific period and place needs to be accurate, or whether a model is able to predict the typical range and average exposure for applications across years, needs to be distinguished. This is a difficulty particularly true of pesticides. Pesticide air concentration is one of the hardest emissions to predict since its emission is episodic on a very fine time scale, as is its dispersion. The timing of the use and emission from a single application can dramatically effect its concentration at any one specific receptor. This is less of a problem for longer time periods and greater frequency of application.

Source –receptor use data domain.

It is presumed in the project framework page 5, that receptor air concentration is limited to a few miles. This has not been demonstrated. The results of the model underestimating lower concentrations suggest that it is not correctly characterizing longer distant sources. Longer distant sources are more important as nearby source applications are more infrequent or lacking altogether. The CDPR study showed air concentrations measured in areas with no uses within the domain (Li et al, 2005). It is necessary to know how low of concentrations are necessary to model in order to evaluate the models presented. According to the conference call, low and high concentrations need to be modeled to determine differences of exposure between different receptors.

Method of Review of Alternative Models.

The regression model approach has many virtues relevant to the goal of this study. The limitations, however, need to be better identified. Some of the limitations are inherent to the model, and others will not be known until it is applied, so can be less certainly predicted.

The difficulties of using the alternative method of numerical dispersion models are stated, but are not altogether convincing, since they many of the difficulties can be overcome with greater effort, albeit with some limitations. Unfortunately, the best way to evaluate the two approaches is to do an inter-comparison study of the construction and application of the two approaches, but this is probably beyond the scope of this study.

Regression Model Precedents.

A strong case can be made for the regression case, based on the success of this approach by California Department of Pesticide Regulations (CDPR). These studies are appropriately well referenced in the document in the introduction and model development. The article published recently (Lit et al., 2005) is concise, comprehensive and useful and should be distributed with this document when possible, or at least excerpted in an appendix.

CDPR has different performance criteria. There is an important difference between the referenced CDPR model (Lit et al., 2005) and the proposed application of the regression. The CDPR performance criterion was to identify a threshold subchronic exposure level of 9ppb MeBr average air concentration, whereas for the present study, levels below this need to be ascertained. From what can be discerned from the background documents, this level will typically occur near a source or in a high usage area. The model's performance was best within 7 miles (11.3km), and less accurate at greater distances. (The reasons that the performance declined at greater distances, was not fully explored in the article. Presumably, the inclusion of distant variables to the regression models developed here was an attempt to address this deficiency.)

This is an example why the document needs to state what levels of air concentration are of importance for its application. 1ppb is indicated as a health effect threshold for children, and is below the target level of 9ppb of the CDPR study. How low of levels are needed to be able to predict and at what degree of

uncertainty is acceptable? As we get to lower levels of air concentration, most model performance goes down for a number of factors (accuracy of input data [meteorological data, use date, etc.] and model uncertainty).

Conventional pollutant regression modeling. Other precedents of the use of regression modeling have been for conventional pollutants such as ozone. Numerical dispersion modeling and regression modeling have been used to predict air concentration data. Regression modeling works well where extensive air concentration data with meteorological data exist. It may be helpful to reference these approaches and their relative successes.

Alternative Numerical Dispersion Models.

Numerical dispersion models have been rapidly developing and improving. Methyl bromide has a long half life in the atmosphere, is in the gas phase, so is more easily modeled than other chemicals. For regional transport of a short duration, destructive processes in the atmosphere and losses from deposition are of less importance in predicting surface air concentration, so inaccuracies in these areas are not likely to be significant. For the more complicated global factors, MeBr and the similar MeCl, have been modeled recently (Reeves 2003; Yoshida et al).

While Guassian numerical dispersion models such as ISCST may be appropriate for short range transport of a limited amount of sources and at high levels of concentration that are of most concern for some regulation purposes, other models are likely to perform better for the convergence of pollutants from longer range sources at lower levels of air concentration. The Guassian models are limited in transport model to the period of averaging and do not allow for buildup of air concentration over more than one averaging period. Eulerian, Lagrangian, and hybrid models are likely to perform better. The ISC3 Guassian model was evaluated to under predict air concentrations more than the CALPUFF Lagrangian model in a recent intercomparison study due to the more complex meteorological phenomenon it was better able to model (Coultier and Eckhoff, 2005).

To know whether numerical dispersion models would be a better approach, depends upon whether it is desired to predict so called background concentration, and lower levels of concentration arising from longer distant sources. Background concentration is a relative term. A global 3D model aims to predict all levels in the atmosphere. Concentrations from beyond a model's domain, is usually referred to background. In the case of typical regression analysis, it shows up as the intercept term. This is

problematic for the case at hand, because distances greater than a certain distance are neglected from the model. This means each region will have a different intercept, depending upon the relative extent of sources near the domain.

The document states the numerical models requirement of computer time to be a disadvantage, especially from multiple sources. This however should not be a criteria to reject this approach, as it is a difficulty that can be addressed by running in parallel by banks of PCs or on a workstation or supercomputer. There are many models out there that use more and less computer time, depending upon complications.

Another objection to the use of numerical models is the uncertainty of precise location and emission profile. This is indeed a difficulty for all modelling attempts, especially to derive parameters from monitoring data. Numerical models however can be employed using emission profiles derived from experimental data, or emissions can be modeled separately as in input to a dispersion model. The unknown location of emission within a region is problematic. It calls into question the construction of a model's parameters (e.g. regression coefficients) from this data. If one is trying to get typical dispersion patterns, it may be preferable to use numerical models with parameters derived from other experimental data, and evaluate the uncertainty due to location, but running the numerical model under different location scenarios, and evaluating the model with the monitoring data. There are a myriad of approaches that can be used, and the specific numerical model selected will shape the methodology.

That said, there are legitimate reasons to select the regression approach. The document acknowledges the problem of predicting low concentrations and low use and documents the development of the regression model. Nevertheless, numerical dispersion modeling is a legitimate alternative, and difficulties can be overcome, but with limitations, as is the case with all models, but limitations of a different sort.

Additional Information Useful for Evaluation.

1) School receptor locations with MeBr use data (mentioned above)
2) Monitoring receptor data set. Spreadsheet or database format. Description, height, sensitivity, quality, number of records.
3) Use data set. Spreadsheet, database or GIS format. Printed maps. Number of records per receptor, and overall.
4) Coefficients and statistics of significance of variables and intercept.

2. What are the overall strengths and weaknesses of the model development process as described?

Strengths:

The base regression approach was informed by the experience with the CDPR regression model. Improvements were attempted to be made by the inclusion of parameters in the regression equation relevant to dispersion and emission processes. Difficulties in creating separate regression terms representative of the processes with interpretable coefficients were acknowledged. A creative approach for developing regression terms was devised. An attempt to mirror the Guassian dispersion equation was made.

The longer period average air concentrations were made from daily predictions. There was acknowledgement that all models have difficulties on smaller time scales. Inaccuracies in input data, model uncertainty tend to average out over time, but are more pronounced in a single time step. It would have been a gross misapplication of a regression model using Guassian dispersion model parameters for a long averaging time, so this approach is welcome.

Tens of thousands of alternative formulations were explored. In many respects, this was done somewhat objectively from a statistical standpoint, with all permutations formulated and run. This approach has the potential of discovering a formulation that one might not have thought would be effective. At its best, it could discover the relative importance of physical processes and conditions that determine pollutant air concentration, highs and lows.

Weaknesses:

The sheer amount of regression model formulations makes the evaluation and ranking the models very difficult to comprehend, manage and evaluate (See Question 4).

Although this approach has the potential to discover relationships of physical factors and their relative importance to determine the distribution of air concentration, this was not fully realized.

Using meteorological data averaging periods of one day has some disadvantages. The Guassian dispersion equation is meant for one averaging period congruent with the time period of meteorological and measurement data. One to two hours averaging period are preferred. Greater averaging periods distort the realities of wind direction and variation of wind speed. In one hour, a plume can travel a great distance at a high wind speed. At a very low wind, concentrations can build up locally. This is why numerical models

make use of the highest time resolutions for best results. This is difficult to do with the regression model and the data available.

The models generated many insignificant regression terms, many with negative coefficients that defy physical reality. When a regression term coefficient has a distribution above and below zero, that is, it is statistically insignificant, that term should not generally be used. Forcing negative coefficients to be positive, was a worthy exercise, but does not give confidence to the results.

Forcing the intercept to zero, necessarily introduces a downward bias for low concentration predictions (as the slope pivots to reach zero), and neglects background sources, hence mis-specifies the model. Ordinarily the intercept is forced to zero when that is what we expect from our knowledge of the phenomenon. In this case, there is a rationale, because there is an attempt to model background. However, background comes from a greater distance than modeled, so we would not expect a zero background. There is the problem that the intercept represents to some extent the unique proximity of the modeled data points to other background sources, or the level of intensity of use in the immediate area, not captured by other regression terms. In any case it is problematic to devise a regression model in this situation that can have an intercept that will be accurate in regions other than what was used to construct its coefficients.

The regression technique, as developed by CDPR and here, appears not to be able to model the cumulative impact of a large number of more distant sources. It appears that it is difficult for the regression technique to capture the more complex processes of transport and environmental fate from longer distances than 8 miles, as developed here.

Overall Assessment: The improvements to the CDPR regression was perhaps overextended to too many formulations and too many variables. Evaluation of the statistical significance of regression terms might be better used to construct a set of candidate models.

3. What are the strengths and weaknesses of the data quality assurance activities conducted during the model development process?

Strengths:

Dramatic improvements were made to data inputs of MeBr usage from PUR data by labor intensive means.

Meteorological data was analyzed and missing data was replaced by appropriate methods.

Outliers that most likely arose from data errors were discovered and taken out with convincing analysis. Errors (differences between predicted and observed values) were presented extensively.

Questions of non-linearity, and normal distribution were addressed by presentation of plots of observed vs predicted observation. A predominance of underestimating low values was presented.

Data sets were run separately and combined by years, counties, and high vs low, to determine if these factors resulted in biases. This provides more confidence to apply the models to other years and regions.

Weaknesses:

Physical process and data factors that resulted in the tendency to underestimate, and have difficulty estimating low predicted values, and estimate zero values, when observed values resulted, should have been further explored. The cases that resulted in those discrepancies should be analyzed to discover what is responsible. For example, in these cases: Is the model domain close but outside, high or low usage areas? Are low or high winds involved? Is there excessive averaging of multiple directions of wind?

4. What are the strengths and weaknesses of the model ranking elements, and the model ranking process? Can you identify alternative ranking measures that would be likely to present significantly different information about model performance that should be considered in model selection? Would these alternative measures be likely to change the selection process outcomes as described?

Strengths:

Regression model R2 and MSE are appropriate statistical measures of model performance and are essential to a ranking process of regression models, but cannot be used alone. Known physical processes of emission and dispersion and interpretability of the model in those terms, is an appropriate guidance to evaluate the application of the model to the real world (conditions in other areas and times).Analysis of the tails of distribution, the 95^{th} percentile, is also appropriate, since the distribution and variance of the predictions, given the inputs, is important to the applicability of the model.

Weaknesses:

Too much focus and importance was given to R2 and MSE in evaluating the models. The simple CDPR model achieved relatively high R2 and MSE. Theoretically, least square regression models and its statistics are only valid if all its assumptions are satisfied, including model specification. Model specification is the first hurdle to cross. It is important that there is an adequately high R2 and low MSE, but model specification is ultimately more important.

The presence of statistically insignificant variables should be a factor in ranking. In the document, these variables were not identified. The problem was identified when it was stated that some of the coefficients were very low, and even negative. A comprehensive analysis of this problem needs to be done. APA provided, in separate correspondence, statistical significance of the coefficients for some of the models. This should be in the report, along with similar data for a larger set of models. Generally, statistically insignificant variables are dropped. The document should provide a better rationale for their inclusion.

Adjusted R2 was not reported. Adjusted R2 corrects for the increasing R2 due to the mere addition of another variable (degrees of freedom relative to sample size). When comparing models of different amount of variables with unadjusted R2 it should be documented that the differences are not due to this statistical effect. In the correspondence from EPA it was stated that there were a large enough sample data set, that the difference from R2 and unadjusted R2 was not significant. This needs to be documented in the report.

It should be noted that since regression models, by their very construction, estimate parameters that determine the midpoint of least squares, some methods used to evaluate under and over estimating numerical dispersion models cannot be as easily used to compare to the regression approach.

More attention to the reasonableness of the model specification should be done. Parameters that will capture differences between regions to be applied, are most important for the ability to generalize and apply the model outside the three counties that were used to generate the models.

Alternative:

Model formulations with insignificant variables should not be used without a convincing rationale. This problem should be addressed before ranking the models by other measures, to some extent. Forcing the

variables to positive coefficients is a worthy exercise, but the results are doubtful, as is forcing the intercept to zero.

5. Are one or more of the identified models capable of characterizing the ambient exposure from multiple fumigant sources to receptors in California for the exposure averaging periods of interest?

The models, as developed, are most appropriate to predict probable ambient air concentrations over a period of 7-8 weeks at a spatial resolution of the 7x7 and 8x8 domains, in domains where frequent applications occur. This is the level of accuracy of the usage data, and the ability of the model. Numerical dispersion modeling could conceivably provide a background term (intercept) to adjust for contributions from longer distant sources.

Models that did not have insignificant variables need to be identified as candidates. They are likely to be improvements over the simple CDPR model, and more applicable to regions outside the three monitored counties.

The models generally have greater difficulty in the low ambient concentrations, below 1 ppb, and the most, below 0.1 ppb MeBr. Most models will have the greatest difficulty accurately predicting low concentration levels, since longer distant sources, and a more complex path of atmospheric transport and fate is at work. If it is desired to have greater accuracy in the distribution of concentrations at the low end, numerical dispersions models are likely to provide better results.

6. Provide any additional comments or recommendations you feel are important to improve the quality of this document.

Overall, the document represents a significant body of work, and as far as I am aware, a remarkable range of model parameterization within the confines of the chosen framework. The use of a nonstandard regression approach that does not break down the independent variables with their own coefficients and the presence of insignificant variables in the models, which are not well documented, makes the evaluation of the models presented here more difficult to evaluate at this stage of development.

Nevertheless, the regression approach followed here should ultimately yield a useful model for estimating differences of air concentration amongst receptors from nearby applications (eg, within 8x8 domain) that improves on the CDPR model.

This approach, at this stage, will be less certain estimating air concentrations at receptors arising from more distant source applications. This situation is likely to be important for receptors that are not nearby heavy applications, or nearby applications are infrequent. To model these situations, numerical dispersion models are likely to be superior and yield more useful results.

In retrospect, the review would have benefited from a conference call with the other reviewers to exchange our views on the charge questions. I believe that we would have more likely come up with more useful comments. Unfortunately, our schedules probably would not have made that practical, considering the time of year.

References.

Coultier, C.T., and P.A. Eckhoff. 1998 A comparison of CALPUFF with ISC3, EPA report EPA-45/R-98-020. December. http://www.epa.gov/scram001/7thconf/calpuff/calisc3.pdf

Li, LinYing, B. Johnson, and R. Segawa. 2005 Empirical Relationship between use, area, and ambient air concentration of methyl bromide. *J. Environ Qual.* 34:420-428.

Reeves, Claire E. 2003 Atmospheric budget implications of the temporal and spatial trends in methyl bromide concentration, *Journal of Geophysical Research,* 108(D11), 4343

Yoshida, Y., Y. Wang, T.Seng, R. Yantsuca. 2004 A three-dimensional model study of atmospheric CH3Cl. *Journal of Geophysical Research*, 109(D24309).

ADDITIONAL REFERENCES SUBMITTED BY

Paul Bartlett, Ph.D.
Principal Modeler and Research Associate
Center for the Biology of Natural Systems
Queens College, City University of New York
Flushing, NY
917-756-8191
paulwoodsbartlett@hotmail.com

United States
Environmental Protection
Agency

Office of Air Quality
Planning and Standards
Research Triangle Park, NC 27711

EPA-454/R-98-020
December 1998

AIR

A Comparison of CALPUFF with ISC3

ACKNOWLEDGMENTS

Special credit and thanks are due John Irwin, NOAA for his technical assistance and advice through all phases of the project, from study design and meteorological data selection to analysis and presentation of results. In the model comparisons, credit is due to Tom Coulter, EPA for his work on the steady state analyses and to Pete Eckhoff for the variable meteorology analyses. Thanks are also due Dave Strimaitis and Joe Scire of Earth Tech for their cooperation and technical assistance with the CALPUFF runs.

DISCLAIMER

This report was reviewed by the Office of Air Quality Planning and Standards, EPA for approval for publication. Mention of trade names or commercial products is not intended to constitute endorsement or recommendation for use.

PREFACE

In this report a comparison is made of two different dispersion models, CALPUFF and ISC3. CALPUFF is a Lagrangian puff model which simulates continuous puffs of pollutants released into the ambient flow, whereas ISC3 is a Gaussian plume model that treats emissions from a source as a contiguous mass. CALPUFF may be configured to treat emissions as integrated *puffs* or as *slugs*. ISC3 is currently recommended for routine use in assessing source impacts involving transport distances of less than 50km. This report is being released to establish part of the basis for review of the consequences resulting from use of CALPUFF in routine dispersion modeling of air pollution impacts.

TABLE OF CONTENTS

1. Introduction

With the initial use of models such as CALPUFF for regulatory applications, there is the question of how the model will behave with respect to more widely used models like the Industrial Source Complex Short Term (ISC3ST) model, hereafter ISC3. Several sensitivity and comparison studies were designed and performed to determine how CALPUFF would behave when set to emulate ISC3. The results of those runs were analyzed and are discussed here.

This evaluation features a systematic, phased series of implementation modes. Section 3.1 involves simple screening modes in which conditions are extremely limited and controlled. Section 3.2 addresses the more general mode in which meteorological conditions are allowed to vary hourly. Section 4 provides a summary and conclusions from this investigation. References are listed in Section 5, followed by the appendices.

2. Technical Background

CALPUFF is a Lagrangian puff model. The model is programmed to simulate continuous puffs of pollutants being emitted from a source into the ambient wind flow. As the wind flow changes from hour to hour, the path each puff takes changes to the new wind flow direction. Puff diffusion is Gaussian and concentrations are based on the contributions of each puff as it passes over or near a receptor point. For these tests, CALPUFF was set to emit 99 puffs per hour (default). A sufficiently large number of puffs is necessary to adequately reproduce the plume solution at near-field receptors.

CALPUFF was originally designed for mesoscale applications and treated emissions as integrated puffs. As features were added to the model for handling local-scale applications, it was realized that use of the integrated puff approach was inefficient. A more efficient approach was developed to treat the emissions as a *slug*, in which the slug is stretched so as to better characterize local source impacts. The slug can be visualized as a group of overlapping circular puffs having very small separation distances. When run in the slug mode, the hourly averaged pollutant mass is spread evenly throughout the slug. For a given hour, if all of the hourly slug has not passed over a receptor, concentrations are reduced by the mass that has not passed over the receptor (Appendix E; Section 2.1 of Reference #2). Note that when run in a *slug* mode, once the slug's lateral dispersion (σ_y) approaches the length of the slug itself (as eventually happens with downwind distance), CALPUFF samples the pollutant mass as a *puff* to improve computational efficiency. At sufficient downwind distance, there becomes no benefit or advantage for the slug simulation.

In the comparison studies described in this report, CALPUFF was run in both the puff mode (emissions simulated as integrated puffs) and the slug mode (emissions simulated as slugs). When the distinction between puffs and slugs is important or significant, they will appear in italics (i.e., *slugs* or *puffs*; see Appendix E). In the generic sense, the use of "puffs" will be used to connote the characterization of a continuous release of a series of overlapping averaged puffs, in which the transport and dispersion of each puff is treated independently, based on local (time and space varying) meteorological conditions. Whereas, the use of "plume" will be used to connote the characterization of a continuous release, in which the release and sampling times are long compared with the travel time from source to receptor, and the meteorological conditions are steady state over the travel time.

3. Results

In this comparison, CALPUFF (Version 4.0, level *960612*) was compared with the latest version of ISC3 (dated *96113*). CALPUFF was run in a mode that enabled ISC3-type meteorological data as input, and therefore winds are horizontally homogeneous for each hour. ISC3 was implemented in the "Regulatory Default" mode and the input file for CALPUFF was configured so as to emulate this to the best extent possible (see Appendix A). Both surface and elevated sources were simulated for *rural* environments in flat terrain, free of obstacles.

3.1 Steady State (screening) Meteorological Conditions

In this approach to the comparison, meteorological conditions were held constant (as in SCREEN3) so as to express true model differences, i.e., without the bias of a varying (temporally and spatially) meteorological regime. Meteorological data sets were synthesized with fixed meteorological conditions (Pasquill-Gifford stability category, wind speed, and mixing height) and were of duration estimated to be sufficient to advect CALPUFF's puffs to the edge of domain (generally 24 - 48 hours). (Of course, ISC3's steady state plume reaches the edge of the domain instantaneously.) For Pasquill-Gifford (P-G) stability category *A*, 5 wind speeds were used, for *B*, there were 9 wind speeds, for *C*, 11 wind speeds, for *D*, 13 wind speeds, for *E*, 9 wind speeds, and for *F*, 7 wind speeds. A matrix describing the basis for the 54 meteorological conditions used is provided in Appendix B.

The elevated point sources were 35m, 100m and 200m, respectively. Surface releases were simulated with a 2m point source, a 500m X 500m area source, and a typical volume source. Characteristics for each source type are described in Appendix C. Sources were placed at the center of a 2 X 2 grid cell domain, with grid spacing set to 150km. While effects within the first 50km are of most interest and significance, straight-line receptors were located with decreasing density out to 100km (Appendix D). The 62 receptors were placed along a radial aligned at 360°, coincident with the bearing used for transport winds.

Unique model runs were made for each combination of source type and meteorological condition (i.e., Pasquill-Gifford stability category, wind speed, and mixing height). Each model was configured to output the highest hourly average concentration for SO_2 (no deposition or chemical transformation).

3.1.1 Residual Analysis

For each pair of model runs (CALPUFF and ISC3), a signed residual (R_i, $\chi_{CALPUFF}$ - χ_{ISC3}, μgm^{-3}) was computed at each of the 62 receptors. From the 62 residuals, a mean ($\bar{R}$, μgm^{-3}), standard deviation (σ_R, μgm^{-3}), and sum of residuals squared (ΣR_i^2) were computed. The statistic $\bar{R}$ provides an indication (sign) of bias along the receptor radial. The statistic σ_R provides general indication of the variance along the receptor radial. Because many of the absolute residuals were quite small, ΣR_i^2 provides a relatively robust indicator of accord along the receptor radial.

Another robust statistic was envisioned in which the absolute residual at each receptor was related to, say, ISC3's predicted concentration value at that receptor. Because of the mathematical problem posed by zero values (can't divide by zero), the statistic $\%R_i$ (*% residual*) was defined in terms of the *maximum* concentration predicted by ISC3 for each run:

$$\%R_i = \left(\frac{R_i}{\chi_{ISC3max}}\right) 100$$

The *mean % residual* follows as:

$$\overline{\%R} = \frac{\Sigma \%R_i}{62}$$

As with $\bar{R}$, the statistic $\overline{\%R}$ provides an indication (sign) of bias along the receptor radial.

Another statistic of interest was the Fractional Bias (FB):

$$FB_i = \frac{R_i}{\frac{\chi_{CALPUFF} + \chi_{ISC3}}{2}}$$

Having by definition a distribution from -2 to +2, a value of zero indicates no bias between $\chi_{CALPUFF}$ and χ_{ISC3}.

One problem that arises with the FB statistic is when the mean paired concentration is very close to zero: the FB statistic can be artificially inflated to a value close to ±2. Since cases in which the mean is close to zero are of little interest in this comparison, a filter was applied:

$$If \quad \left(\frac{\chi_{CALPUFF} + \chi_{ISC3}}{2}\right) < 0.001 \mu g m^{-3}, \quad then \; FB_i \quad 0.0$$

For each run pair (i.e., CALPUFF versus ISC3), a mean fractional bias was computed as:

$$\overline{FB} \quad \frac{FB_i}{62} \qquad \text{(62 receptors)}$$

As with $\overline{R}$ and $\overline{\%R}$, $\overline{FB}$ provides an indication (sign) of bias along the receptor radial. While a value of zero would be ideal for $\overline{FB}$, the following was established as a "goal":

$$-0.10 \leq \overline{FB} \leq 0.10$$

Specific instances for which this goal was not met were noted.

There are some caveats to the interpretation of FB. Its behavior is closely related to its structure. Its value is influenced not only by the absolute difference of the paired concentrations, but by their relative magnitude as well. Thus, modest R_i's related to "large" $\overline{\chi}$'s (e.g., from a low level release) yield modest FB_i's (and a modest $\overline{FB}$). Such a scenario can include a fairly large variance (σ_R = 56 µgm^{-3}) and mean residual (e.g., $\overline{R}$ = −32 $\mu g m^{-3}$) along the receptor radial but still result in a fairly low $\overline{FB}$ (e.g., $\overline{FB}$ = -0.06). Conversely, modest R_i's related to "small" $\overline{\chi}$'s (e.g., from an elevated release) may yield substantial FB_i's. Such a scenario can include a modest variance (σ_R = 0.5 µgm^{-3}) and mean residual (e.g., $\overline{R}$ 0.3 $\mu g m^{-3}$) along the receptor radial but still result in a sizeable $\overline{FB}$ (e.g., $\overline{FB}$ = 0.35). While a useful indicator of correspondence between two quantities, the FB must be interpreted in the context of other comparison statistics.

At the conclusion of the runs, a performance matrix was created and aggregate statistics were compiled. For basic residual analysis, the value, run (distinct combination of source type, wind speed, P-G category, mixing height) and receptor for $R_{i(min)}$ and $R_{i(max)}$ were noted. Likewise, across all runs, the value and run for $\overline{\%R}_{min}$ and $\overline{\%R}_{max}$ were noted, as were the value and run for $\overline{R}_{min}$ and $\overline{R}_{max}$. Across all runs, the value and run for $\sigma_{R(min)}$ and $\sigma_{R(max)}$ were also noted.

Finally, for the FB statistic, the value, run and receptor for $FB_{i(min)}$ and $FB_{i(max)}$ were noted. Across all runs, the value and run for $\overline{FB}_{min}$ and $\overline{FB}_{max}$ were noted. The values and cases in which $\overline{FB}$ did not meet the "10% goal" were also noted.

3.1.2 Point Sources (surface and elevated)[1]

3000m mixing height

To model the four point sources, CALPUFF had to be run 216 times while ISC3 was run 54 times.[2] As indicated in Appendix A, CALPUFF was run in the *slug* mode to emulate ISC3's Gaussian plume simulation.[3] The results indicated good accord (Appendix F). For all cases, $|\overline{FB}| \leq 0.10$ ($\overline{FB}_{max} = 0.02$). The *maximum* residual was 25.0 μgm^{-3} (0.13% of the concentration mean at the incident receptor), while the *minimum* residual was -8.0 μgm^{-3} (0.03% of the concentration mean at the incident receptor). Mean residuals for any run were less than one μgm^{-3}, and total range for σ_R was 0.0 - 3.2 μgm^{-3}. Overall, perhaps the most practical performance parameter was $\overline{\%R}$, which indicates accord well within one percent across all release heights, meteorological conditions and receptors (the value for $\overline{\%R}_{min}$ was -0.04% and $\overline{\%R}_{max}$ was 0.13%). A qualitative inspection of residuals as they appear along the receptor array indicated no distinct pattern of bias for any case. Across all runs, a slight negative bias (CALPUFF relative to ISC3) is apparent for the 2m source, and the greatest variance is associated with the 2m source, especially for P-G category *A*.

500m mixing height

The array of runs was redone (again, using *slugs*) with mixing height reduced to 500m to assess CALPUFF's response to reflection and to evaluate whether reflection is handled equivalently. The results were quite good. In 43 cases, the plume centerline computed by ISC3 exceeded the mixing height and set ground level concentrations to zero. CALPUFF treated the same cases equivalently. For the remaining 173 cases, $|\overline{FB}| \leq 0.10$ ($\overline{FB}_{max} = 0.02$). The comparison statistics bear a striking resemblance to those for Z_i = 3000m. Mean residuals for

---

[1]Certain runs may be referenced, e.g., D20H100 or B1p5H2. Under this nomenclature, the first signifies a 100m source running under *D* stability with 20 ms^{-1} winds. The second would be a 2m source running under *B* stability with 1.5 ms^{-1} winds.

[2]Each source was modeled 54 times for each of two mixing heights. In the current version of CALPUFF, it is impossible to isolate impacts from more than one source per run. ISC3, however, may be configured to simulate multiple sources during a single run and isolate impacts individually.

[3]For a description of integrated *puff* and *slug* formulations, see Sections 2.1.1 and 2.1.2 of the CALPUFF User's Guide (Reference #2) and Appendix E of this report.

any run were also less than one μgm^{-3}, and $\overline{\%R}$ indicates accord to well within one percent across all release heights, meteorological conditions and receptors (the value for $\overline{\%R}_{min}$ was 0.0% and $\overline{\%R}_{max}$ was 0.08%). A qualitative inspection of residuals as they appear along the receptor array also indicated no distinct pattern of bias for any case. As with the 3000m Z_i case, a slight negative bias is apparent for the 2m source, and the greatest variance is associated with the 2m source, especially for P-G category *A*.

3.1.3 Area Source

The area source was modeled with emissions simulated as *slugs*. While a significant difference would be expected between the behavior of *puffs* and *slugs*, *slugs* are considered to treat the area source more closely to the way of ISC3. This is because the "line-source" integrator, similar to that used in ISC3 to model area sources, is only implemented when emissions are simulated as *slugs*. *Puffs* use the effective σ_y treatment for area sources. If there are receptors within or very near an area source, the *slug* treatment is a better representation. If receptors are farther away, the *puff* treatment is reasonable, and less time-consuming. Mixing height was fixed at 3000m. These runs were done both for $\sigma_{z(init)} = 0$ and for $\sigma_{z(init)} = 2.5$m (specification of non-zero $\sigma_{z(init)}$ is optional in both models). The best accord was seen for the set in which $\sigma_{z(init)} = 0$ (Appendix G). For about one fifth of the cases, $|\overline{FB}| > 0.10$ ($\overline{FB}_{min} = -0.16$). The *maximum* residual was 561 μgm^{-3} (2.2% of the concentration mean at the incident receptor), while the *minimum* residual was -1537 μgm^{-3} (33% of the concentration mean at the incident receptor). Mean residuals and mean standard deviations among runs ranged over three orders of magnitude. Analysis of the residuals and fractional biases indicate a definite trend toward negative bias (CALPUFF relative to ISC3), and best accord for any P-G category was seen for the *higher wind speeds*. Also, within any P-G category, the variance falls off with higher wind speed. The parameter $\overline{\%R}$ indicates accord within two percent across meteorological conditions and receptors (the value for $\overline{\%R}_{min}$ was -1.5% and $\overline{\%R}_{max}$ was -0.07%) and again, the tendency toward negative bias is indicated. A qualitative inspection of residuals as they appear along the receptor array indicated no distinct pattern of bias for any case.

3.1.4 Volume Source

The volume source was modeled with emissions simulated as *slugs*. Because ISC3 does not compute concentrations for receptors within $2.15\sigma_y$ of the source (it's actually $2.15\sigma_y$ + 1m), no residuals were analyzed for receptors closer than 200m.

There is a fundamental feature of the way in which ISCST3 treats virtual sources (such as the volume source in question) that is at odds with the way in which CALPUFF treats such sources. The phenomenon is described and illustrated in Appendix H. A modified version of ISCST3 was created to ensure conformity in the treatment of virtual sources by both models. Once this modification was made, the accord between CALPUFF and ISC3 was quite good (Appendix I).

For all cases $|\overline{FB}| = 0.0$. The *maximum* residual was 0.15 μgm^{-3} (0.1% of the concentration mean at the incident receptor), while the *minimum* residual was -0.92 μgm^{-3} (0.4% of the concentration mean at the incident receptor). Mean residuals for any run ranged from -0.2 μgm^{-3} to 0.0 μgm^{-3}, and total range for σ_R was 0.0 - 0.22 μgm^{-3}. The parameter $\overline{\%R}$ indicates accord well within a tenth of one percent across all meteorological conditions and receptors (the value for $\overline{\%R}_{min}$ was -0.07% and $\overline{\%R}_{max}$ was 0.01%). A slight tendency for negative bias was apparent for the stable P-G categories. As seen for the area source, for any of the stable P-G categories, variance falls off with higher wind speed. A qualitative inspection of residuals as they appear along the receptor array indicated slightly more bias for receptors in the near field of the source.

3.2 Variable Meteorological Conditions

3.2.1 Scenarios for Sensitivity Study

For the sensitivity study comparing CALPUFF and ISC3, meteorological conditions were allowed to vary hourly. The first test scenario was devised to see what effects variable meteorology would have on hourly averaged concentrations. One annual period of hourly averaged meteorological data was selected from each of three climatically different regions of the United States. The concentrations between CALPUFF (emissions simulated as a continuous series of puffs) and ISC3 (emission release simulated as a continuous plume) were compared in time and space. The comparisons were examined to try to find the underlying cause of significant differences. The second scenario was a rerun of the first case with some modifications. The averaging times were extended to 3-, 24-hour and annual periods. Maximum concentrations were compared for individual receptor rings at 15 downwind distances. The suite of four point sources described in Appendix C was used in these comparisons.

The meteorological data consist of hourly values of wind speed and direction, ambient temperature, stability class, and mixing heights. The three sites selected were: 1991 Boise, Idaho; 1990 Medford, Oregon; and 1964 Pittsburgh, Pennsylvania.

The Boise data set was selected because of the very directional nature of it winds (see 1991 Boise wind rose, Appendix J). Over 33% of the winds have a northwesterly component and over 33% of the winds have a southeasterly component with the majority of those winds having speeds greater than 2 ms^{-1}. With such persistence in wind direction, the puffs simulated by CALPUFF would be expected to be transported to the most distant receptors.

The Medford data set was selected because of the high number of calm wind situations (see 1990 Medford wind rose, Appendix J). In 1990, Medford Oregon recorded a value of 22.5% of calm winds. This compares to the average of 6.5% for the other two sets of data. Since CALPUFF processes calm winds and ISC3 "zeros" concentrations during calm wind events, there is good reason to expect differences to be seen in the simulated patterns of surface concentration values estimated by the two models.

The 1964 Pittsburgh data set was selected because it has been used as a standard test set for a number of years and because of its fairly well distributed wind directions and wind speeds (see 1964 Pittsburgh wind rose, Appendix J). Although there is a bias in the wind direction toward the southwest, this set was included because many data sets show a similar bias for a particular wind direction and also have a low number of calm winds.

The receptor placement consisted of 15 rings of 36 receptors each for a total of 540 receptors. The rings were spaced at distances of 0.5, 1, 2, 3, 5, 10, 15, 20, 30, 50, 100, 150, 200, 250, and 300km from the source. On each ring, the receptors were spaced every 10° starting at 360°.

3.2.2 Preliminary Studies

Three preliminary studies were done prior to the sensitivity study. In the first preliminary study, CALPUFF and ISC3 were run to create a plot of concentration curves under steady state conditions for centerline and laterally placed receptors. If there were differences in the way dispersion coefficients were calculated between the two models, that would become apparent in plots of concentration distributions. In the second preliminary study, the *puff* and *slug* models were run for a two-hour segment where a large wind shift occurred in the second hour. The purpose was to compare concentration footprints from *puff* and *slug* mode results. This study highlights the different manner in which *puffs* and *slugs* are treated in CALPUFF. In the third preliminary study, a detailed examination was made of the concentration output from CALPUFF (*puff* mode) and ISC3 using the Boise meteorological data to help understand the large differences in concentrations between these two models over a multi-hour period involving calm winds and a wind shift.

First Study

The first study was done to see whether CALPUFF would calculate σ_y and σ_z values differently than ISC3. The same standard input file was created for ISC3 and CALPUFF with the idea being that any difference in the way the sigmas were calculated would be evident in the concentration results. In this comparison, CALPUFF was run in both the *puff* and *slug* modes. The models were run for a 2m point source and the basic switch settings for CALPUFF set per Appendix A. The meteorological data were kept constant except for P-G stability category. For each run, the stability category was changed until all six stability categories, A through F, were used for all three models (i.e., ISC3, CALPUFF *puff* model, and CALPUFF *slug* model). A preliminary group of receptors was created with the centerline along the 360° axis and the receptors spaced every 1° for 44°.

The resulting concentrations were compared on a receptor-by-receptor basis. When the same input data were used, all three models produced concentrations that were within a few fractions of a percent of one another (Figure 1). Figure 1 displays six sets of three curves, one set of curves for each stability category. Each curve in each set overlaps the other curves in that set. The only common difference in each set is that both CALPUFF curves are truncated. This can be seen by the extrapolation of the ISC3 thin dashed line after the thick dashed line and thin solid lines of the two CALPUFF curves. This disparity results from CALPUFF concentration values set to zero for receptors that are more than $3\sigma_y$ from the centerline (Appendix E), whereas ISC3 sets concentration values to zero for receptors that are more than $11.75\sigma_y$ from the centerline. However, lateral plume spread in ISC3 is limited to 50° either side of the centerline and may be further decreased by vertical mixing conditions.

Second Study

In the second study, CALPUFF's treatment of emissions, *puffs* versus *slugs*, was evaluated (Appendix E), using synthesized meteorological data. There is a general difference in the extent of the hourly CALPUFF concentration "footprints" using the *puff* and *slug* models (Appendix K). Concentrations produced by the puff model produce a concentration field similar to a concentration field produced by ISC3 but are restricted to the trajectory algorithms in CALPUFF. The extent of each CALPUFF downwind concentration field is limited by the average wind speed occurring over a particular hour. The extent of the downwind concentration field in ISC3 is limited only by the farthest downwind receptor. The extent of the downwind concentration field when the *slug* model is used is the same as that for the *puff* model. However, when the wind direction changes from one hour and to the next, the directional orientation of the *slug* is maintained while the *slug* is advected downwind (Figure 2). During Hour 1, the wind was from

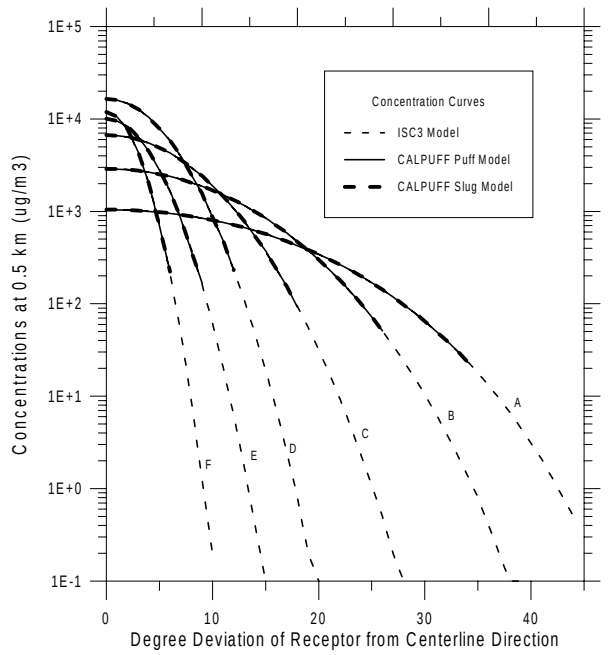

Figure 1. Plot of ISC3 and CALPUFF *slug* and *puff* model concentrations at a distance of 0.5 km from the source for all stability classes. The curves for CALPUFF are truncated because CALPUFF and ISC3 use different y/σ_y criteria for deciding whether to compute a concentration for a given receptor.

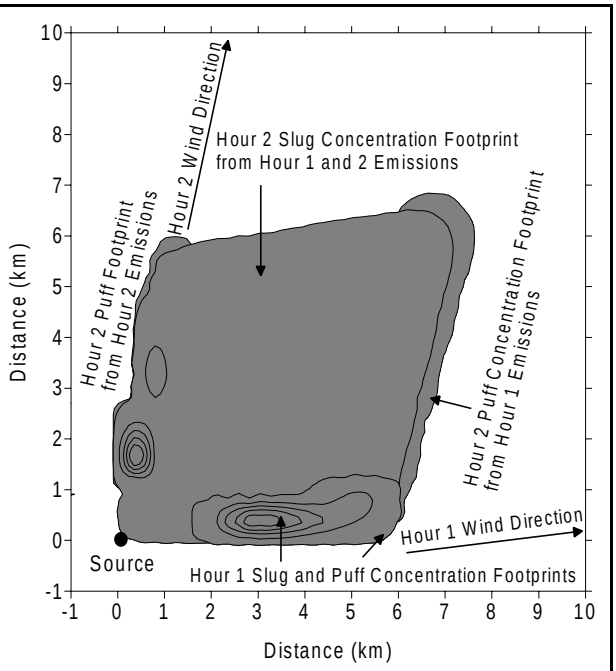

Figure 2. Plot of CALPUFF *slug* and *puff* one-hour concentration footprints during a 2-hour, 70 degree wind shift. Note the broad Hour 2 *slug* area which was advected from the area of the Hour 1 *slug* footprint. This area was coupled with the Hour 2 emissions.

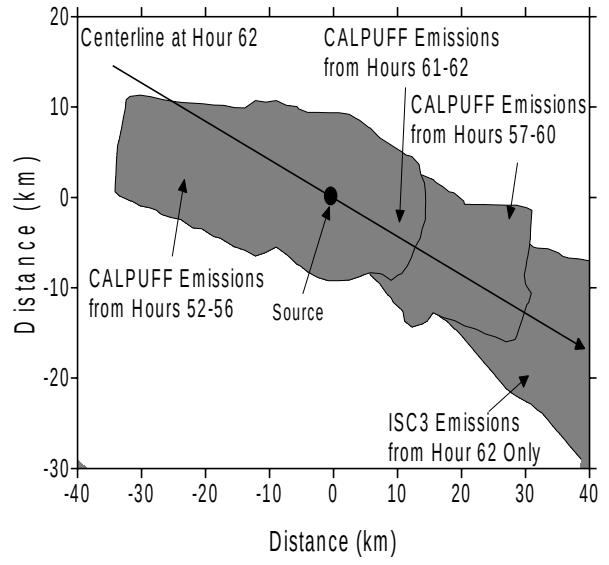

Figure 3. Plot of concentration footprints at Hour 62 from three CALPUFF hourly emission groups and one ISC3 emission group. The Hour 62 ISC3 plume centerline orientation is drawn through the source location. Note the overlap of groups in the 5 to 15km downwind range.

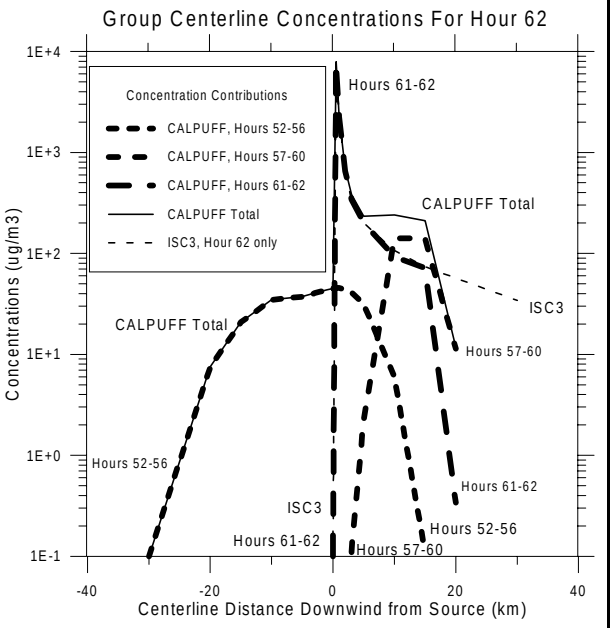

Figure 4. Plot of Figure 3 CALPUFF group and total and ISC3 one-hour concentrations at Hour 62. Note that the CALPUFF total is approximately 50% greater than ISC3 concentrations at 15km.

263°; during Hour 2, the wind switched to 193°. In Hour 1, the *puff* and *slug* model concentration footprints are almost exactly the same. However, in the next hour, the east-west oriented slug is advected north-northeastward. This results in a number of receptors being impacted but at a much lower concentration of about 280 $\mu g m^{-3}$. At the end of Hour 2, an area of approximately 25 km^2 has been impacted by the *slug* model. The puff impacts are restricted to relatively narrow corridors.

Note that during Hour 2, the *slug* and *puff* models have been simulating emissions from the source. The emissions have been transported north-northeastward (Figure 2). The concentrations produced by both models are similar but the puff concentrations are higher in the area of the maximum (Appendix K), due to the way in which dispersion is treated in the *slug* model. Since the slug is elongated and the mass of effluent is spread evenly throughout its volume, the newly emitted effluent close to the end of the hour has not had time to be transported past the receptors farther out. At distances of 0.5, 1, 2, 3 and 5km along the 10 degree radial, the Hour 2 slug concentrations are 91, 82, 64, 46, and 11 percent of the respective puff concentrations. While the *slug* model may have a broader spatial impact, its average concentrations are generally lower than those of the *puff* model.

Remember that receptors were placed on rings within the modeled domain and that there were no rings between 5km and 10km. With this arrangement a truncation appeared in the *puff* concentration footprint for Hour 2 beyond 5km from the source, and the actual footprint (appearing as right side Hour 2 in Figure 2) was not detected. (This truncation was not as evident for the Hour 2 *slug* footprint). To address this artifact, a finer Cartesian grid was developed for the second preliminary study that used a spacing of 400 meters and the right side Hour 2 *puff* footprint was then detected and expressed (Fig. 2). Note that the right side Hour 2 *puff* footprint originates from the terminus of the Hour 1 *puff*. The left side Hour 2 *puff* footprint is the result of Hour 2 emissions from the source. Also note the 400 meter grid resolution was not fine enough to properly contour the left side Hour 2 *puff* concentration isopleths. There was no such contouring problem evident within the other *puff* and *slug* concentration footprints. Note that the Hour 2 *slug* footprint is superimposed by the Hour 1 and Hour 2 *puff* footprints and by the exposed area between them.

Third Study

In the third study, a detailed examination was done on the concentration output from CALPUFF (*puff* mode) and ISC3 using the Boise meteorological data to examine the cause of a large difference in concentrations between these two models' results. These concentrations

occurred 5 to 15km downwind from the source at Hour 62 and after a 4-hour period of calm winds and then a wind reversal (Figure 3).

During the 10 hours preceding Hour 62, hourly emissions were released into one of three wind regimes. First, there were 5 hours of east-southeasterly winds, followed by 4 hours of calm winds, followed by a 180-degree wind shift for 2 hours. Emissions were advected west-northwesterly, then stagnated but the puffs spread out evenly during this calm wind regime, and finally all emissions were advected east-southeasterly until Hour 62.

The CALPUFF concentration field at Hour 62 consists of three groups of concentrations based upon the prevailing wind direction at the time of emission release. One group had releases during Hours 52 through 56. The next group had releases during the calm wind Hours 57 through 60, and the final group had releases during Hours 61 and 62. The fields were depicted to show their respective group concentration footprints at Hour 62.

In Figure 3, note that all three groups overlap each other in the 5 to 12km range downwind. This is also affirmed in Figure 4, which shows the centerline concentrations oriented on the Hour 62 wind direction for each group, the total of the three groups, and the ISC3 centerline concentrations for the receptors nearest the centerline. The centerline concentrations from the three groups were added together to produce concentrations a factor of two greater than those estimated by ISC3 at 15km.

Leading up to Hour 62, there were four hours of calm wind conditions. During calm winds, CALPUFF assumes that the wind speed is zero. However, unlike ISC3 which treats the calm hour as missing, CALPUFF increases the sigma values of each puff with respect to time. During an hour of calm winds, the puffs have grown to the point that ground-level concentrations in this study were calculated at 0.5 and 1.0 km from the puff centers in all directions for the first hour of calm. After two hours, the effluent reached as far as 2km. The broadness of the Hour 52-56 and Hour 57-60 groups is reflective of the puff spreading during the calm wind period.

Details of this type of dispersion phenomena can be seen in Table 1. During Hour 57, the Hour 57 puff releases penetrated a low mixing height (inversion) and continued to spread horizontally without any concentrations contacting the ground. During the inversion rise in Hour 58, emissions were then mixed to the ground and Hour 57 emissions impacted receptors 0.5, 1 and 2km distance from the source while Hour 58 emissions were dispersed only to receptors at 0.5 and 1 km distance from the source.

3.2.3 Sensitivity Study

One of the major tasks of this study is to understand what types of concentrations will be produced by CALPUFF with respect to ISC3. The results of ISC3 versus CALPUFF using the *puff* and *slug* models were compared for three different climatological regions of the country. The results are displayed as a series of figures plotting the percent difference in concentrations at various downwind distances with only ISC3 results in the denominator. Results consist of maximum and highest of the second highest percent differences for 1-, 3-, 24-hour and annual averages.

Table 1
CALPUFF Concentration Estimates under Calm Wind Conditions

Receptor Coordinates		Concentrations (μgm^{-3}) produced by:		
X	Y	Hour 57 emissions at Hour 57	Hour 57 emissions at Hour 58	Hour 58 emissions at Hour 58
0.00	0.50	0.00	1340.44	2989.86
0.00	1.00	0.00	822.80	315.08
0.00	2.00	0.00	115.98	0.00
0.00	3.00	0.00	0.00	0.00
0.00	5.00	0.00	0.00	0.00
0.09	0.49	0.00	1340.68	2992.90
0.17	0.99	0.00	822.44	314.55
0.35	1.97	0.00	115.86	0.00
0.52	2.95	0.00	0.00	0.00
0.87	4.92	0.00	0.00	0.00

As illustrated in Figures 3 and 4, the explanation of why and how one model produces higher concentrations than another can be complex. The effects of inversions, calm winds, wind shifts, wind reversals, and plume and puff trajectory differences can all lead to enhanced or reduced effluent impact. The results of these interactions are shown in Figures 5 and 6 (the series is continued as Figures L-1 through L-7 in Appendix L).

As shown in Figure 5, the Medford plots contain the largest number of positive percentage differences over the widest range of downwind distances. As was seen in Figures 3 and 4, the results of calm winds and wind reversals can lead to higher than ISC3 average concentrations at

respective downwind distances. With the high percentage of calm winds, note also in the annual average panel (Figure 5d) how the differences increase dramatically for the higher stacks as the downwind distance decreases. This is caused by the ISC3 plume not reaching the ground, or not fully dispersing to the ground, whereas CALPUFF can model effluent dispersion with wind reversals for receptors near the stack base.

As shown in Figure 6, the overall difference pattern with respect to stack height and downwind distances among the three sites is remarkably similar. Only the magnitude of the differences and the downwind distance at which the values initially converge is different. The Pittsburgh plots tend to slope downward with respect to the others but overall the patterns remain the same with respect to stack height and downwind distance.

As illustrated in Figures L - 1 through L - 7 (Appendix L), sometimes a pattern or trend can be seen by comparing subsequent or related figures only to find an exception in another figure. All of this may be the result of complex interactions that are likely to occur in any of the climatological regimes. For instance, Medford, Oregon has a high percentage of calm winds. If these calm wind events are coupled with a wind reversal, the same situation illustrated in Figure 3 for Boise, Idaho can occur. The patterns in the percentage differences may reflect a general pattern found at that site but the pattern can be overlaid by a situation often found at another site.

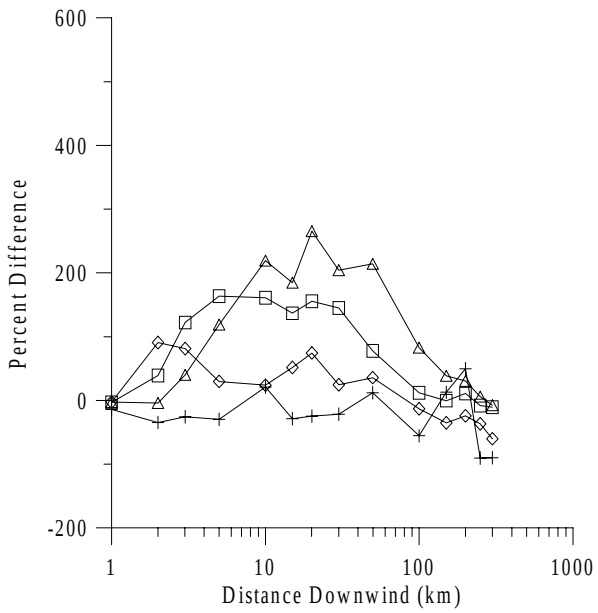

Figure 5a. Results for 1-hour averages using 1990 Medford data.

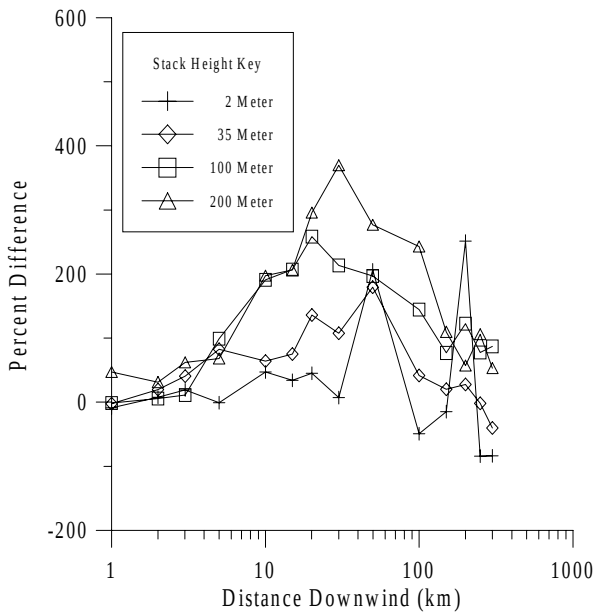

Figure 5b. Results for 3-hour averages using 1990 Medford data.

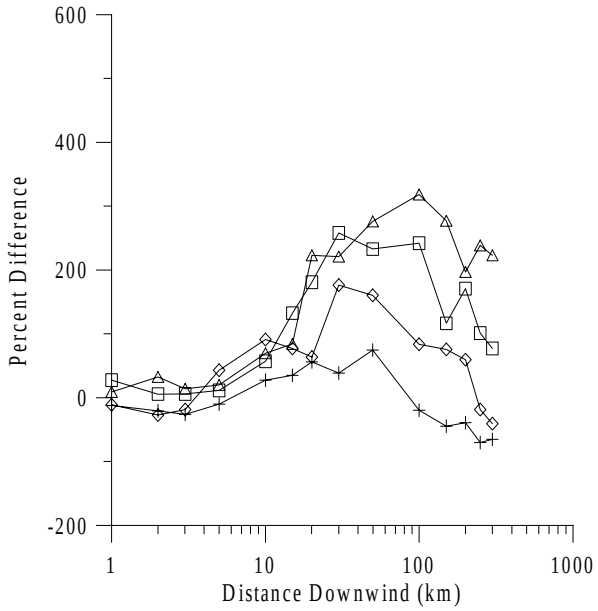

Figure 5c. Results for 24-hour averages using 1990 Medford data.

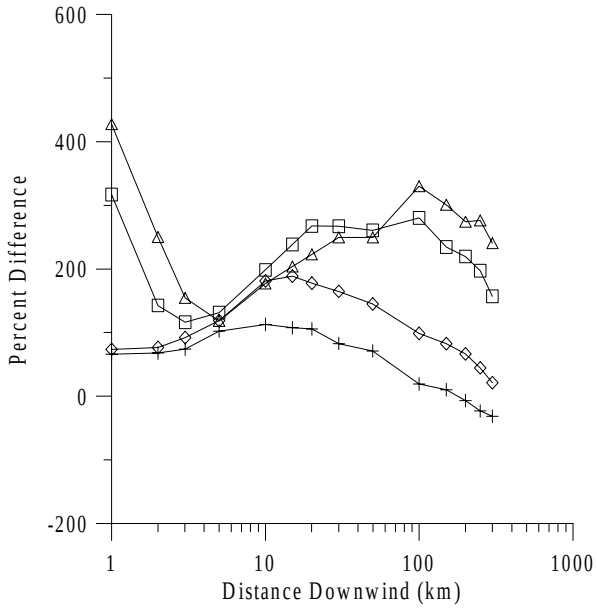

Figure 5d. Results for annual averages using 1990 Medford data.

Figure 5. Percent differences (ISC3 vs. CALPUFF *slug* model) as a function of downwind distance for the highest 2nd high concentrations; 1-, 3-, 24-, and annual averages. Data are for Medford, Oregon. Note: $\%\ Difference \quad 100\ (\frac{\chi_{CALPUFF} - \chi_{ISC3}}{\chi_{ISC3}})$.

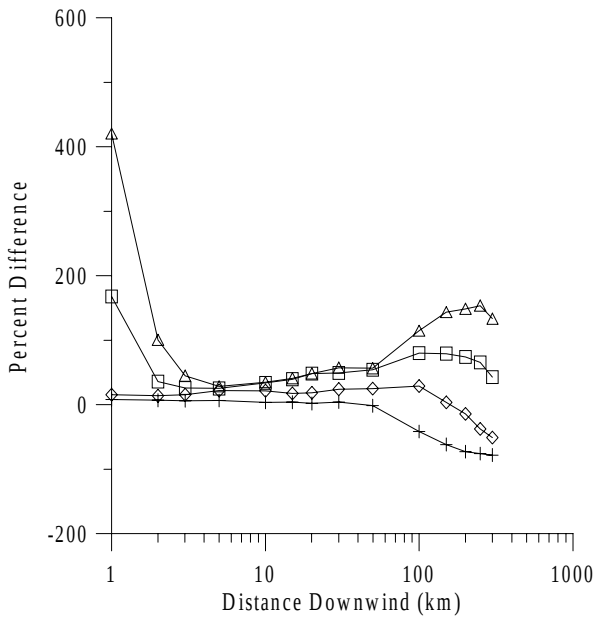

Figure 6a. Results for annual averages using 1991 Boise data.

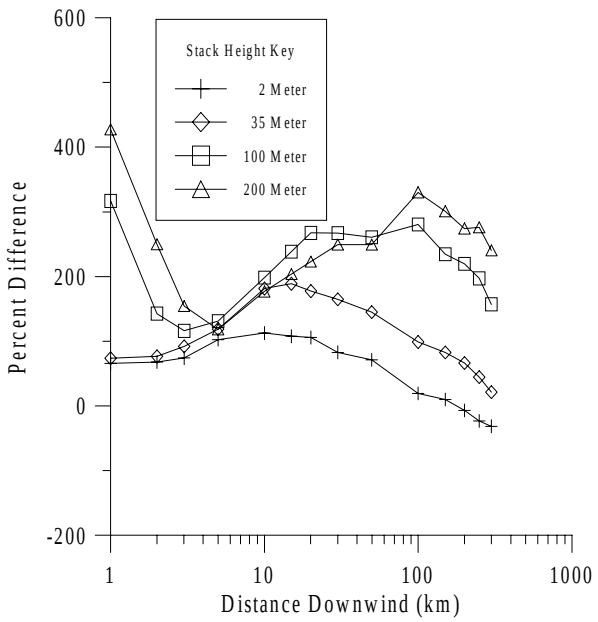

Figure 6b. Results for annual averages using 1990 Medford data (repeat of Fig. 5d).

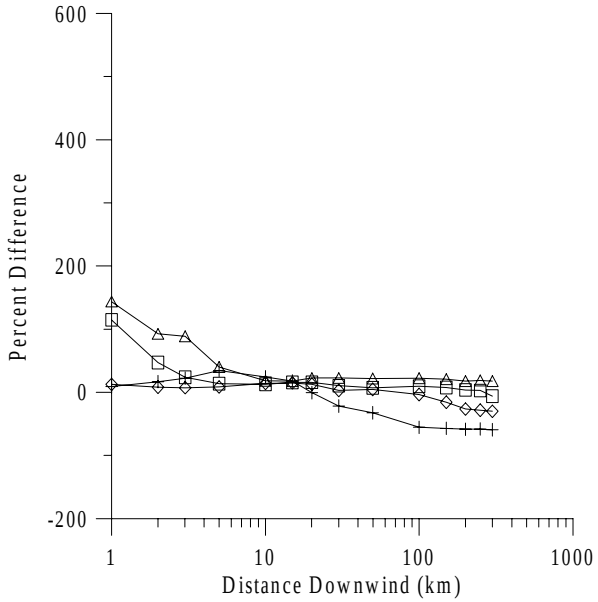

Figure 6c. Results for annual averages using 1964 Pittsburgh data.

Figure 6. Percent differences (ISC3 vs. CALPUFF *slug* model) as a function of downwind distance for annual averages, all three sites. Note: $\%\ Difference \quad 100\ (\frac{\chi_{CALPUFF} - \chi_{ISC3}}{\chi_{ISC3}})$.

4. Summary and Conclusions

4.1 Steady State Meteorological Conditions

CALPUFF and ISCST3 were run with identical meteorological data sets to compare their estimates. The meteorological data sets were synthesized to represent a variety of wind speeds in each of the six P-G stability categories (54 cases in all). ISC3 was run in the "regulatory default" mode and CALPUFF runs were configured to emulate this mode, which included the simulation of emission releases as *slugs* (versus *integrated puffs*). Receptors were located along a straight line ("due north") at successively distant intervals. Sources included three elevated point sources (35m, 100m and 200m). Surface releases included a 2m point source and a rectangular area source 500m on a side. A typical volume source was also examined. For point sources, model runs were done for two regimes, one in which the mixing height (Z_i) was set to 3000m, and the other for Z_i = 500m. The latter regime was explored to inspect CALPUFF's treatment of reflection. For each source type, a comparison matrix was created to assess comparison across all meteorological conditions in terms of a variety of robust statistical indicators.

For all point sources (with Z_i = 3000m), the results indicated good accord between the two dispersion models. For all meteorological conditions, the mean fractional bias across the receptor radial was well below 10%. Maximum residuals at any receptor were on the order of 0.1% of the concentration mean at the incident receptor. While a qualitative inspection of residuals as they appear along the receptor array indicated no distinct pattern of bias, a slight negative bias (CALPUFF relative to ISC3) is apparent for the 2m source, while the reverse is true for the elevated sources. For the low mixing height regime (Z_i = 500m), the comparison results were strikingly similar, suggesting that both CALPUFF and ISC3 treated reflection identically.

The area source was simulated with mixing height set to 3000m. One set of runs was done with initial σ_z set to 0, while the other was set to 2.5m. The best accord was seen for the former case, but for about one fifth of the cases, the mean fractional bias was greater than 10%. The maximum absolute residual was 33% of the concentration mean at the incident receptor. There was an apparent trend toward negative bias (CALPUFF relative to ISC3), but there was substantial variance as well. Mean residuals and mean standard deviations ranged over three orders of magnitude. Accord improved (and variance diminished) with higher wind speeds, which is expected as the slugs are stretched from the point of origin.

With a test version of ISC3 in which the virtual source treatment was "corrected", the models showed close agreement in their treatment of the volume source. Maximum absolute residual was well below one percent of respective concentration means at incident receptors. For all cases, mean fractional bias was zero. A very slight tendency for negative bias was seen for the stable stability categories, and (as for the area source) variance diminished with higher wind

speed. A qualitative inspection of residuals as they appear along the receptor array indicated slightly more bias for receptors in the near field of the source.

4.2 Variable Meteorological Conditions

To examine differences in model estimates when variable meteorological data are used, several studies were done. Actual full-year data sets from three climatologically different sites were used. The sites chosen were Boise, Idaho (1991), Medford, Oregon (1990) and Pittsburgh, Pennsylvania (1964). Using a synthesized meteorological data set, a preliminary set of studies was done to examine (1) differences in the way both models treat lateral σ's (CALPUFF was run using both *puffs* and *slugs*), and (2) *puff* versus *slug* differences within CALPUFF alone. Another study was done using the Boise data to examine the occurrence and location of concentration maxima estimated by ISC3 and the CALPUFF *puff* model. Then for all three sites, extensive sensitivity studies were done in which estimates by ISC3 were compared to CALPUFF (*puff* and *slug* models). In general, 36 - 45 receptors were placed on each of 15 concentric rings at successively more distant intervals.

In general, the differences between CALPUFF and ISC3 concentration results are caused by how emissions are transported and dispersed. CALPUFF limits downwind transport in based on the wind speed while there is no such limitation in ISC3 (it is a plume model). Under calm wind conditions, CALPUFF continues to disperse each puff while the ISC3 model is arbitrarily set to not determine concentrations when the wind speed is less than 1 ms^{-1}. CALPUFF is capable of tracking the puff emitted before, during and after wind shifts and reversals while ISC3 is only concerned with the current hour transport of its plume(s). CALPUFF continues to disperse each puff even when they are above an inversion layer while ISC3 determines its plume is above the inversion layer and cannot be advected to the ground (e.g,. concentrations = 0.0). When the inversion rises above the old puffs, they are dispersed to the ground creating impacts for any nearby receptors.

When all these and other meteorological conditions are recorded on an hourly basis and form a complete year of meteorological data, the effects on concentrations vary between the models and from region to region. The meteorologically induced variations in concentrations do not appear to be so much a regional phenomena, but the variations are related to how the hourly meteorological conditions occur preceding and during a given averaging period. It is possible to have 4 or 5 hours of winds in one general direction followed by 4 hours of calm winds, and then followed by several hours of reversed wind flow. This can occur in any one of the regions. However, the potential frequency of this occurrence may be higher for one region than another. Since calm winds have a causal relationship leading to higher concentrations, then a site such as Medford with a relatively greater incidence of calms (i.e., 22% calm hours versus the other regions having around 6%) will have higher concentrations associated with CALPUFF.

4.3 Conclusion

Even though ISC3 and CALPUFF can be made to produce the same concentrations in a steady state environment, a variable state environment can produce higher-than-ISC3 ground-level concentrations with CALPUFF. Climatological characteristics of a region appear to be a factor, but the accumulation of hour by hour meteorological conditions on the transport of CALPUFF puffs is the key to understanding the differences that are produced by these two models. This should come as no surprise as the meteorological assumptions used in formulating the downwind transport of the ISC3 and CALPUFF effluents and the dispersion from the respective plumes and puffs are different. This is also compounded by the different treatment of dispersion during calm wind conditions.

This complex interaction of transport, vertical mixing, and dispersion have an effect on concentrations with respect to downwind distances in CALPUFF. Occasionally, the accumulation of mass released over several hours will be transported in such a manner that the combined effect is to produce sharp localized maxima in simulated concentration values. The occurrence of such events is not predictable. It seems to occur with greater frequency at Medford. Calm winds play a part in these events. These maxima seem to occur at most locations in the receptor network, at all downwind distances. When they occur, they seem to affect in particular the results for the shorter averaging periods.

Overall trends have been noted in the percentage difference comparisons in simulated concentration values between CALPUFF and ISC3. For taller point sources, there is a trend toward higher concentrations being simulated by CALPUFF in comparison to ISC3. For annual averages, the closer a receptor is to the source and the taller the stack, the greater the chance that the CALPUFF concentration values will be higher than those simulated by ISC3. At the more distant downwind receptor rings, the bias changes direction from CALPUFF yielding higher concentrations, to CALPUFF yielding relatively lower concentrations and sometimes these concentrations are lower than their respective ISC3 counterpart.

5. References

1. Environmental Protection Agency, 1995. User's Guide for the Industrial Source Complex (ISC3) Dispersion Models. Volumes I - III. EPA-454/B-95-003a-c.

2. Environmental Protection Agency, 1995. A User's Guide for the CALPUFF Dispersion Model. EPA-454/B-95-006.

3. Environmental Protection Agency, 1995. SCREEN3 User's Guide. EPA-454/B-95-004.

Appendix A

Switch settings for CALPUFF input file to emulate ISC3's "Regulatory Default" mode

For these comparisons, CALPUFF was run to emulate ISC3's "regulatory mode" (i.e., default). Thus, to ensure equivalence for this emulation, certain of CALPUFF's switches were set as follows:

METFM	= 2	ASCII input file used for input
MSLUG	= 1	Puffs emitted as *slugs*
MDRY	= 0	Dry deposition NOT used, unless specified otherwise
MWET	= 0	Wet deposition NOT used, unless specified otherwise
MSHEAR	= 0	Vertical wind shear NOT modeled
WSCALM	= 0.9999	A value of 1 ms^{-1} for the calm wind speed threshold causes a rounding problem
AVET	= 3	Averaging times for σ's is 60 min; σ_y is adjusted as $(AVET/60)^{0.2}$
MTRANS	= 0	NO transitional plume rise (i.e., final plume rise only)
MDISP	= 3	PG dispersion coefficients for RURAL areas, computed using the ISC multi-segment approximation
MGAUSS	= 1	Vertical dispersion used in the near-field is Gaussian
MCHEM	= 0	NO chemical treatment used
MROUGH	= 0	PG σ_y and σ_z NOT adjusted for roughness
MPARTL	= 0	No partial plume penetration of elevated inversion
MCTADJ	= 1	ISC-type of terrain adjustment
MTIP	= 1	Stack tip downwash used
PLXO(6)		Default wind speed profile power-law exponents for P-G categories A-F
PTGO(2)		Default vertical Θ gradient (Km^{-1}) for stable P-G categories E & F

For all applicable sources, CALPUFF employs buoyancy induced dispersion (BID); a feature enabled in ISC3's regulatory mode. Consistent with ISC3's regulatory default mode, missing data processing was NOT used.

Appendix B

Meteorological conditions for the steady state CALPUFF/ISC3 comparisons[1]

P-G	Wind Speed (ms^{-1})												
A	1.0	1.5	2.0	2.5	3.0								
B	1.0	1.5	2.0	2.5	3.0	3.5	4.0	4.5	5.0				
C	1.0	1.5	2.0	2.5	3.0	3.5	4.0	4.5	5.0	8.0	10.0		
D	1.0	1.5	2.0	2.5	3.0	3.5	4.0	4.5	5.0	8.0	10.0	15.0	20.0
E	1.0	1.5	2.0	2.5	3.0	3.5	4.0	4.5	5.0				
F	1.0	1.5	2.0	2.5	3.0	3.5	4.0						

[1]Wind speed is at 10m and values are the same as those used in SCREEN3. For each combination of P-G stability category, comparisons for point sources were made with Z_i = 500m and 3000m. For the area and volume source, Z_i = 3000m.

Appendix C

Characteristics for sources used in the CALPUFF/ISC3 comparisons

Point Sources					
Stack height (m)	X,Y location & base elevation (m)	Emission rate (gs^{-1})	Exit velocity (ms^{-1})	Stack diameter (m)	Temperature (K)
2	0, 0, 0	100	10.0	0.5	300
35	0, 0, 0	100	11.7	2.4	432
100	0, 0, 0	100	18.8	4.6	416
200	0, 0, 0	100	26.5	5.6	425

Ground-level Area Source				
Area (m^2)	Length of side (m)	Emission rate ($gs^{-1}m^{-2}$)	Effective Release Height (m)	Initial σ_z (m)[1]
250,000	500	0.0004	1.0	2.5

Volume Source[2]	
Emission Rate (gs^{-1}):	1.0
Release height (m):	10
Initial σ_y (m):	50
Initial σ_z (m):	20

[1]In one set of comparisons, $\sigma_{z(init)}$ was set to zero.

[2]Parameter values taken from Figure 9 of SCREEN3 User's Guide (Reference 3); buoyancy flux and momentum flux = 0; rural option.

Appendix D

Receptor array used in the steady state CALPUFF/ISC3 comparisons

Receptors are aligned along a 360° radial at these distances (m):

1	100	32	4000
2	200	33	4500
3	300	34	5000
4	400	35	5500
5	500	36	6000
6	600	37	6500
7	700	38	7000
8	800	39	7500
9	900	40	8000
10	1000	41	8500
11	1100	42	9000
12	1200	43	9500
13	1300	44	10000
14	1400	45	15000
15	1500	46	20000
16	1600	47	25000
17	1700	48	30000
18	1800	49	35000
19	1900	50	40000
20	2000	51	45000
21	2100	52	50000
22	2200	53	55000
23	2300	54	60000
24	2400	55	65000
25	2500	56	70000
26	2600	57	75000
27	2700	58	80000
28	2800	59	85000
29	2900	60	90000
30	3000	61	95000
31	3500	62	100000

Appendix E

Puffs versus Slugs: CALPUFF's Two Simulation Modes

CALPUFF may be operated in one of two modes for simulating emissions: *puff* or *slug*. In the *puff* mode, a continuous plume is represented as a number of discrete packets of pollutant material. Most puff models evaluate the contributions of a puff to the concentration at a receptor by a "snapshot" approach, where each puff is "frozen" at particular time intervals, the concentration due to the frozen puff at that time is computed, and the puff is then allowed to move, evolving in size, strength, etc. until the next sampling step. The total concentration at a receptor is the sum of the contributions of all nearby puffs averaged for all sampling steps within the basic time step. A traditional drawback of the puff approach has been the need for the release of many puffs to adequately represent a continuous plume close to the source. Another potential problem arises if the puffs do not overlap sufficiently, causing concentrations at receptors located in the gap between puffs at the time of the "snapshot" to be underestimated, while those at the puff centers are overestimated. One alternative to the problems posed by the "snapshot" approach is the use of the integrated sampling function (originally implemented in MESOPUFF II). This technique is available in CALPUFF as the *integrated puff* approach, and is fully described in Section 2.1.1 of the CALPUFF User's Guide (Reference 2).

Another approach available in CALPUFF uses a non-circular puff (*slug*) elongated in the direction of the wind to eliminate the need for frequent releases of puffs. Thus in the *slug* model, the "puffs" consist of Gaussian packets of pollutant material stretched in the along wind direction. A slug can be visualized as a group of overlapping circular puffs having very small puff separation distances. Actually, the slug represents the continuous emission of puffs, each containing an infinitesimal mass. The concentrations near the endpoints of the slug (both inside and outside of the body of the slug) fall off in such a way that if adjacent slugs are present, the plume predictions will be reproduced when the contributions of those slugs are included (and this is with steady state conditions). As with circular puffs, each slug is free to evolve independently in response to local effects of dispersion, chemical transformation, removal, etc. However, unlike puffs, the endpoints of adjacent slugs are constrained to remain connected (like country sausages). This ensures continuity of a simulated plume without the gaps associated with the puff approach. It should be noted that all receptors lying outside of the slug's $\pm 3\sigma_y$ envelope during the entire averaging time interval are eliminated from consideration. And for those receptors remaining, integration time limits are computed such that sampling is not performed when the receptor is outside of the $\pm 3\sigma_y$ envelope. This technique is available in CALPUFF as the *slug* approach, and is fully described in Section 2.1.2 of the CALPUFF User's Guide (Reference 2).

When initial CALPUFF runs were made for point sources, a disparity was seen between concentration estimates produced by CALPUFF run in the *slug* mode versus those produced by ISC3. This discrepancy was unexpected and the matter was brought to the attention of Earth Tech (CALPUFF's developer). Earth Tech determined that the reason the *slug* model in Version *960612* did not reproduce the plume model (ISC3) was due to the computation algorithm for sigmas. In the *960612* version, the receptor-specific sigma was computed by determining the

sigma that the puff would have at the receptor, even if the puff hasn't reached the receptor yet (as does a plume model). This gave nearly exact reproduction of plume results under steady-state conditions.

However, under non-steady conditions and very high sigma growth rates (e.g., under P-G category *A*), this extrapolation can produce puff impacts prematurely (and hence the *causality* effect is compromised somewhat). Therefore, the sigmas were "clipped" at the value at the end of the slug when the receptor is beyond the end of the slug. This arrangement did reasonably well for *causality* effects, but caused some deviation from the plume results under steady state conditions.

As a result of Earth Tech's investigation of this disparity, an experimental version of CALPUFF was made available to EPA for the purposes of this comparison, and all analyses were done with this version. This version compromised between the two solutions described above. The version only allows concentrations to be computed for receptors that are within 4 σ_x (where σ_x is the horizontal puff dispersion parameter) of a puff centroid. This technique was seen to perform much better with respect to both treating *causality* and reproducing plume results, and will be incorporated in the next model to be released (Joe Scire, *pers. comm.*, December 1997).

Appendix F

Summary statistics from performance matrix - point sources (Z_i = 3000m)

Emissions simulated as:	SLUGS[a]
$\overline{\%R}_{min}$ (%)	-0.04 (C1H200)
$\overline{\%R}_{max}$ (%)	0.13 (D1H100)
$R_{i(min)}$ (μgm^{-3})	-8.0 (A3H2 @ 100m)[b]
$R_{i(max)}$ (μgm^{-3})	25.0 (F2p5H2 @ 500m)[c]
$\overline{R}_{min}$ (μgm^{-3})	-0.1 (see footnote e)
$\overline{R}_{max}$ (μgm^{-3})	0.4 (F2p5H2)
$\sigma_{R(min)}$ (μgm^{-3})	0.0 (see footnote e)
$\sigma_{R(max)}$ (μgm^{-3})	3.2 (F2p5H2)
# cases $\overline{FB}$ "out of range":[d]	NONE
$\overline{FB}_{min}$	0.0 (see footnote e)
$\overline{FB}_{max}$	0.02 (D20H100)
$FB_{i(min)}$	-0.18 (A1H2 @ 100km)
$FB_{i(max)}$	0.53 (D20H100 @ 800m)

[a] See text for explanation of (C1H200), etc.

[b] This value for R_i is 0.03% of $\overline{\chi}$ ($\frac{\chi_{CALPUFF} + \chi_{ISC3}}{2}$) at this receptor. $\chi_{CALPUFF}$ = 24836 μgm^{-3}; χ_{ISC3} = 24844 μgm^{-3}

[c] This value for R_i is 0.13% of $\overline{\chi}$ at this receptor. $\chi_{CALPUFF}$ = 19040 μgm^{-3}; χ_{ISC3} = 19015 μgm^{-3}

[d] There were 216 distinct cases. The "goal" for this range is: $-0.10 \leq \overline{FB} \leq 0.10$

[e] There is no unique run associated with this value.

Appendix G

Summary statistics from performance matrix - area source (emissions simulated as *slugs*)

Initial σ_z (m):	0		2.5	
$\overline{\%R}_{min}$ (%)	-1.5	(F1AREA)	-3.2	(F1AREA)
$\overline{\%R}_{max}$ (%)	-0.07	(see footnote a)	-0.66	(see footnote a)
$R_{i(min)}$ (μgm^{-3})	-1537	(F1AREA @ 3500m)[b]	-4212	(F1AREA @ 300m)
$R_{i(max)}$ (μgm^{-3})	561	(E1AREA @ 100m)[c]	0.08	(A1AREA @ 85km)
$\overline{R}_{min}$ (μgm^{-3})	-548	(F1AREA)	-969	(F1AREA)
$\overline{R}_{max}$ (μgm^{-3})	-1.1	(D20AREA)	-10.5	(D20AREA)
$\sigma_{R(min)}$ (μgm^{-3})	2.4	(D20AREA)	28.3	(D20AREA)
$\sigma_{R(max)}$ (μgm^{-3})	510	(F1AREA)	895	(F1AREA)
# cases $\overline{FB}$ "out of range":[d]	10		19	
$\overline{FB}_{min}$	-0.16	(see footnote a)	-0.19	(F1AREA)
$\overline{FB}_{max}$	-0.02	(see footnote a)	-0.04	(see footnote a)
$FB_{i(min)}$	-0.39	(E1AREA @ 4000m)	-0.40	(E1AREA @ 4000m)
$FB_{i(max)}$	0.05	(A1AREA @ 85km)	0.05	(A1AREA @ 85km)

[a]There is no unique run associated with this value.

[b]This value for R_i is 33% of $\overline{\chi}$ ($\frac{\chi_{CALPUFF} + \chi_{ISC3}}{2}$) at this receptor. $\chi_{CALPUFF}$ = 3869 μgm^{-3}; χ_{ISC3} = 5406 μgm^{-3}

[c]This value for R_i is 2.2% of $\overline{\chi}$ at this receptor. $\chi_{CALPUFF}$ = 25719 μgm^{-3}; χ_{ISC3} = 25158 μgm^{-3}

[d]There are 54 distinct cases. The "goal" for this range is: $-0.10 \leq \overline{FB} \leq 0.10$

Appendix H

ISCST3's Treatment of Virtual Sources

For volume sources and point sources subject to building wake dispersion, ISC3 makes use of a *virtual source* to simulate an initial plume size. That is, if a source has a finite size at the point of release, its initial σ_y and σ_z are "matched" to a point on the corresponding dispersion curve. Because these curves prescribe the dispersion parameters as a function of distance (starting with a value of zero at a downwind distance equal to zero), matching the curve to a source with a non-zero initial sigma entails shifting the apparent position of the source upwind. This shift is known as the *virtual position* of the source. If x_v denotes the distance of the virtual location of the source upwind of its actual location, then the value of the dispersion parameter at some distance (x) downwind of the source should be evaluated at the modified distance $(x + x_v)$.

ISC3 adopts this general method, but modifies its implementation in the following way. Because the P-G curves for σ_z are expressed as the function ax^b, where the parameters a and b themselves depend on the distance, "the ISC model programs check to ensure that the x_v used to calculate σ_z at $(x + x_v)$ is calculated using coefficients a and b that correspond to the distance category specified by the quantity $(x + x_v)$." (Vol. II of the ISC3 User's Guide (Section 1.1.5.2, p. 1-20) with the notation for the virtual distance changed from x_z to x_v. The term x_v is calculated using Equation 1-36.)

The result of this implementation is that the virtual distance becomes a function of receptor distance downwind of the source, and in fact x_v is reevaluated at each receptor the plume encounters as it moves downwind. Thus, the computed curve of σ_z as a function of distance is no longer the continuous P-G curve. This error is illustrated in the following figures. ISC3 was applied to a volume source with an initial σ_z of 5m and 20m, respectively, and concentrations were obtained at receptors within 1000m, for both P-G stability classes A and F (Figs. H-1 to H-4). Using strategically placed write statements in CALC1.FOR (one of ISCST3's files), the computed virtual distances and the corresponding σ_z values were written to a diagnostic file. These values were then plotted in the figures below as open squares (virtual distances) and as solid circles (σ_z) in the figures below. Figures H-1 and H-2 are for the P-G A stability category, while Figures H-3 and H-4 are for P-G F.

In Figure H-1, the virtual distance begins at 33.76m, and grows in steps corresponding to the "distance ranges" (Table 1-3 of Vol. II) for this P-G curve to almost 120m. The corresponding σ_z values "jump" each time a new virtual distance is used. The same phenomenon can be seen in the other figures, and the departure (ISC3 σ_z versus P-G σ_z) increases with downwind distance. Had more receptors been placed near each of the transition points, a clear "break" in the σ_z curve would have been resolved.

For the purpose of the CALPUFF/ISC3 comparison, ISCST3 was re-configured so that a single value of the virtual distance is computed as a joint function of P-G category and initial σ_z, with due regard for the distance ranges imposed on selecting a & b. This single value is then added to all receptor distances, and the corresponding value for σ_z computed. Figure H-1 indicates the resulting contour (depicted with open triangles) and suggests the *continuous* P-G curve for stability class A, for a virtual location 33.76m upwind of x = 0m.

A version of ISC3 with a corrected virtual source algorithm (dated *97363*), as was used in this comparison, was released in January 1998 and uploaded to EPA's SCRAM web site for public use.

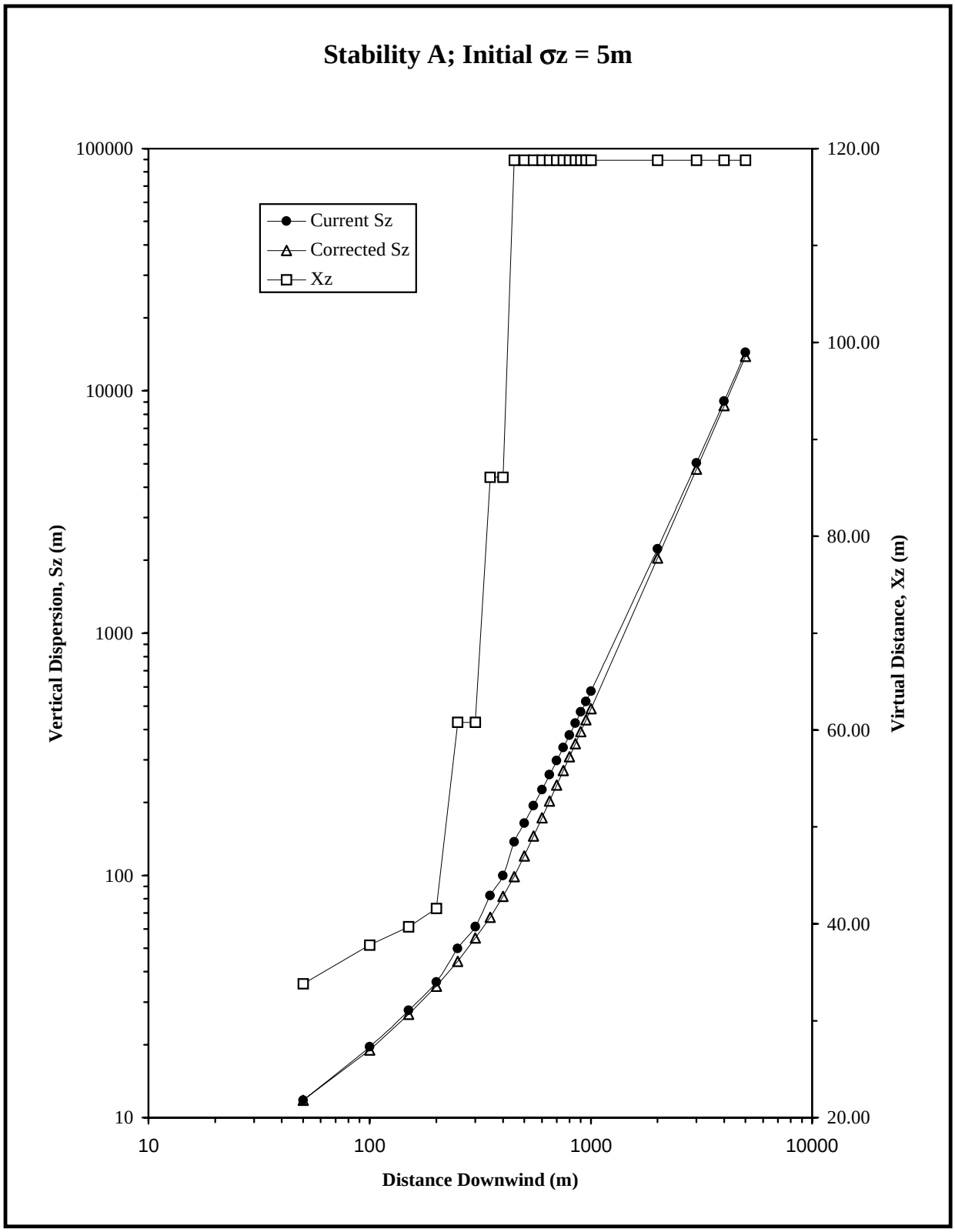

Figure H-1. Profile of σ_z with distance (m); P-G A and $\sigma_{z(init)}$ = 5m.

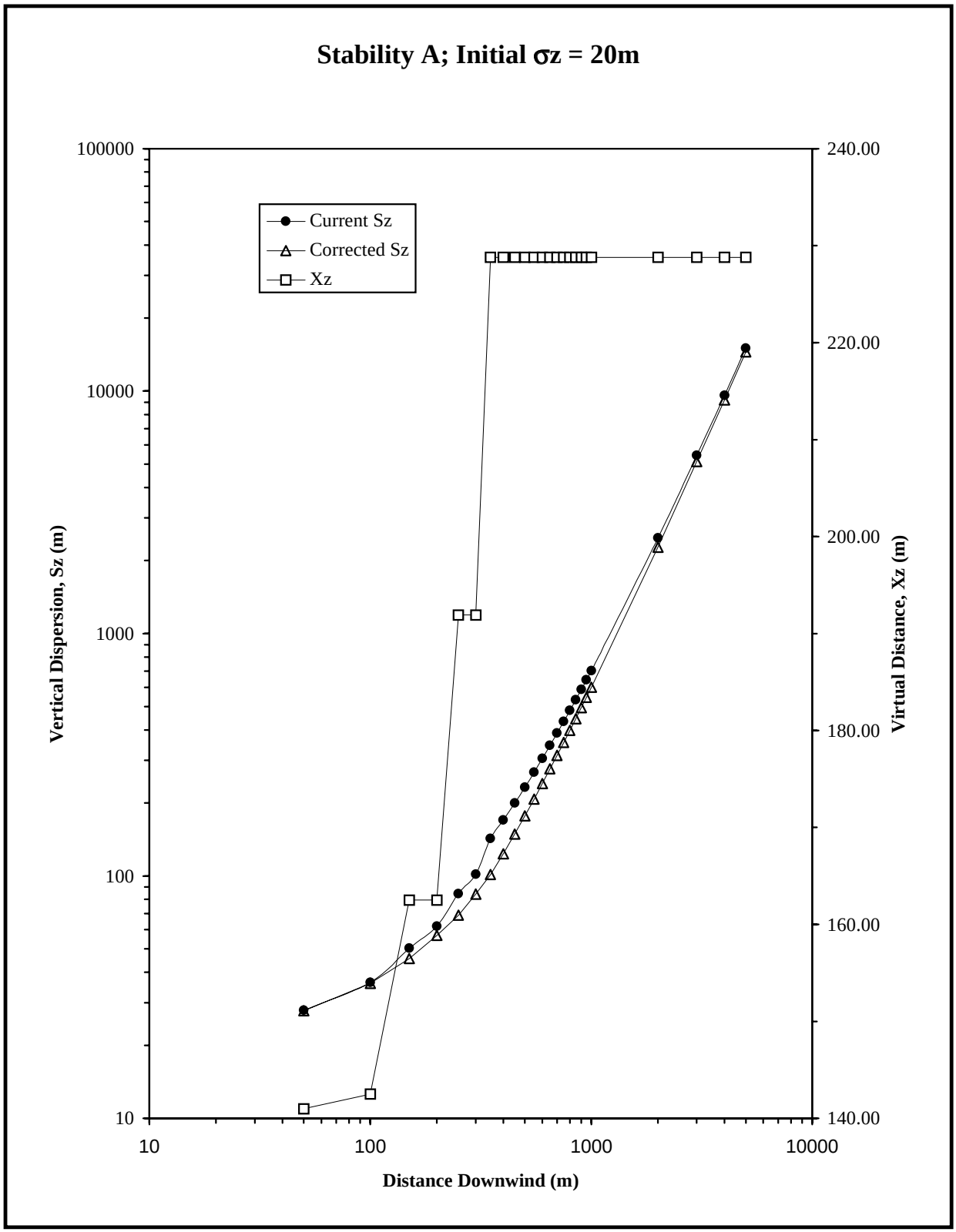

Figure H-2. Profile of σ_z with distance (m); P-G A and $\sigma_{z(init)}$ = 20m.

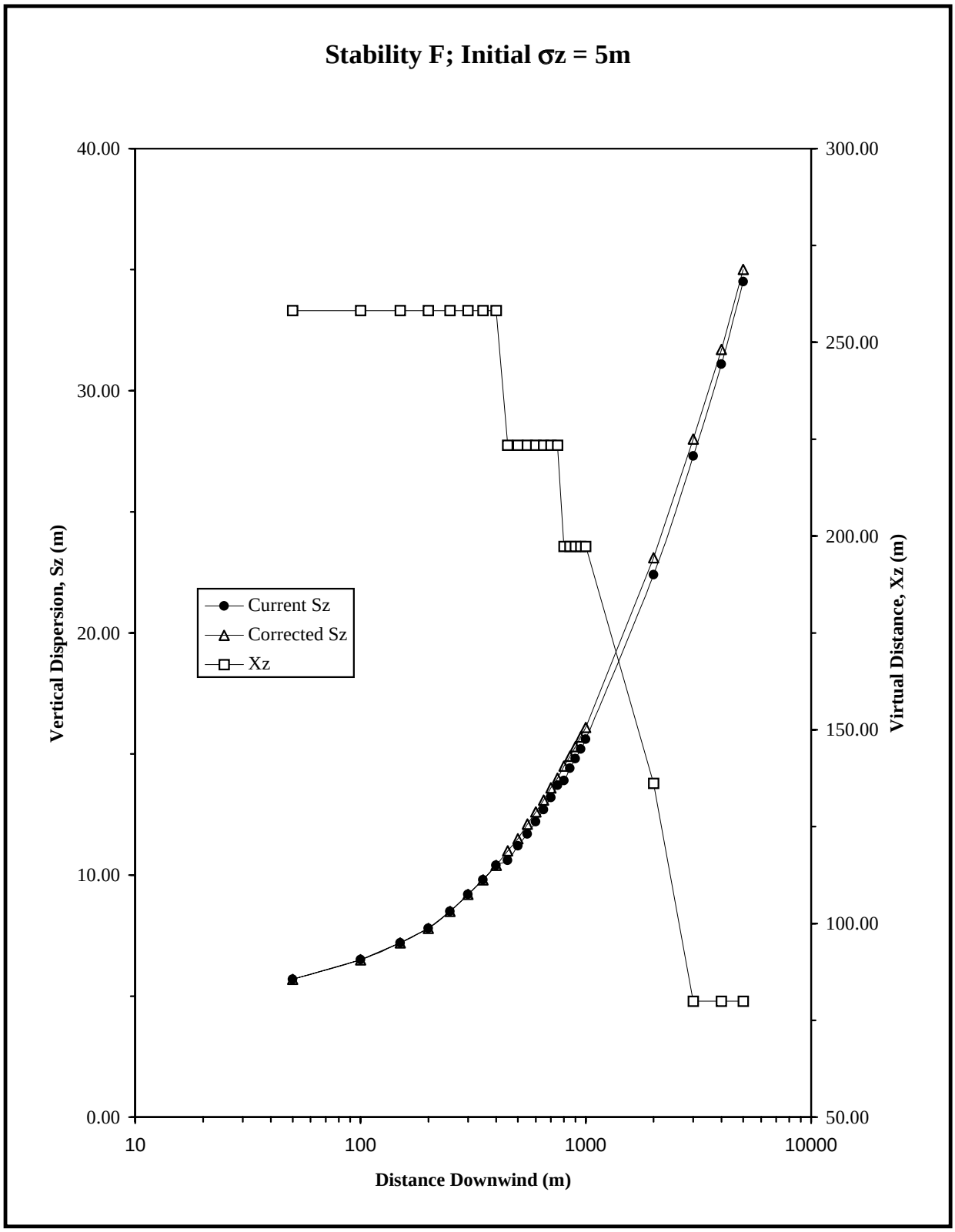

Figure H-3. Profile of σ_z with distance (m); P-G F and $\sigma_{z(init)}$ = 5m.

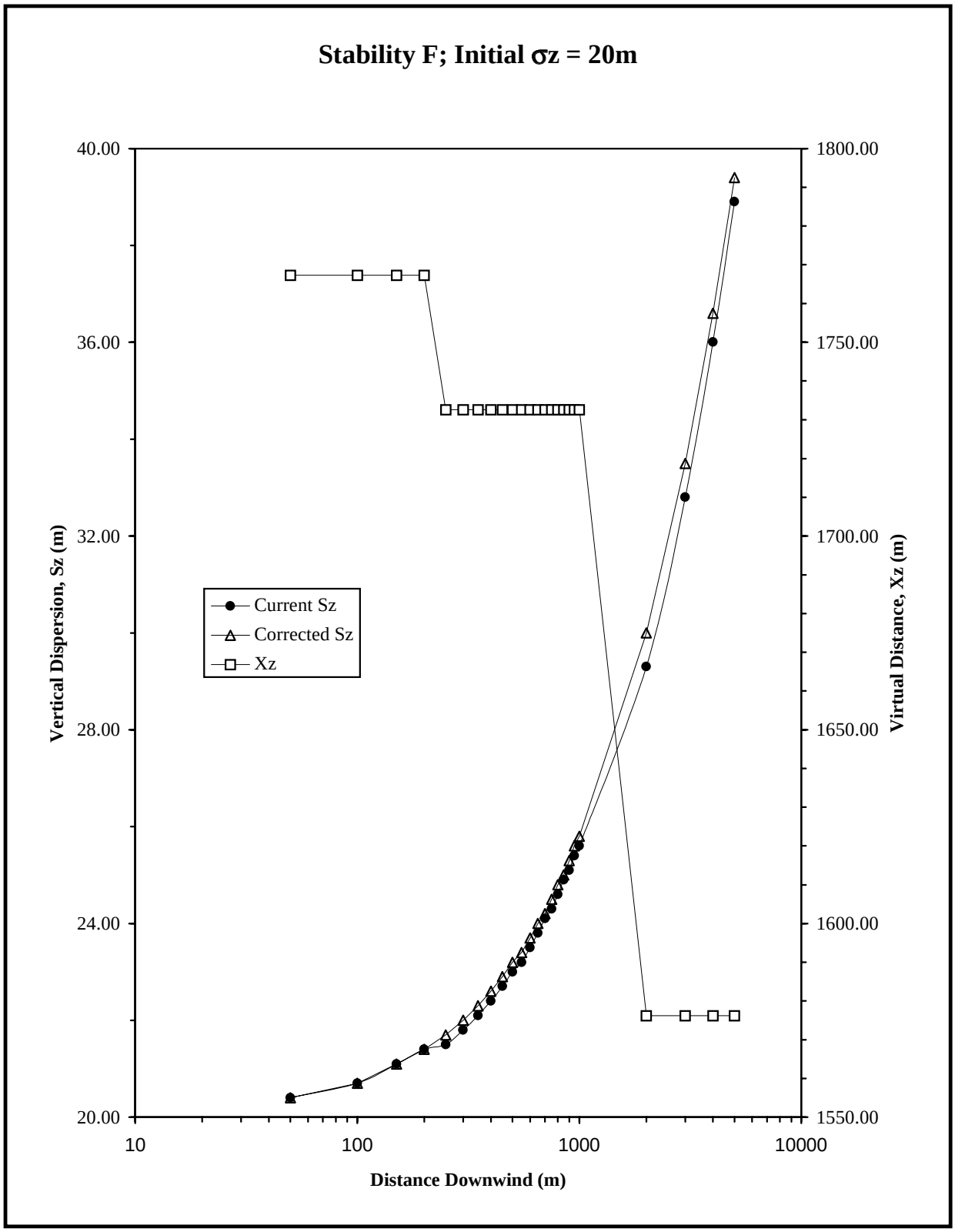

Figure H-4. Profile of σ_z with distance (m); P-G F and $\sigma_{z(init)}$ = 20m.

Appendix I

Summary statistics from performance matrix - volume source

Emissions simulated as:	**SLUGS**
$\overline{\%R}_{min}$ (%)	-0.07 (see footnote a)
$\overline{\%R}_{max}$ (%)	0.01 (see footnote a)
$R_{i(min)}$ (μgm^{-3})	-0.92 (F1VOL @ 200m)[b]
$R_{i(max)}$ (μgm^{-3})	0.15 (C1VOL @ 200m)[c]
$\bar{R}_{min}$ (μgm^{-3})	-0.2 (F1VOL)
$\bar{R}_{max}$ (μgm^{-3})	0.0 (see footnote a)
$\sigma_{R(min)}$ (μgm^{-3})	0.0 (see footnote a)
$\sigma_{R(max)}$ (μgm^{-3})	0.22 (F1VOL)
# cases $\overline{FB}$ "out of range":[d]	NONE
$\overline{FB}_{min}$	0.0 (see footnote a)
$\overline{FB}_{max}$	0.0 (see footnote a)
$FB_{i(min)}$	-0.18 (A1VOL @ 100km)
$FB_{i(max)}$	0.06 (A1VOL @ 85km)

[a]There is no unique run associated with this value.

[b]This value for R_i is 0.4% of $\bar{\chi}$ ($\frac{\chi_{CALPUFF} + \chi_{ISC3}}{2}$) at this receptor. $\chi_{CALPUFF}$ = 238.6 μgm^{-3}; χ_{ISC3} = 239.5 μgm^{-3}

[c]This value for R_i is 0.1% of $\bar{\chi}$ at this receptor. $\chi_{CALPUFF}$ = 135.1 μgm^{-3}; χ_{ISC3} = 135.0 μgm^{-3}

[d]There were 54 distinct cases. The "goal" for this range is: $-0.10 \leq \overline{FB} \leq 0.10$

Appendix J
Wind Rose Patterns

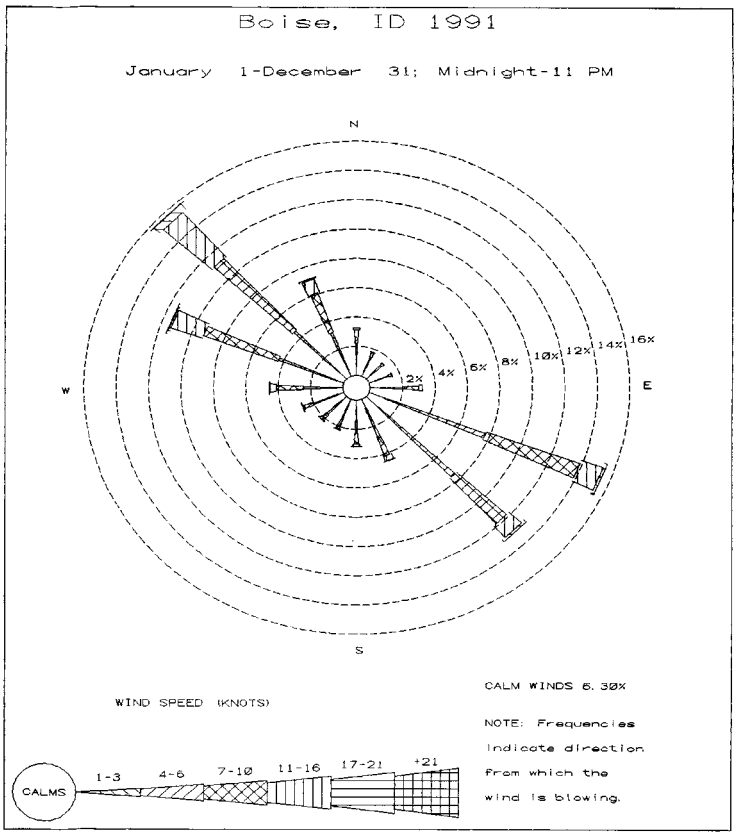

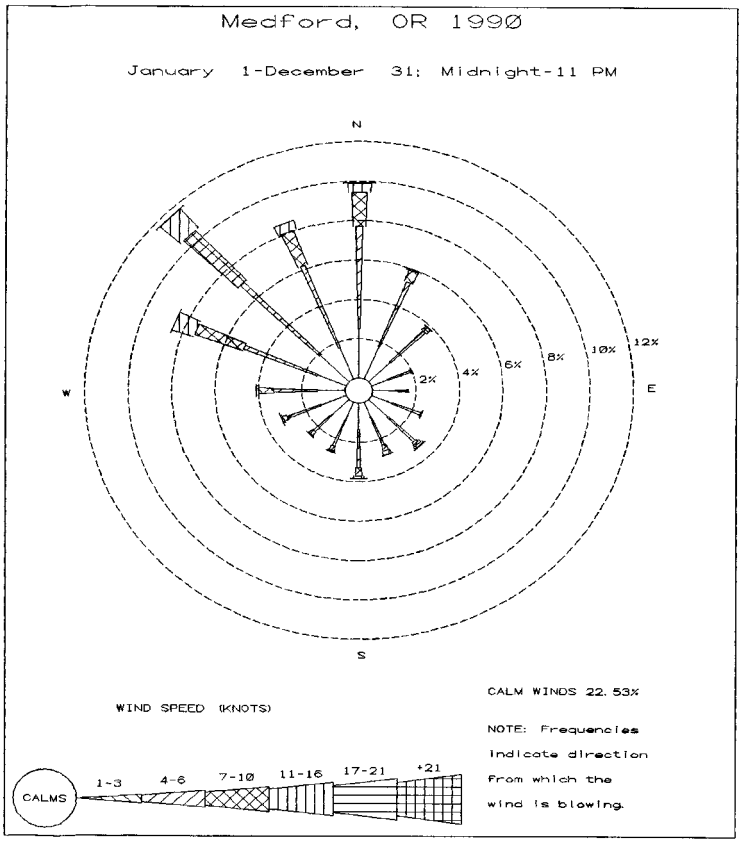

Appendix J, continued.

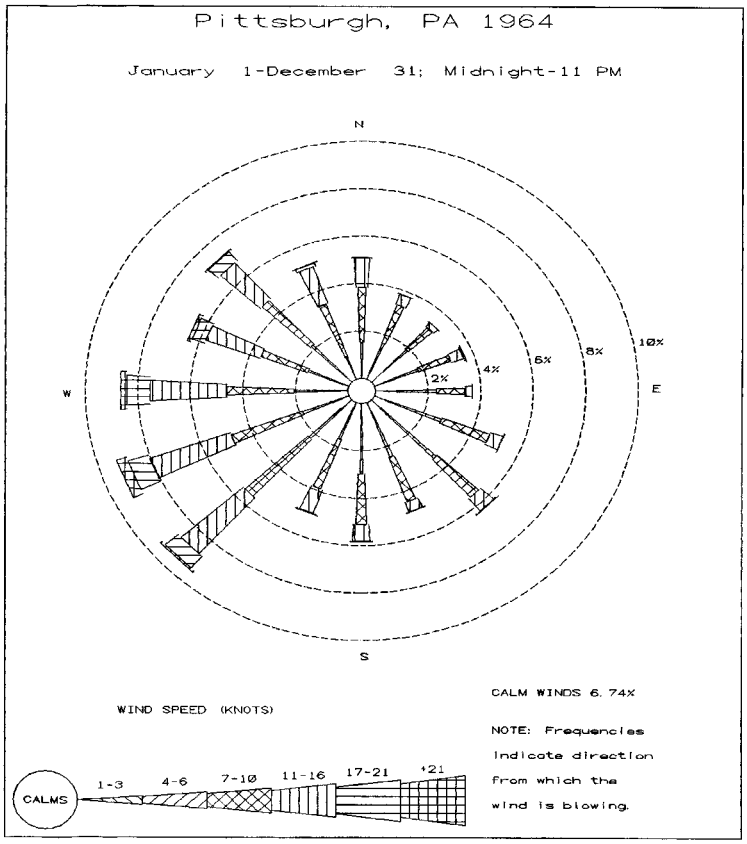

Appendix K

CALPUFF Concentrations Estimated by *Integrated Puff* and *Slug* Model

Coordinates		Hour 1	Hour 2	
X	Y	Puff	Puff	Slug
0	0.5	0	0	0
0	1	0	0	0
0	2	0	0	0
0	3	0	0	0
0	5	0	0	0
0.09	0.49	0	4400.88	4011.7
0.17	0.99	0	4606.96	3785.43
0.35	1.97	0	2366.87	1525.9
0.52	2.95	0	1408.23	658.51
0.87	4.92	0	670.78	74.94
0.17	0.47	0	0	75.18
0.34	0.94	0	0	211.99
0.68	1.88	0	0	284.43
3.19	2.82	0	0	271.96
1.71	4.7	0	0	233.71
0.25	0.43	0	0	93.83
0.5	0.87	0	0	234.87
1	1.73	0	0	284.04
1.5	2.6	0	0	266.32
2.5	4.33	0	0	229.02
0.32	0.38	0	0	108.62
0.64	0.77	0	0	248.26
1.29	1.53	0	0	282.78
1.93	2.3	0	0	262.57
3.21	3.83	0	0	226.52
0.38	0.32	0	0	118.39
0.77	0.64	0	0	254.07
1.53	1.29	0	0	261.61
2.3	1.93	0	0	261.61
3.83	3.21	0	0	226.13
0.43	0.25	0	0	122.47
0.87	0.5	0	0	255.92
1.73	1	0	0	281.55
2.6	1.5	0	0	261.75
4.33	2.5	0	0	227.49
0.47	0.17	0	0	120.31
0.94	0.34	0	0	254.23
1.88	0.68	0	0	282.08
2.82	1.03	0	0	263.61
4.7	1.71	0	0	230.65
0.49	0.09	4445.83	0	103.69
0.99	0.17	4593.7	0	234.05
1.97	0.35	2440.53	0	269.69
2.95	0.52	1413.91	0	254.14
4.92	0.87	678.28	0	226.08
0.5	0	0	0	0

Puff vs. ISC3

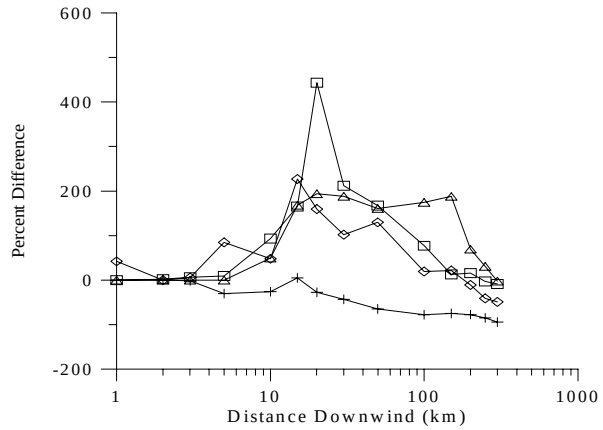

Figure L-1(a). Boise meteorological data.

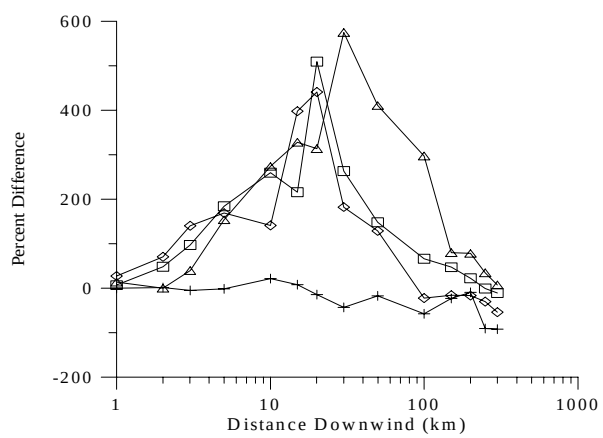

Figure L-1(c). Medford meteorological data.

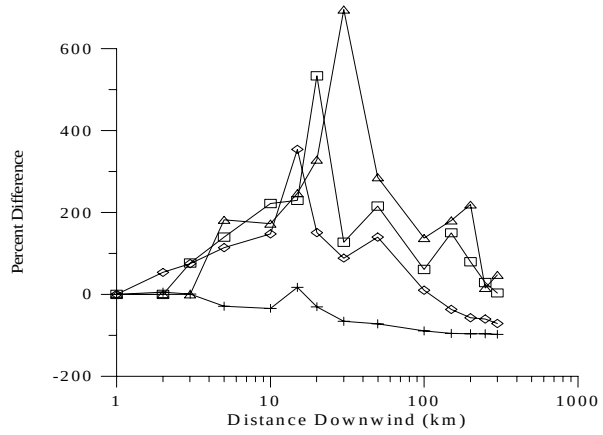

Figure L-1(e). Pittsburgh meteorological data.

Slug vs. ISC3

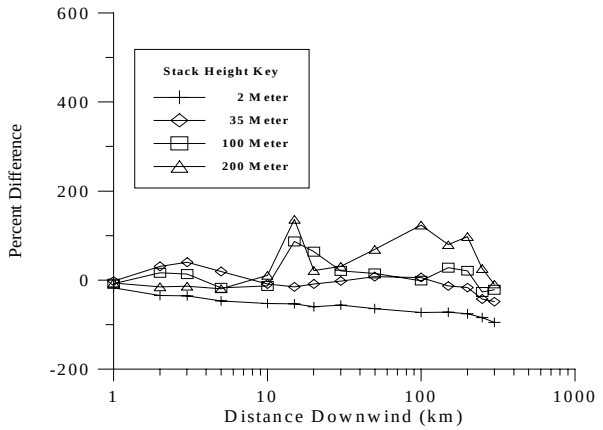

Figure L-1(b). Boise meteorological data.

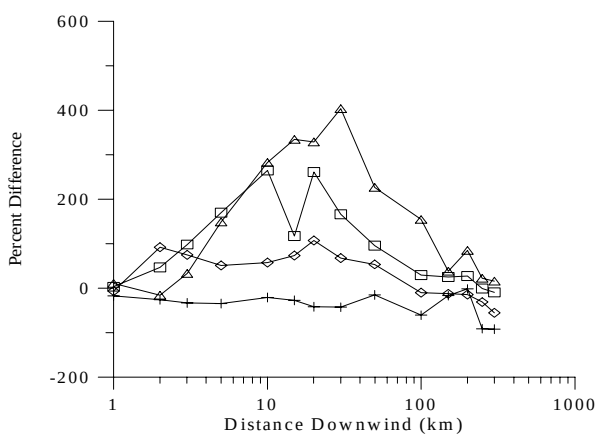

Figure L-1(d). Medford meteorological Data.

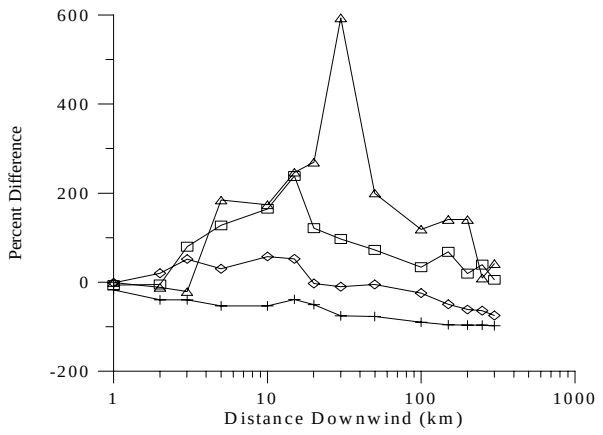

Figure L-1(f). Pittsburgh meteorological data.

Figure L-1. Maximum 1-hour average concentrations by distance. Figures a, c, & e show CALPUFF *puffs*, whereas figures b, d, & f show *slugs*.
Note: $\%\ Difference \quad 100\ (\frac{\chi_{CALPUFF} - \chi_{ISC3}}{\chi_{ISC3}})$.

Puff vs. ISC3

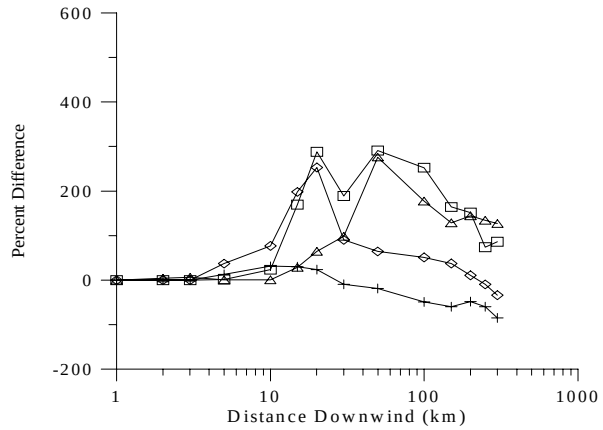

Figure L-2(a). Boise meteorological data.

Slug vs. ISC3

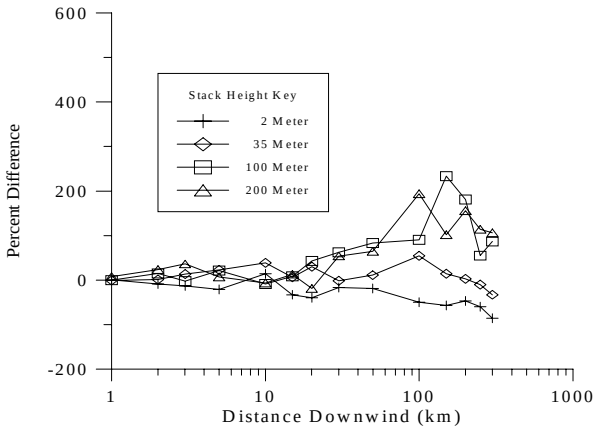

Figure L-2(b). Boise meteorological data.

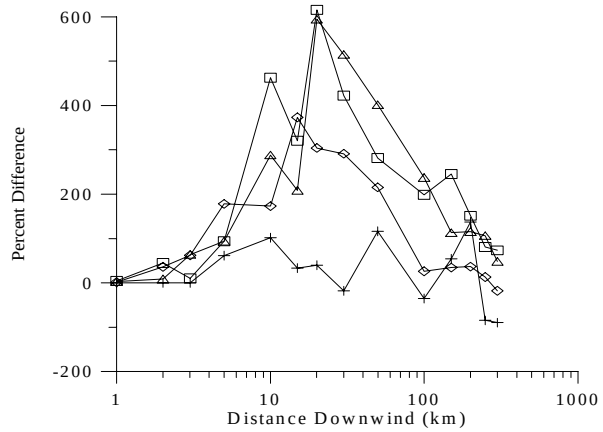

Figure L-2(c). Medford Meteorological Data.

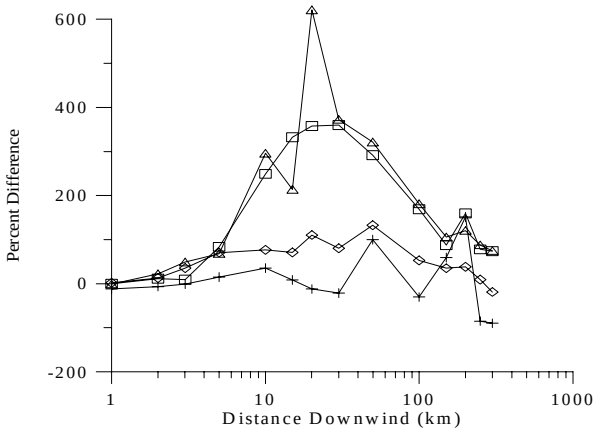

Figure L-2(d). Medford meteorological Data.

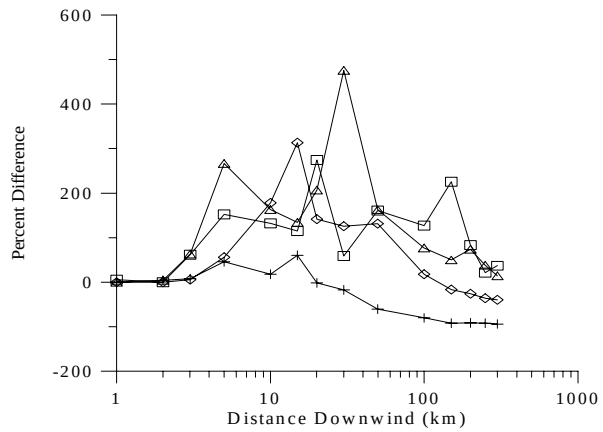

Figure L-2(e). Pittsburgh meteorological data.

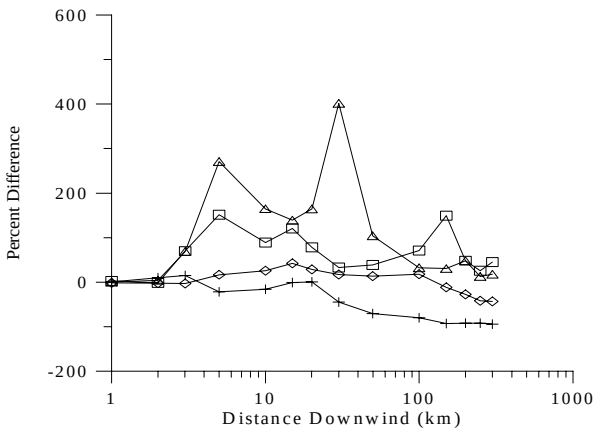

Figure L-2(f). Pittsburgh meteorological data.

Figure L-2. Maximum 3-hour average concentrations by distance. Figures a, c, & e show CALPUFF *puffs*, whereas figures b, d, & f show *slugs*.
Note: $\%\ Difference \quad 100\ (\frac{\chi_{CALPUFF} - \chi_{ISC3}}{\chi_{ISC3}})$.

Puff vs. ISC3

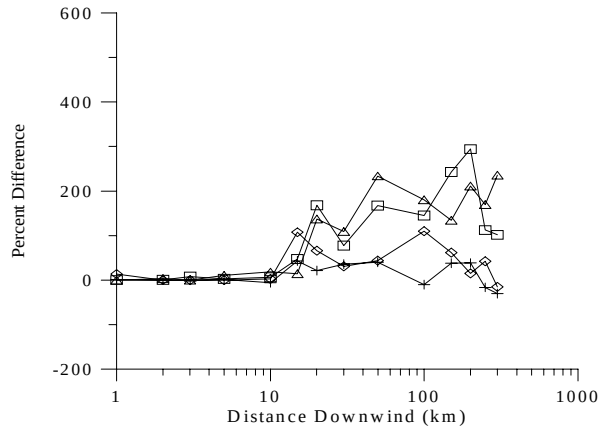

Figure L-3(a). Boise meteorological data.

Slug vs. ISC3

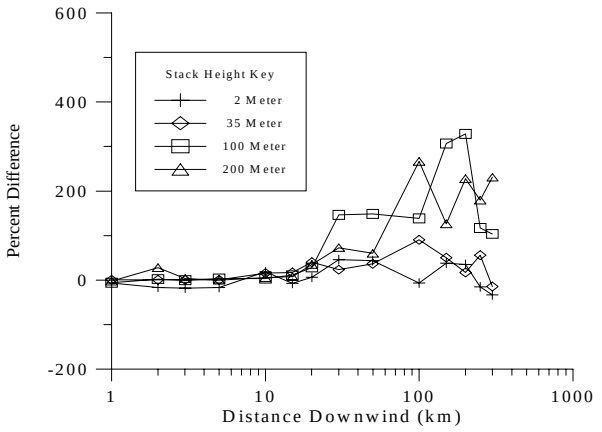

Figure L-3(b). Boise meteorological data.

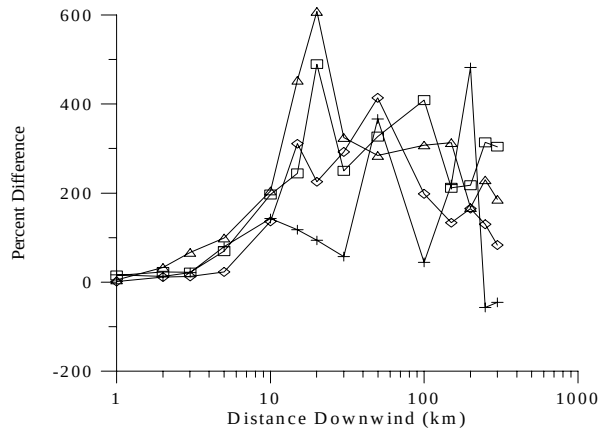

Figure L-3(c). Medford meteorological data.

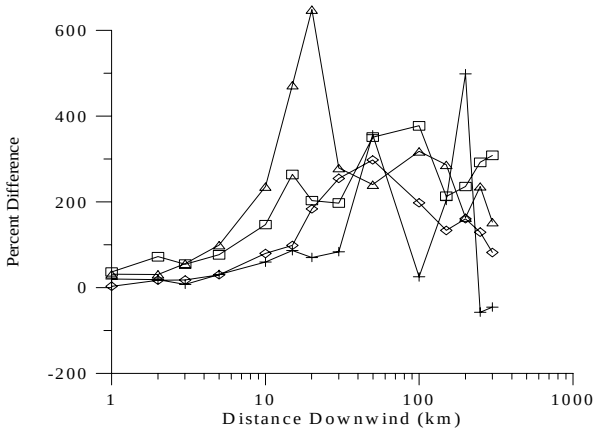

Figure L-3(d). Medford meteorological data.

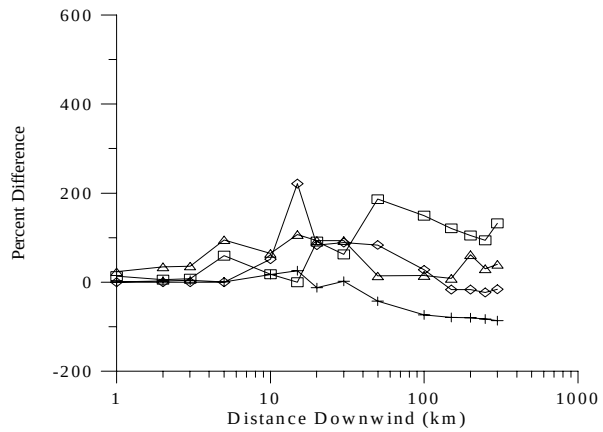

Figure L-3(e). Pittsburgh meteorological data.

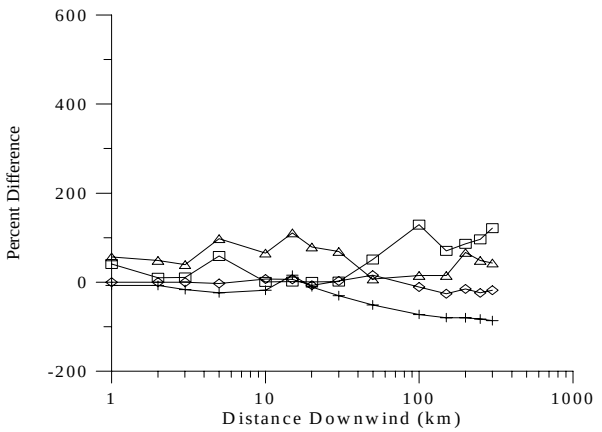

Figure L-3(f). Pittsburgh meteorological data.

Figure L-3. Maximum 24-hour average concentrations by distance. Figures a, c, & e show CALPUFF *puffs*, whereas figures b, d, & f show *slugs*.
Note: $\%\ Difference \quad 100\ (\frac{\chi_{CALPUFF} - \chi_{ISC3}}{\chi_{ISC3}})$.

Puff vs. ISC3

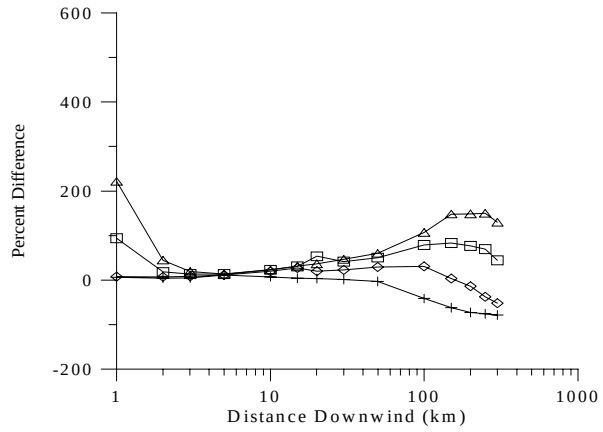

Figure L-4(a). Boise meteorological data.

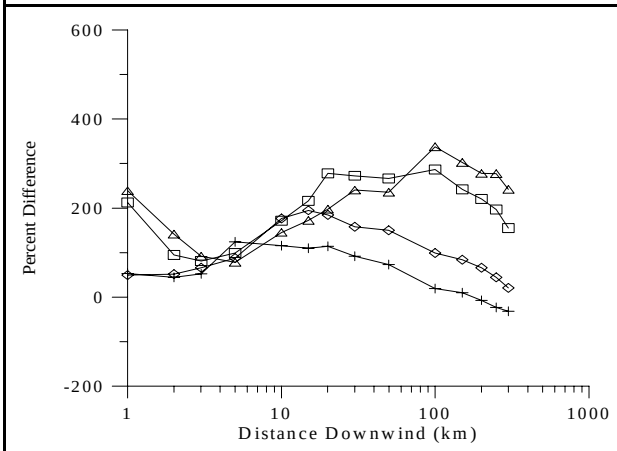

Figure L-4(c). Medford meteorological data.

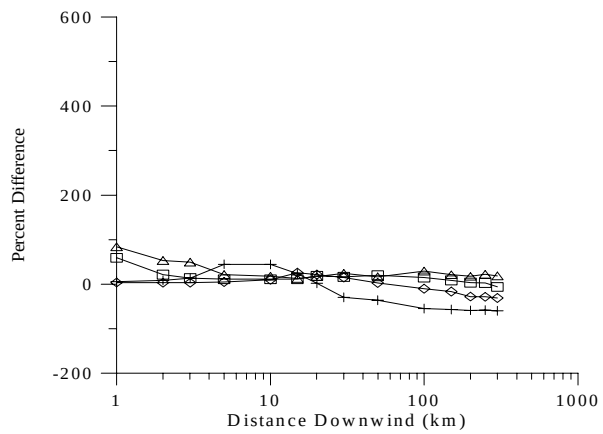

Figure L-4(e). Pittsburgh meteorological data.

Slug vs. ISC3

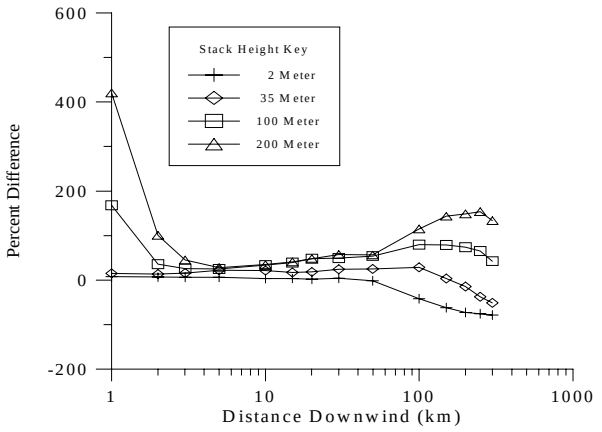

Figure L-4(b). Boise meteorological data.

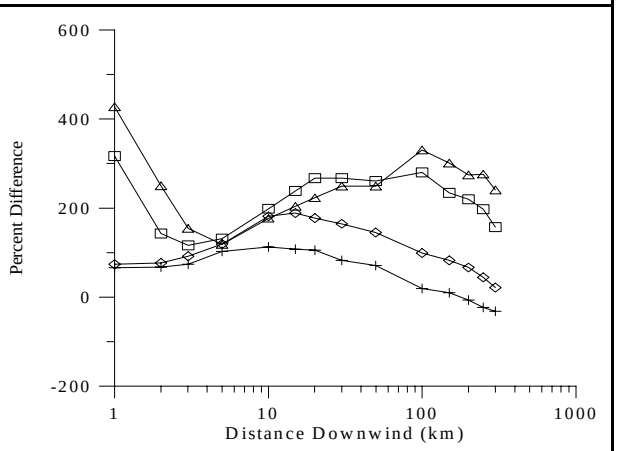

Figure L-4(d). Medford meteorological data.

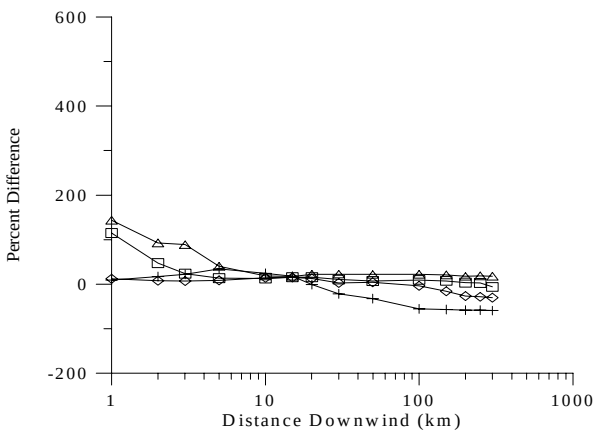

Figure L-4(f). Pittsburgh meteorological data.

Figure L-4. Maximum annual average concentrations by distance. Figures a, c, & e show CALPUFF *puffs*, whereas figures b, d, & f show *slugs*.
Note: % *Difference* $100\ (\frac{\chi_{CALPUFF} - \chi_{ISC3}}{\chi_{ISC3}})$.

Puff vs. ISC3

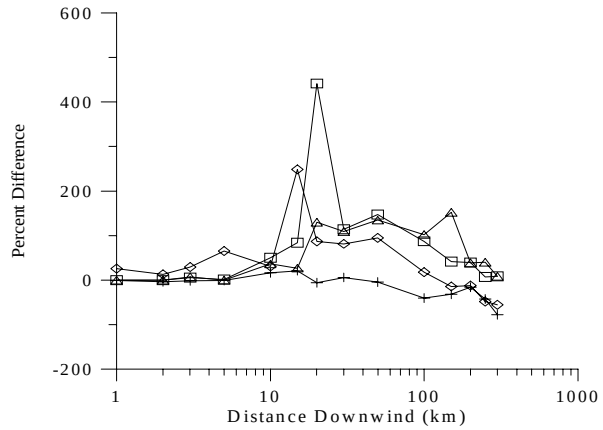

Figure L-5(a). Boise meteorological data.

Slug vs. ISC3

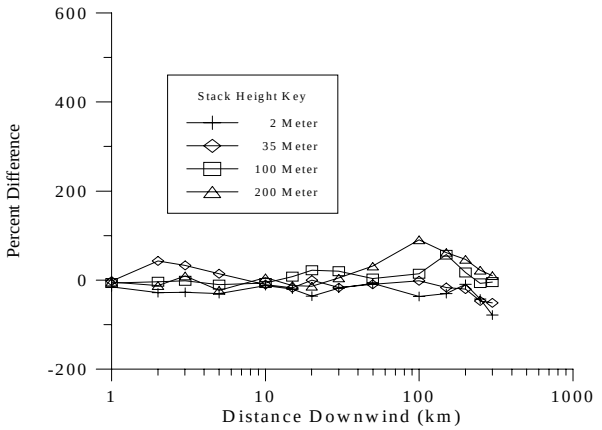

Figure L-5(b). Boise meteorological data.

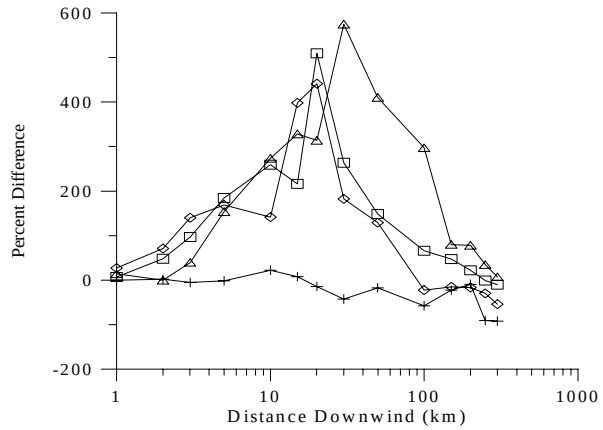

Figure L-5(c). Medford meteorological data.

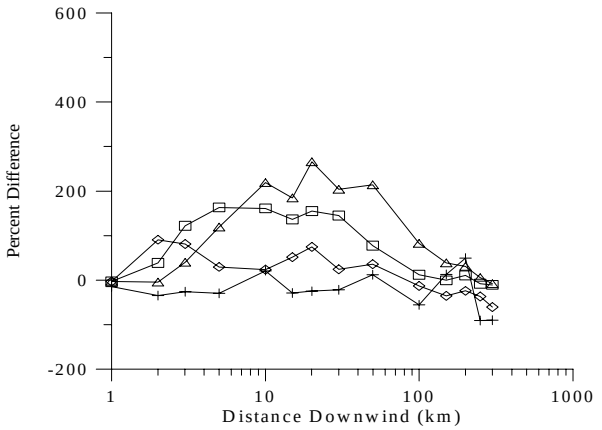

Figure L-5(d). Medford meteorological data.

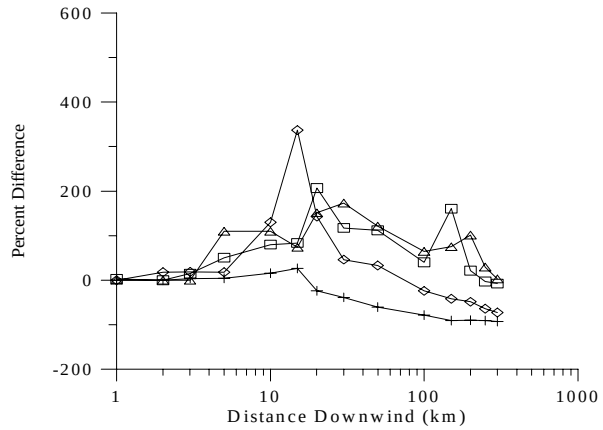

Figure L-5(e). Pittsburgh meteorological data.

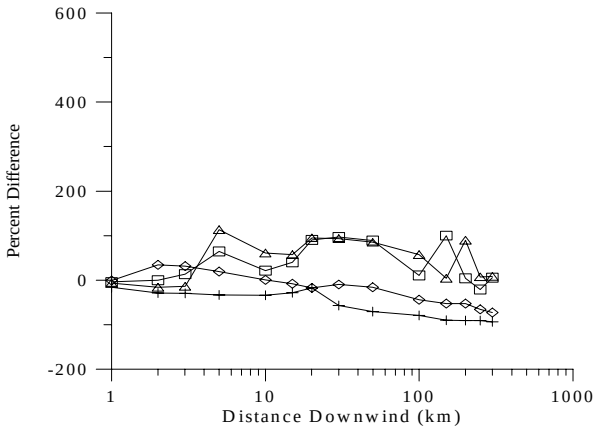

Figure L-5(f). Pittsburgh meteorological data.

Figure L-5. Highest of the second highest 1-hour average concentrations by distance. Figures a, c, & e show CALPUFF *puffs*, whereas figures b, d, & f show *slugs*.
Note: % *Difference* $100\ (\frac{\chi_{CALPUFF} - \chi_{ISC3}}{\chi_{ISC3}})$.

Puff vs. ISC3

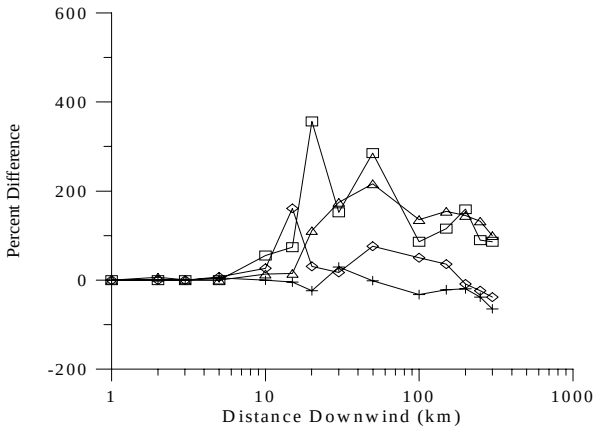

Figure L-6(a). Boise meteorological data.

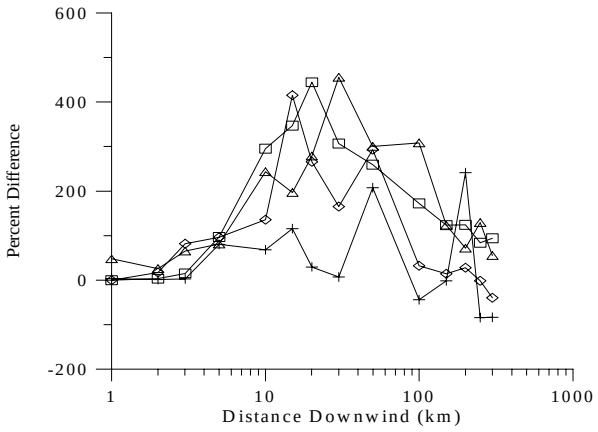

Figure L-6(c). Medford meteorological data.

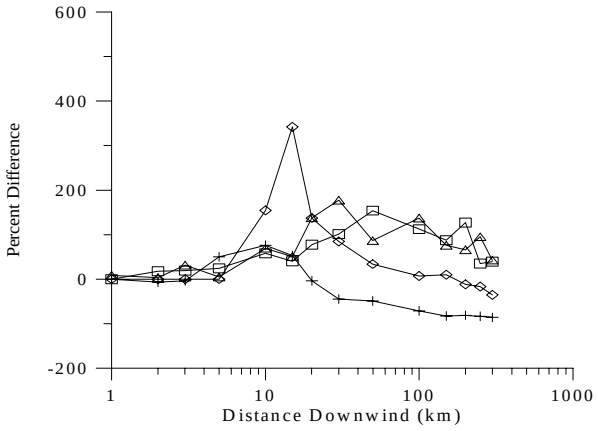

Figure L-6(e). Pittsburgh meteorological data.

Slug vs ISC3

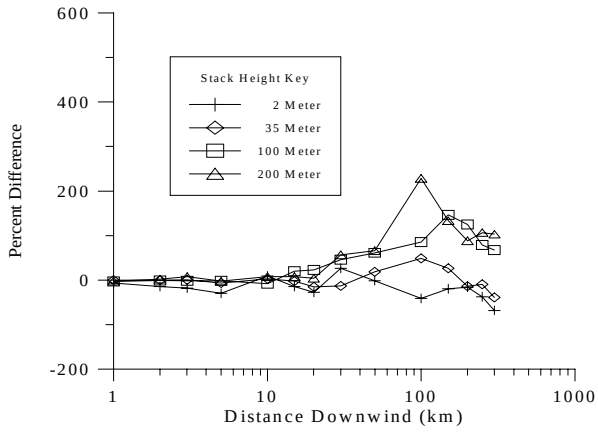

Figure L-6(b). Boise meteorological data.

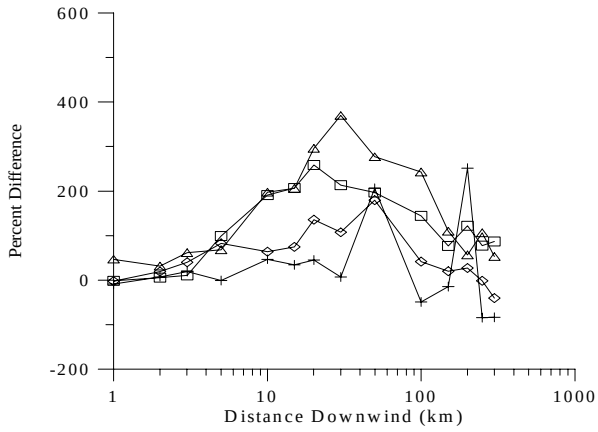

Figure L-6(d). Medford meteorological data.

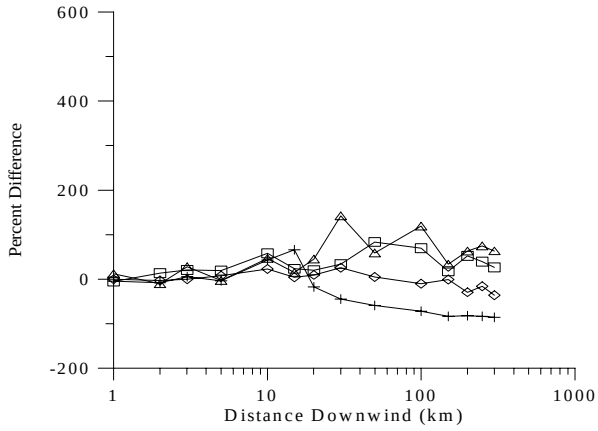

Figure L-6(f). Pittsburgh meteorological data.

Figure L-6. Highest of the second highest 3-hour average concentrations by distance. Figures a, c, & e show CALPUFF *puffs*, whereas figures b, d, & f show *slugs*.
Note: $\%\ Difference \quad 100\ (\frac{\chi_{CALPUFF} - \chi_{ISC3}}{\chi_{ISC3}})$.

Puff vs. ISC3

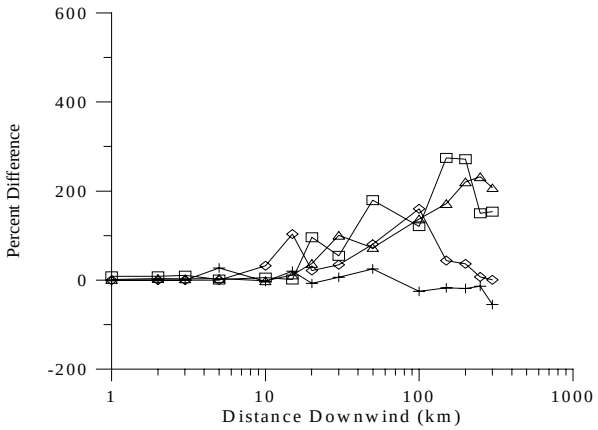

Figure L-7(a). Boise meteorological data.

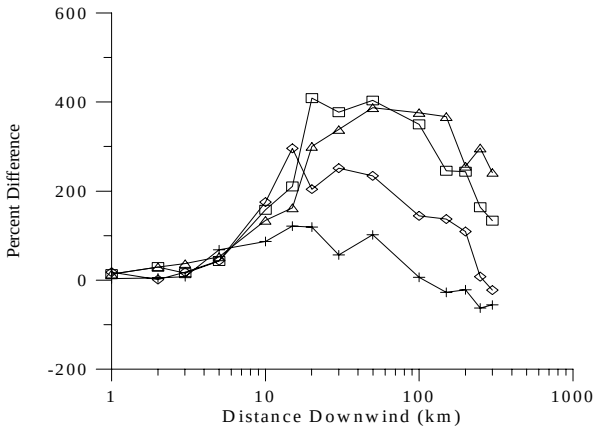

Figure L-7(c). Medford meteorological data.

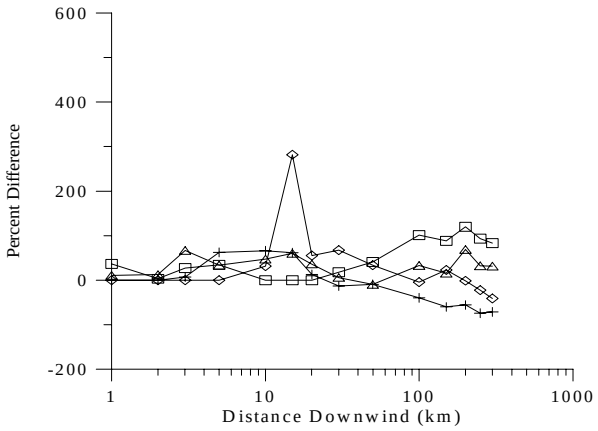

Figure L-7(e). Pittsburgh meteorological data.

Slug vs. ISC3

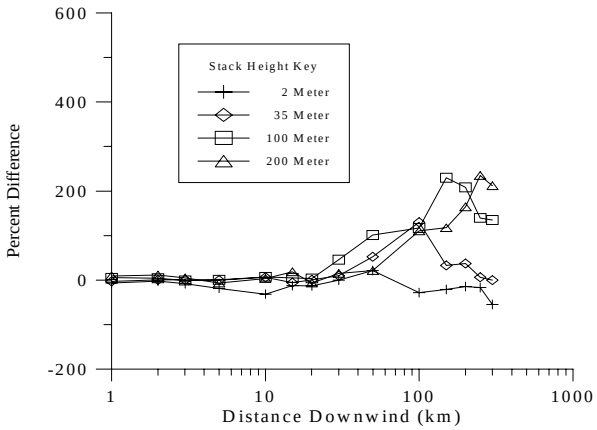

Figure L-7(b). Boise meteorological data.

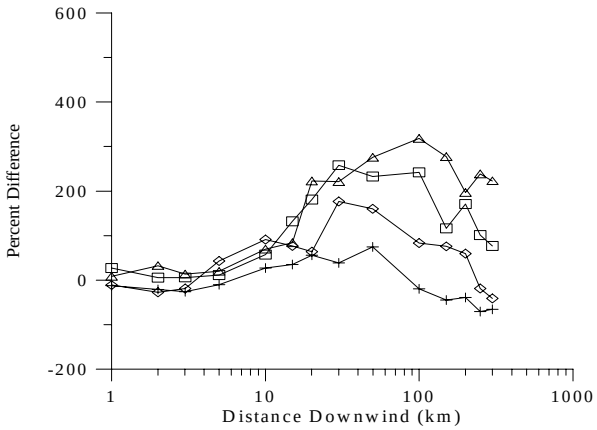

Figure L-7(d). Medford meteorological data.

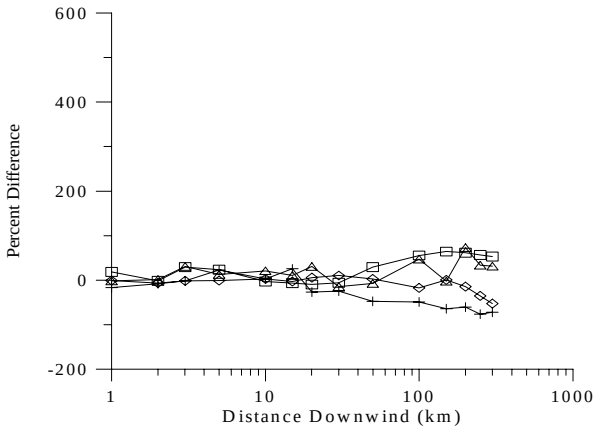

Figure L-7(f). Pittsburgh meteorological data.

Figure L-7. Highest of the second highest 24-hour average concentrations by distance. Figures a, c, & e show CALPUFF *puffs*, whereas figures b, d, & f show *slugs*. Note: $\%\ Difference \quad 100\ (\frac{\chi_{CALPUFF} - \chi_{ISC3}}{\chi_{ISC3}})$.

TECHNICAL REPORT DATA

(Please read Instructions on reverse before completing)

1. REPORT NO.	2.	3. RECIPIENT'S ACCESSION NO.
EPA-454/R-98-020		

4. TITLE AND SUBTITLE	5. REPORT DATE
A Comparison of CALPUFF with ISC3	December 1998
	6. PERFORMING ORGANIZATION CODE

7. AUTHOR(S)	8. PERFORMING ORGANIZATION REPORT NO.
C. Thomas Coulter & Peter A. Eckhoff	

9. PERFORMING ORGANIZATION NAME AND ADDRESS	10. PROGRAM ELEMENT NO.
U.S. Environmental Protection Agency Office of Air Quality Planning and Standards Emissions, Monitoring, and Analysis Division Research Triangle Park, NC 27711	11. CONTRACT/GRANT NO.

12. SPONSORING AGENCY NAME AND ADDRESS	13. TYPE OF REPORT AND PERIOD COVERED
	14. SPONSORING AGENCY CODE

15. SUPPLEMENTARY NOTES

16. ABSTRACT

We examined CALPUFF for equivalency to ISC3, both in a steady-state mode, as well as non-steady-state (i.e., meteorological conditions were allowed to vary hourly). For 4 standard point sources, an array of persistent "screening" meteorological conditions and all 6 P-G categories, we completed 432 CALPUFF runs (216 for Z_i = 3000m; 216 for Z_i = 500m to assess reflection) and 108 ISC3 runs (54 for Z_i = 3000m; 54 for Z_i = 500m) for receptors out to 100km. Using a simple custom FORTRAN postprocessor, we analyzed paired residuals in a systematic way to characterize the two models' equivalence. Results were reduced and expressed in a tabular form. CALPUFF was seen to mimic ISC3 to a substantial degree. In non-steady state conditions, we ran CALPUFF and ISC3 to estimate impacts from standard point sources and results compared using meteorological data from Boise, ID, Medford, OR, and Pittsburgh, PA. Occurrences of calms and recirculations resulted in higher source impacts with CALPUFF than for ISC3 for most comparisons made.

17. KEY WORDS AND DOCUMENT ANALYSIS

a. DESCRIPTORS	b. IDENTIFIERS/OPEN ENDED TERMS	c. COSATI Field/Group
Air Pollution Atmospheric Dispersion Modeling		

18. DISTRIBUTION STATEMENT	19. SECURITY CLASS *(Report)*	21. NO. OF PAGES
Release Unlimited	Unclassified	21 (+ 12 apps.)
	20. SECURITY CLASS *(Page)*	22. PRICE
	Unclassified	

JOURNAL OF GEOPHYSICAL RESEARCH, VOL. 108, NO. D11, 4343, doi:10.1029/2002JD002943, 2003

Atmospheric budget implications of the temporal and spatial trends in methyl bromide concentration

Claire E. Reeves

School of Environmental Sciences, University of East Anglia, Norwich, UK

Received 13 September 2002; revised 14 February 2003; accepted 5 March 2003; published 11 June 2003.

[1] Methyl bromide (CH_3Br) is an important ozone-depleting gas for which 20th century trends of the atmospheric concentration have recently been derived from air trapped in Antarctic firn. In this paper, a two-dimensional (2-D) global model, with a coupled atmosphere and ocean, is used to examine this historical trend, analyzing its implication for the various source strengths and the lifetime of CH_3Br. The results illustrate that not only is the current understanding of the present-day atmospheric budget of CH_3Br incomplete but so too is our understanding of the budget of CH_3Br prior to major industrial emissions and anthropogenic changes to it. This difference cannot be explained by the overall error in the model results as determined from the uncertainties in the major source and sink terms. Either the estimate of the sink strength is too large or there is an underestimate of a known ''nonindustrial'' source or an unaccounted ''nonindustrial'' source, or some combination of these. Further, the results imply that the increase in the ''anthropogenically influenced'' sources during the 20th century is underestimated or that the sink strength is too strong. Since this applies to both before and after 1950, this suggests that the increase in nonfumigant sources and possibly fumigant sources is underestimated, assuming the sinks not to be overestimated. A longer lifetime has the effect of not only increasing the absolute concentrations but also increasing the rate of growth in concentrations and thus improving the agreement with the firn data. The sensitivity of the results to the uncertainties in the individual source and sink terms is assessed. The budget is also examined in terms of the properties of an artificial source necessary to provide balance. Other data sets of observed CH_3Br concentration are also used to evaluate the modeled source and sink scenarios in terms of seasonal and latitudinal variations. *INDEX TERMS:* 0312 Atmospheric Composition and Structure: Air/sea constituent fluxes (3339, 4504); 0315 Atmospheric Composition and Structure: Biosphere/atmosphere interactions; 0322 Atmospheric Composition and Structure: Constituent sources and sinks; 1610 Global Change: Atmosphere (0315, 0325); *KEYWORDS:* methyl bromide, atmospheric budget, long-term trends, natural and anthropogenic sources, atmospheric lifetime

Citation: Reeves, C. E., Atmospheric budget implications of the temporal and spatial trends in methyl bromide concentration, *J. Geophys. Res.*, *108*(D11), 4343, doi:10.1029/2002JD002943, 2003.

1. Introduction

[2] With a mean, global, background, tropospheric concentration of 10 pptv [e.g., *Schauffler et al.*, 1998; *Kurylo et al.*, 1999], methyl bromide (CH_3Br) makes the largest single contribution to stratospheric bromine. When considered as equivalent chlorine this amounts to a loading of 580 pptv: 13% of the total equivalent tropospheric chlorine loading [*Pyle et al.*, 1999]. However, unlike many of the other ozone-depleting gases (e.g., chlorofluorocarbons and hydrochlorofluorocarbons), CH_3Br has both natural and anthropogenic sources. Furthermore, the strengths of these sources, along with the sinks of CH_3Br, are relatively poorly quantified, such that the present-day atmospheric budget of CH_3Br, based on current understanding, does not balance [*Kurylo et al.*, 1999; *Pyle et al.*, 1999].

0148-0227/03/2002JD002943$09.00

[3] Recently 20th century trends of the atmospheric concentration of CH_3Br have been derived from air trapped in Antarctic firn (unconsolidated snow) [*Butler et al.*, 1999; *Sturges et al.*, 2001a]. These data are extremely important as they indicate the concentrations that existed prior to major, known, industrial production of CH_3Br, which can be used to ascertain the nonindustrial budget of CH_3Br. Furthermore, the increase in concentration over the last century can be used to quantify the anthropogenic contribution to the budget. The main objective of this paper is to use a two-dimensional (2-D) (latitude versus altitude) global model, with a coupled atmosphere and ocean, to examine this historical trend, analysing its implication for the various source strengths and lifetime of CH_3Br.

[4] The major known sources of CH_3Br are fumigation, mostly in the agricultural industry, exhaust emissions from automobiles combusting leaded fuel, biomass burning, the oceans and coastal salt marshes. The first two sources

clearly have anthropogenic origins. However, biomass burning is very often anthropogenically induced. Therefore in this paper the term "nonindustrial" refers to the ocean, coastal salt marshes and biomass burning, the term "industrial" refers to fumigation and automobile exhausts, while the term "anthropogenically influenced" sources refers to fumigation, automobile exhausts and biomass burning.

2. Model

[5] The model is described below largely in terms of how each source and sink of CH_3Br is prescribed in the base case model run.

2.1. Physical Description

[6] The atmospheric component is basically the same as in our previous study of CH_3Br [*Reeves and Penkett*, 1993] and in studies of other halocarbons [*Oram et al.*, 1995, 1996]. The atmospheric grid is divided into 18 equal area, zonally averaged bands and has 6 vertical layers each 2.5 km in height. Seasonally varying advective and diffusive transport is simulated using the mean meridional circulation of *Newel et al.* [1972] and eddy diffusion coefficients of *Louis* [1975]. The ocean is treated as a single layer with 18 boxes each linked to the overlying box of the lowest layer of the atmospheric component, but with no transport between adjacent ocean boxes.

2.2. Atmospheric in situ Losses

[7] The hydroxyl radical (OH) field employed, with an average tropospheric concentration of $6.5(+3/-2) \times 10^5$ molecules cm^{-3}, is that derived by *Volz et al.* [1981], based on ^{14}CO measurements. Using a temperature-dependent rate constant calculated from the expression $4.0 \times 10^{-12}\exp(-1470/T)$ [*DeMore et al.*, 1997] the lifetime for CH_3Br within the model domain with respect to reaction with OH (τ_{OH}) is 1.84 yr (Table 1). The model also includes a sink through the upper boundary to simulate stratospheric loss. The gradient across this boundary is defined to give a diffusive loss from the model domain equivalent to a lifetime of 31.5 yr (τ_{STRAT}) in agreement with that of *Kurylo et al.* [1999]. The OH concentrations vary seasonally, but they are assumed to have no long-term trend, unlike that recently proposed by *Prinn et al.* [2001].

2.3. Soil Sink

[8] The deposition velocities for each of the 18 zonally averaged bands in the model were assigned according to the amount of each type of land cover in each band and deposition velocities assumed for each type of land cover. One degree land cover data, divided into 11 classes, were obtained from the Advanced Very High Resolution Radiometer (AVHRR) [*Defries and Townshend*, 1994] and for each class a deposition velocity was assumed based on those reported by *Shorter et al.* [1995], *Serca et al.* [1998], and *Varner et al.* [1999a]. This gives a global average deposition velocity of 0.011 cm s^{-1} with a latitudinal distribution as shown in Figure 1. The global average value is reduced slightly when seasonality is considered as no deposition is assumed to frozen land. The land is assumed to be frozen for 6 months of the year at high latitudes (bands 1 and 18: 63°–90°) and for 4 months for latitudes between 51° and 63° (bands 2 and 17). The soil sink was assumed to have no historical trend.

Table 1. Modeled Atmospheric Lifetimes

Lifetime	Years
τ_{OH}	1.84
τ_{STRAT}	31.5
τ_{SOIL}	2.47
τ_{OCEAN}	1.75
τ_{ATM}	0.64
τ_{ATM} (O1a, τ_{OCEAN} increased to 2.33 yr)	0.71
τ_{ATM} (O1b, τ_{OCEAN} decreased to 1.58 yr)	0.62
τ_{ATM} (S1, τ_{SOIL} decreased to 1.00 yr)	0.47
τ_{ATM} (S2, τ_{SOIL} increased to 3.54 yr)	0.70
τ_{ATM} (OH1, τ_{OH} increased to 2.45 yr)	0.71
τ_{ATM} (OH2, τ_{OH} decreased to 1.47 yr)	0.59
τ_{ATM} (L, no soil nor stratospheric sinks and τ_{OH} increased to 2.45 yr)	1.02

[9] *Shorter et al.* [1995] calculated a lifetime of atmospheric CH_3Br with respect to deposition to soil (τ_{SOIL}) of 3.4 yr, equivalent to a sink strength of 42 ± 32 Gg yr^{-1}. *Serca et al.* [1998] obtained similar deposition velocities to *Shorter et al.* [1995] for temperate woods shrubland and grassland, but larger deposition velocities for agricultural lands and bogs. *Varner et al.* [1999a] updated the work of *Shorter et al.* [1995] by examining a far greater range of agricultural soils and increased their estimated deposition velocity by a factor of three, but their new estimate of this deposition velocity was still only approximately 10% of the value derived by *Serca et al.* [1998]. *Serca et al.* [1998] calculated a total sink strength of 143 ± 70 Gg yr^{-1}, but noted that the largest discrepancy between their evaluation and that of *Shorter et al.* [1995] was the biome area estimates. Using mean deposition velocities from the 2 studies (except bog) *Serca et al.* [1998] estimated a flux of 94 ± 54 Gg yr^{-1} using their biome areas equivalent to a lifetime of 0.97–3.54 yr. The current model's atmospheric lifetime with respect to soil loss is 2.47 yr (τ_{SOIL}, Table 1) and is in agreement with those of *Shorter et al.* [1995] and *Serca et al.* [1998], given the uncertainties.

2.4. Fumigation

[10] Much information on the recent temporal trend and geographical distribution of CH_3Br use was obtained from *Methyl Bromide Technical Options Committee* (*MBTOC*) [1998]. This provided data on the total annual amount of CH_3Br used in the years 1984 to 1996. The 1984–1996 data showed that the usage was divided into 4 categories: preplanting (73%); postharvesting (21%) (13% durables and 8% perishables); structural (3%); and chemical intermediates (3%). No CH_3Br from the latter use is emitted into the atmosphere. The latitudinal distribution of these sources was based on the national data provided by *Thomas* [1999] (available at http://www.epa.gov/ozone/mbr/background.html) and M. Miller (personal communication, 2002) (Figure 1).

[11] Information on the usage of CH_3Br prior to 1984 is not very quantitative. The insecticide properties of CH_3Br were discovered in 1930 [*Le Goupil*, 1930] with early scientific papers discussing postharvesting use for flowers and apples published in 1937–39 [*Monro*, 1979; and references therein]. It was therefore assumed that postharvesting

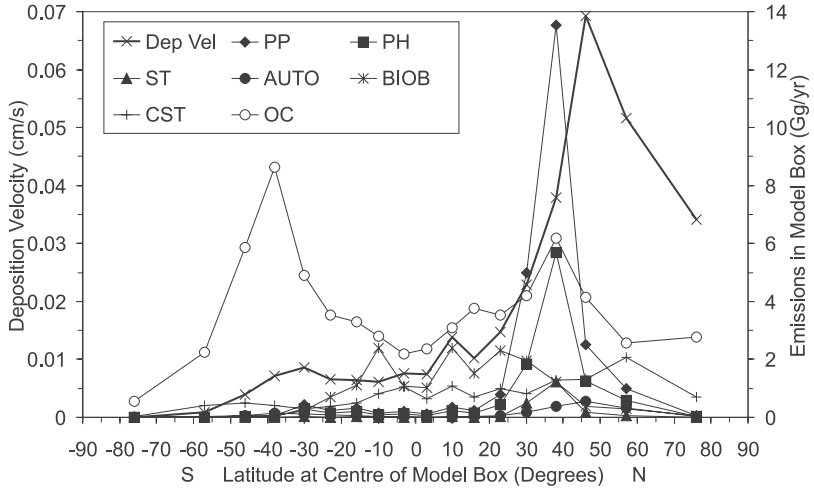

Figure 1. The CH_3Br deposition velocities and strengths of individual sources assigned to each model box. These distributions were held constant with time except for the automobile source (see text). The sources are designated as PP, preplanting fumigation; PH, postharvesting fumigation; ST, structural fumigation; AUTO, automobiles; BIOB, biomass burning; CST, coastal salt marshes; OC, ocean emission.

usage started in 1937. Usage then spread to grain and by 1944–47 fumigation of shipping containers and factories were mentioned in scientific papers. It was therefore assumed that structural usage began in 1945 and that both the postharvesting and structural usages rose exponentially at 10% yr^{-1} until they reached their 1984 values (Figure 2). Preplanting fumigation of strawberries began in 1961 and by 1965 almost all strawberries grown in California had been fumigated in this way, using about 1 Gg that year [*Wilhelm and Paulus*, 1980]. In 1972, machinery had been developed for application and tarping leading to use over an increased acreage. Also the use had spread to other cultivars. It was therefore assumed that preplanting usage of CH_3Br began in 1961 and rose exponentially at 20% yr^{-1} until it reached the 1984 values (Figure 2). Consumption of CH_3Br for 1998 is estimated on the basis of consumption data officially reported by Parties to the Ozone Secretariat (M. Miller, personal communication, 2002) and for 1997 is interpolated between the data for 1996 and 1998. The Montreal Protocol regulations state that for developed countries, usage in 1995 should have been frozen at 1991 levels and by 1999 usage should be cut by 25%. Therefore for 1999 a cut of 25% from 1991 usage is assumed in the preplanting for North America and Europe with no change in the rest of the world. For postharvesting and structural uses, 1999 usage is assumed to be the same as 1998, since much of this will be exempt as quarantine and preshipment uses.

[12] Although the usage rates of CH_3Br are quite well quantified, at least for recent years, there is a large uncertainty in the actual emission rates. *Kurylo et al.* [1999] quote emission factors of 50% (30–90%) for preplanting, 51–88% for durables, 85–95% for perishables and 100% for structural uses. On the basis of the fraction of postharvesting use that is for durables and perishables, it was

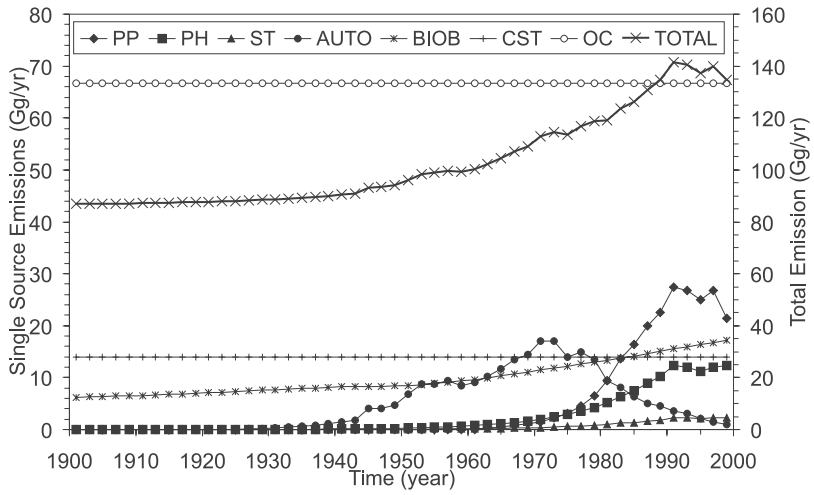

Figure 2. The historical trends assigned to the strengths of individual sources of CH_3Br in the base case. Abbreviations are the same as Figure 1. The trend in total emissions from all these sources is plotted against the right hand axis.

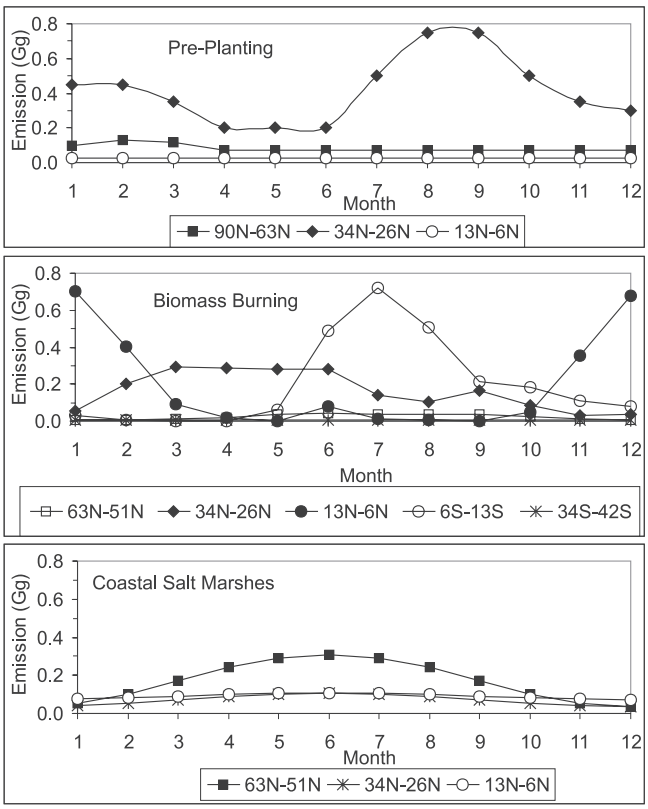

Figure 3. The seasonal variation assigned to the strengths of individual sources of CH_3Br shown as amount emitted each month into the specified latitudinal box. The latitudinal boxes have been selected to illustrate the change in seasonal variation with latitude. For preplanting and coastal salt marshes no boxes in the Southern Hemisphere are shown since their seasonal variations mirror those in boxes of equivalent latitude in the Northern Hemisphere. The boxes are described by their latitudinal extent given in degrees.

assumed that for postharvesting the emission factor was 78%. 50% was adopted for the preplanting and 100% for the structural.

[13] Little quantitative information is available about the seasonality in the use of CH_3Br in fumigation. On the basis of information from EPA (W. B. Thomas, personal communication, 2000) and *Lee-Taylor et al.* [1998], preplanting was given a late winter/early spring maximum at high latitudes, a late summer/autumn max with a secondary spring peak in midlatitudes and no seasonality in the tropics (Figure 3). This is based on the assumption that a single planting occurs in the high latitudes, while for midlatitudes it is assumed that a second planting occurs later in the growing season and for the tropics planting can occur all year-round. No seasonality was given to postharvesting or structural uses.

2.5. Automobiles

[14] Data are available on the historical bromine (Br in the form of ethylene dibromide (EDB)) usage in gasoline between 1925 and 1995 by hemisphere [*Thomas et al.*, 1997]. After 1995 it was assumed that the EDB usage in the Northern Hemisphere continued to decline at a similar rate to previous years, while in the Southern Hemisphere its decline leveled off. The latter assumption is based on measurements of EDB in Antarctic firn air (W. T. Sturges, personal communication, 2001). Within each hemisphere the latitudinal distribution of the automobile emission was based on that used for anthropogenic/industrial sources by *Hough* [1989, 1991]. It should be noted that in Figure 1 the distribution for the automobile emission shown is that for 1995. The interhemispheric ratio and hence latitudinal distribution of the automobile source changes with time, with the Southern Hemisphere accounting for only 5–10% of the global emissions prior to the early 1980s, after which it increases up to 50% as the northern hemispheric emissions rapidly drop. The distribution within each hemisphere was assumed to be constant with time.

[15] There is much debate concerning the amount of EDB that is emitted as CH_3Br. *Hao* [1986] quotes 0.1%, *Baumann and Heumann* [1987] 15–25%, *Baker et al.* [1998] 7.5%, *Chen et al.* [1999] 10% and *Bertram and Kolowich* [2000] 2.4%. Furthermore, it is possible that the emission factor has changed over time with changing fuel composition, engines and operating conditions. A constant emission factor of 10% was adopted for this study.

2.6. Biomass Burning

[16] The biomass burning source strength and geographical distribution of CH_3Br emissions was based on the data for methyl chloride (CH_3Cl) as derived by *Lobert et al.* [1999] as part of the Reactive Chlorine Emission Inventory. *Lobert et al.* [1999] estimate that their data are reliable to within a factor of 2 or 3. The CH_3Br:CH_3Cl emission ratio is approximately 1% (molecule/molecule), although there is evidence for it being slightly higher in boreal forests compared to savannas and tropical forests [*Manö and Andreae*, 1994; *Andreae et al.*, 1996; *Blake et al.*, 1996]. A value of 1% is adopted in this current study, which gives a source strength of 17 Gg yr^{-1}. This is within the uncertainty quoted by other studies (10–50 Gg yr^{-1} [*Manö and Andreae*, 1994], 14–24 Gg yr^{-1} [*Blake et al.*, 1996], 20 Gg yr^{-1} [*Andreae et al.*, 1996] and 20 (10–40) Gg yr^{-1} [*Kurylo et al.*, 1999]). It was assumed that this source strength applied to 1999 and that 10% of this biomass burning was natural and that the remaining anthropogenic portion (90%) was a linear function of the global population [*United Nations*, 1999] (available at http://www.undp.org/popin/wdtrends/p98/p98.htm) as suggested by *Lobert et al.* [1999]. This gives an emission strength of 6.22 Gg yr^{-1} in 1900, 36% of that in 1999 (Figure 2).

[17] The seasonality in the biomass burning source of CH_3Br was taken to be that determined for black carbon biomass burning emissions by the Global Emissions Inventory Activity (http://weather.engin.umich.edu/geia/). This is a combination of a modified version of *Hao et al.* [1991] and some assumptions for extra-tropical forest fires. In addition satellite observations were used to modify the seasonality of vegetation fires in Africa [*Cooke et al.*, 1996]. The latitudinal and seasonal trends in CH_3Br emissions from biomass burning adopted in the model are shown in Figures 1 and 3.

2.7. Coastal Salt Marshes

[18] *Rhew et al.* [2000] calculated a global net flux of 14 (7–29) Gg yr^{-1} from coastal salt marshes based on an area

of 0.38×10^{12} m^2 [*Woodwell et al.*, 1973]. There is an uncertainty of greater than 50% in this area estimate. A source of 14 Gg yr^{-1} was included in the model and was distributed according to the fraction of global coastal area in each latitude band, which was derived assuming an equal width band along all coast lines, except that covered by ice [*Baker et al.*, 2001]. *Rhew et al.* [2000] found a maximum in this source during the growing season, which for this study is assumed to be April to August with a maximum in June in the Northern Hemisphere and October to February with a maximum in December in the Southern Hemisphere. It was also assumed that the amplitude of this seasonal variation reduced toward the equator. No historical trend was given to this coastal source. The latitudinal and seasonal trends in CH_3Br emissions from coastal regions adopted in the model are shown in Figures 1 and 3. It should be noted that the flux reported by *Rhew et al.* [2000] is a net flux. The coastal source included in the model is a gross flux since the soil sink is treated as a separate loss. This may lead to an underestimate of the strength of this source in the model.

2.8. Ocean

[19] The coupling between each ocean box and its overlying atmospheric box was set up as defined by *Butler* [1994] for his simple 2-box model, with the fractional area of each model box occupied by ocean surface taken from *Gross* [1972]. The transfer velocity required for parameterization of the rate of air-sea exchange was calculated as a function of wind speed. Wind speeds, including latitudinal and seasonal variations, were taken from the Oregon State University/Climatic Research Institute (OSU/CRI) global monthly data sets (DS209.0) via the National Center for Atmospheric Research Data Support Section (NCAR DSS). Since these are climatological wind fields and the transfer velocity is nonlinear with respect to wind speed, the relationship that *Wanninkhof* [1992] derived for long-term winds was used. The Schmidt number for CH_3Br is required to convert the transfer velocity from that for CO_2 to one for CH_3Br. This was calculated from the diffusivity of CH_3Br [*De Bruyn and Saltzman*, 1997] and the kinematic viscosity, derived from the viscosities of pure water [*Korson et al.*, 1969] and seawater [*Millero*, 1974]. Eddy diffusion loss downward out of the ocean layer was calculated using latitudinally varying vertical mixing coefficients and mixed layer depths from *Li et al.* [1984].

[20] Sea surface temperatures, including latitudinal and seasonal variations, were acquired from OSU/CRI global monthly data sets (DS209.0). These are required to calculate the solubility of CH_3Br, which was done using the expression determined by *Elliott and Rowland* [1993]. Furthermore, the rates of loss of CH_3Br from seawater via hydrolysis and chloride ion substitution were calculated using expressions from *Moelwyn-Hughes* [1938] and *Elliott and Rowland* [1993] respectively, both of which processes are temperature dependent. *King and Saltzman* [1997] first observed biological degradation of CH_3Br in tropical waters at a rate of 0.10 day^{-1}. *Tokarczyk and Saltzman* [2001] and *Tokarczyk et al.* [2001] have since measured this biological degradation in waters between 8° and 58°N and found it to exhibit no relationship to seawater temperature or latitude. *Tokarczyk and Saltzman* [2001] observed mean rates of 0.11, 0.03 and 0.04 day^{-1} during the 3 legs of their cruise, while *Tokarczyk et al.* [2001] observed rates ranging from 0.01 to 0.20 day^{-1}. For the current study a constant rate of 0.05 day^{-1} was used.

[21] CH_3Br has been observed to be produced in marine phytoplankton cultures [*Moore et al.*, 1996; *Sæmundsdóttir and Matrai*, 1998; *Scarrat and Moore*, 1998] and its concentration in seawater has been found to correlate with various pigments and phytoplankton species [*Moore and Webb*, 1996; *Baker et al.*, 1999]. However, since the in situ oceanic production rates are poorly known, a model run was performed in which the observed 1990s atmospheric concentrations and saturation anomalies were used to constrain the model such that production rates could be calculated. The saturation anomalies were set in the model according to the relationship with sea surface temperature (SST) defined by *King et al.* [2000] based on the anomalies observed by *Lobert et al.* [1995, 1996, 1997], *Groszko and Moore* [1998] and *King et al.* [2000]. This created both a latitudinal and seasonal variation in the saturation anomalies (Figure 4) with a global annual average of −11%. The amplitude of the seasonal variation maximizes in midlatitudes and, because the relationship with SST gives a maximum saturation anomaly at 16°C, the months at which the maximum and minimum occur are not the same for each latitude band. The atmospheric concentrations were varied latitudinally on the basis of *Lobert et al.* [1995], *Wingenter et al.* [1998], and *Kurylo et al.* [1999] such that the average northern hemispheric concentration was 10.7 ppt and the average southern hemispheric concentration was 8.4 ppt. No seasonal variation was given to the atmospheric concentrations; these varied far less than the saturation anomaly and for this purpose could be neglected.

[22] Under these conditions the model gives a net flux of −15 Gg yr^{-1} (i.e., 15 Gg yr^{-1} from the atmosphere to the ocean), which is in the ranges quoted by *King et al.* [2000] (−11 to −20 Gg yr^{-1}) and *Kurylo et al.* [1999] (−3 to −32 Gg yr^{-1}). The average production rate calculated by the model is 9.2×10^{-4} g m^{-2} yr^{-1}. The seasonality in this production rate was similar to that of the saturation, but slightly moderated by the variability in the chemical losses, which strongly increases with seawater temperature. It is this temperature effect that gives rise to the largest average production rates in the warm tropical waters (Figure 4) despite the larger saturation anomalies at midlatitudes. The latitudinal variation in the oceanic production is similar to that calculated by *Lee-Taylor et al.* [1998]. The calculated production rates were then used as input data for all subsequent model runs with the atmospheric concentrations and saturation anomalies as free variables.

[23] The emission rate is simply the CH_3Br that is produced in situ in the ocean, which is emitted into the atmosphere and not lost by in situ loss or diffusion down through the mixed layer. It is therefore independent of the atmospheric concentrations and, since the oceanic production rate is assumed to be constant from year to year, so is the emission rate (Figure 2). The uptake is defined as the flux of CH_3Br from the atmosphere to the ocean mixed layer that is then lost by oceanic removal processes. It will therefore increase with increasing atmospheric concentrations. Consequently, the net flux, which is equal to the emission minus the uptake, will decrease with increasing

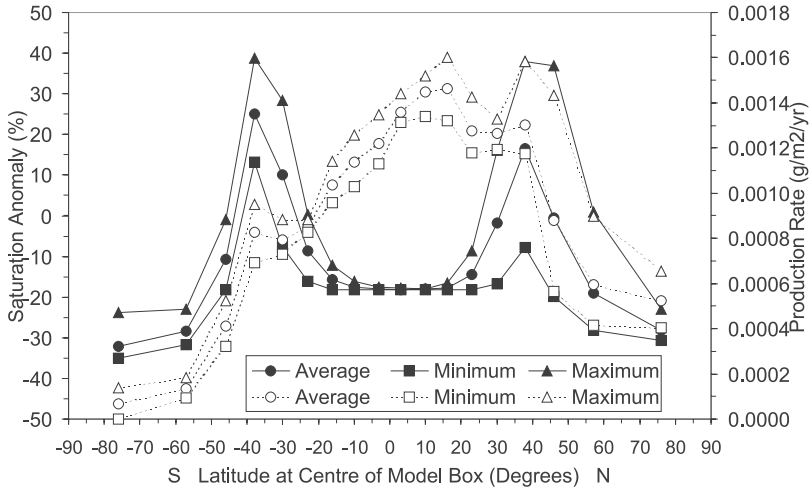

Figure 4. The latitudinal variation in the average and seasonal maximum and minimum CH_3Br saturation anomalies (solid lines and filled symbols) and the calculated oceanic production rates (dashed lines and open symbols) assigned to each oceanic model box.

atmospheric concentrations in this model. Effectively the oceanic production rates were calculated to give an emission rate that would balance the uptake plus the net flux for 1990s conditions. The latitudinal variation in the oceanic emission is shown in Figure 1. Despite below-average production rates, the maximum values occur in southern midlatitudes, because the ocean makes up over 90% of the area of these model boxes and the highest wind speeds are found here, while the chemical loss is greatest in the warmer tropical waters.

[24] The uptake for 1990s atmospheric conditions was calculated to be 81 Gg yr^{-1}, which is in reasonable agreement with the estimate of 77 Gg yr^{-1} by *Yvon-Lewis and Butler* [1997] and well within the uncertainty from the biological loss rate (see section 7.1). The model atmospheric lifetime with respect to oceanic loss (τ_{OCEAN}) is 1.75 yr, again in agreement with that determined by *Yvon-Lewis and Butler* [1997] (1.85 yr with a range of 1.1–3.9 yr), given the affect of the uncertainties in the biological loss term (Table 1). Despite the calculated uptakes being similar between the two studies, the emission rate of 67 Gg yr^{-1} in the present study is larger than the value of 56 Gg yr^{-1} given by *Yvon-Lewis and Butler* [1997], since they used the larger net flux of -21 Gg yr^{-1} to calculate their emission rate. However, given the uncertainties in the biological loss rate, and the saturation anomalies used to constrain the net flux, this difference in emission rate is not significant (see section 7.1).

3. Model Runs

[25] The model base case run was with the model set up as described above. Various runs were also performed involving modifications to individual source and sink terms as indicated in Table 2. Most of these runs were to examine the sensitivity of the results to uncertainties in individual source and sink terms. More details of these modifications are presented below, along side the results. Further, by considering these runs together, the overall uncertainty in the results was assessed.

[26] Additional runs were also performed in which an artificial source was added to the model to examine how the budget imbalance could be rectified (Ar) (Table 2). Again the details of these runs are given when the results are discussed.

4. Model Evaluation and Error Analysis

[27] The transport in the model has previously been evaluated by comparison of observed and calculated concentrations of CFCs, which have no tropospheric sinks and well known emissions, mostly in northern midlatitudes. The model reproduces the observed concentrations at Cape Grim, Tasmania (42°S) [*Derwent and Volz-Thomas*, 1990], which suggests that the timescale for transport from the surface at northern midlatitudes to the surface at southern midlatitudes is well simulated. *Derwent and Volz-Thomas* [1990] concluded that the transport scheme adequately represented the gross features of halocarbon transport. However, on close inspection the model slightly underestimated concentrations of CFC-11 as measured by the Atmospheric Lifetime Experiment (ALE) at Ragged Point, Barbados (13°N). The model has been rerun for CFC-11 and compared to more recent data from the ALE/Global Atmospheric Gases Experiment (GAGE)/Advanced GAGE network [*Prinn et al.*, 2000], but again similar results were found. Interhemispheric exchange in the model occurs via the meridional circulation that lifts halocarbon-laden air from the lower troposphere of the Northern Hemisphere upward and over the tropical region at altitude before depositing it at midlatitudes in the Southern Hemisphere [*Derwent and Eggleton*, 1978]. The above results perhaps suggest that the low-altitude transport between the northern midlatitudes and northern tropics of the model is too slow, but is compensated for by enhanced upper level transport between the Northern and Southern Hemispheres.

[28] To evaluate the model OH field, the model was run for methyl chloroform (CH_3CCl_3). Using a rate calculated from the expression $1.8 \times 10^{-12}\exp(-1550/T)$ [*DeMore et*

al., 1997] and a stratospheric lifetime of 45 yr [*Ko et al.*, 1994] the model gave a lifetime of 5.1 yr. Including a partial atmospheric lifetime of 85 yr for oceanic removal of CH_3CCl_3 would give an overall lifetime of 4.8 yr, which agrees well with the estimate derived from the ALE-GAGE CH_3CCl_3 observations [*Prinn et al.*, 1995].

[29] To give an estimate of the overall error in the results presented, the runs in which the major source and sink terms were individually set at their upper and lower estimated uncertainty ranges were considered together. The results presented are primarily the absolute concentration in surface air above the Antarctic throughout the 20th century, the change in this concentration over the periods 1904 to 1950 and 1950 to 1995, and the hemispheric averages and interhemispheric ratio (IHR) in 1995. The upper and lower ranges of these values were determined by calculating the root mean square (RMS) value for all runs that increased and decreased these values, respectively. These ranges are presented below in the discussion of the base case. They are large as they consider the often substantial uncertainties in the automobile emission factor (A1, A2), fumigation emission factor (F1, F2), coastal salt marsh source strength (C1, C2), biomass burning source strength (B1, B2) and historical trend (B3, B4), ocean saturation used to determine the oceanic productivity (O3a, O3b), oceanic biological loss (O1a, O1b), loss due to reaction with OH (OH1, OH2) and soil sink strength (S1, S2).

5. Results

[30] The hemispheric average concentrations and interhemispheric ratio (N/S) (IHR) for each model run for the years 1920, 1950, 1975 and 1995 are given in Table 3. Table 4 gives the changes in concentration during the first and second halves of the century for the southerly most surface model box (63°S to 90°S).

6. Base Case: Best Estimate and Uncertainty

[31] The base case run represents the best estimates of the major known individual source and sink terms. The sum of the sources for 1995 (137 Gg yr^{-1}) is in excellent agreement with that determined by *Yvon-Lewis and Butler* [1997]. The model atmospheric lifetime (τ_{ATM}) of 0.64 yr is in reasonable agreement with the value of 0.7 determined by *Yvon-Lewis and Butler* [1997]. The discrepancy is largely due to the different values for τ_{SOILS} ($\approx$3 yr compared to 2.47 yr in the current study), which is well within the uncertainty for this sink strength.

[32] The calculated northern and southern hemispheric averages of 6.6 (4.2–8.6) and 5.4 (3.7–6.8) ppt (RMS ranges in brackets) in 1995 (Table 3) are both below the values of around 10–12 and 8–9 ppt indicated by observations [*Lobert et al.*, 1995, 1997; *Wingenter et al.*, 1998; *Yokouchi et al.*, 2000], clearly illustrating that the best estimate of the total sink strength far out-weighs that of the total source strength for recent years, as previously reported [e.g., *Kurylo et al.*, 1999]. The annual average IHR of 1.22 (1.06–1.37) is, however, in agreement with the equal area, seasonally weighted, average IHR of 1.21 ± 0.03 derived by *Wingenter et al.* [1998] and within the larger range of 1.3 ± 0.1 quoted by *Kurylo et al.* [1999].

[33] Figure 5 compares the concentration of CH_3Br in the southerly most surface model box with Antarctic concentrations derived from the firn air data [*Butler et al.*, 1999; *Sturges et al.*, 2001a]. The trends obtained from the firn air data suggest that the CH_3Br concentration in Antarctica was about 5–6 ppt in 1940 compared to 8 ppt in the 1990s. It should be noted that the dates given for the firn air equate to the mean age of air extracted from a particular depth within the firn. As the depth increases within the diffusive zone, so the range of ages represented at any particular depth increases such that air with a mean age of 40 yr may actually be made up of air ranging from near present-day to over 100 yr old [*Sturges et al.*, 2001b], depending on the structure of the firn and properties of the molecule concerned. Furthermore the atmospheric trends are calculated from the depth profiles using models that consider the rate of diffusion of the particular molecule through the firn. In Figure 5 scenarios 2, 4 and 5 are plotted from *Sturges et al.* [2001a]. These 3 atmospheric concentration scenarios all fitted the depth profiles quite well, such that it cannot be said with any confidence that any one is better than the others. In fact scenarios 2 and 4 gave almost identical depth profiles [*Sturges et al.*, 2001a] from which it can be deduced that the modeling of these firn profiles is relatively insensitive to the trend before 1940, effectively establishing a limit to the time period represented by these firn data for CH_3Br. The *Butler et al.* [1999] atmospheric historical trend comes from different Antarctic sites, where the diffusive column extended to lower depths allowing older air to be sampled, giving more confidence in the concentrations for the earlier dates. Both *Butler et al.* [1999] and *Sturges et al.* [2001a] report elevated concentrations of CH_3Br in air extracted from the bottom of Arctic firn, suggesting some form of in situ production. Despite no evidence for this in the Antarctic samples, the possibility of production or loss in the firn cannot be eliminated completely.

[34] It is only prior to 1920 that the base case results, and prior to 1940 that the upper RMS values, fall within the large range given by the scenarios of *Sturges et al.* [2001a] (Figure 5a), which as discussed above are relatively insensitive to atmospheric concentrations prior to 1940. The base case severely underestimates by 1.5–2.0 ppt the concentrations prior to 1940 as inferred by *Butler et al.* [1999], which are also above the upper RMS values. This suggests that not only is there an imbalance in the budget for recent years, but an imbalance exists for the early part of the last century, as suggested by *Butler et al.* [1999], and throughout the whole of the century.

[35] The firn air data indicate that the atmospheric concentration of CH_3Br over Antarctica increased by 2 to 3 ppt during the last century with by far the majority of this increase (2.0–2.5 ppt) occurring in the latter half of the century. This equates to a growth rate of around 0.04 to 0.05 ppt yr^{-1} for the second half of the century. Recent analysis of air collected between 1979 and 1998 and stored in the Cape Grim Air Archive [*Langenfelds et al.*, 1996] gives a CH_3Br abundance of 7.9 ppt in 1998 with a trend of 0.03 ppt yr^{-1} [*Miller*, 1998]. *Khalil et al.* [1993] also measured CH_3Br in flask samples collected at Cape Grim between 1983 and 1992, but because of the interannual variability no trend could be discerned. *Butler et al.* [1999] also inferred an increase of about 0.7 ppt prior to 1950 from the firn air data.

Table 2. Emission Strengths for Each Model Run

Run	Comment, Changes From Base Case	Source	1920 Gg yr^{-1}	1950 Gg yr^{-1}	1975 Gg yr^{-1}	1995 Gg yr^{-1}
Base	As described in text	Preplanting	0.0	0.0	3.2	25.0
		Postharvest	0.0	0.3	2.9	11.2
		Structural	0.0	0.1	0.6	2.1
		Automobiles	0.0	6.1	14.0	2.1
		Biomass Burning	7.0	8.3	12.2	16.3
		Coastal	14.0	14.0	14.0	14.0
		Ocean	66.6	66.6	66.6	66.6
		Total[a]	87.6	95.4	113.5	137.3
A1	Emission factor = 25% for automobiles	Automobiles	0.0	15.4	34.9	5.3
		Total[a]	87.6	104.7	134.4	140.5
A2	Emission factor = 0.1% for automobiles	Automobiles	0.0	0.1	0.1	0.0
		Total[a]	87.6	89.4	99.6	135.2
B1	CH_3Br/CH_3Cl = 2% for biomass burning	Biomass Burning	14.1	16.6	24.5	32.7
		Total[a]	94.7	103.7	125.8	153.7
B2	CH_3Br/CH_3Cl = 0.5% for biomass burning	Biomass Burning	3.5	4.1	6.1	8.2
		Total[a]	84.1	91.2	107.4	129.2
B3	No historical trend in biomass burning	Biomass Burning	17.1	17.1	17.1	17.1
		Total[a]	97.7	104.2	118.4	138.1
B4	Zero emission in 1900, increasing with population	Biomass Burning	1.3	3.3	9.4	15.9
		Total[a]	81.9	90.4	110.7	136.9
B5	B1 + B3	Biomass Burning	34.3	34.3	34.3	34.3
		Total[a]	114.9	121.4	135.6	155.3
F1	Emission factor = 90% for preplanting and 91% for postharvesting	Preplanting	0.0	0.0	5.7	45.0
		Postharvest	0.0	0.3	3.4	13.1
		Structural	0.0	0.1	0.6	2.1
		Total[a]	87.6	95.4	116.5	159.2
F2	Emission factor = 30% for preplanting and 64% for postharvesting	Preplanting	0.0	0.0	1.9	15.0
		Postharvest	0.0	0.2	2.4	9.2
		Structural	0.0	0.1	0.6	2.1
		Total[a]	87.6	95.3	111.7	125.3
O1a	Bio. loss = 0.0 day^{-1}, τ_{ATM} = 0.71 yrs, production adjusted	Ocean	42.5	42.5	42.5	42.5
		Total[a]	63.5	71.3	89.4	113.2
O1b	Bio. loss = 0.1 day^{-1}, τ_{ATM} = 0.62 yrs, production adjusted	Ocean	77.8	77.8	77.8	77.8
		Total[a]	98.8	106.6	124.7	148.5
O2a	Saturation Anomaly = -8%, Net Flux = -11 Gg yr^{-1}	Ocean	70.5	70.5	70.5	70.5
		Total[a]	91.5	99.3	117.4	141.2
O2b	Saturation Anomaly = -15%, Net Flux = −20 Gg yr^{-1}	Ocean	61.5	61.5	61.5	61.5
		Total[a]	82.5	90.3	108.4	132.2
O3a	Saturation Anomaly = -2%, Net Flux = -3 Gg yr^{-1}	Ocean	78.3	78.3	78.3	78.3
		Total[a]	99.3	107.1	125.2	149.0
O3b	Saturation Anomaly = -24%, Net Flux = -31 Gg yr^{-1}	Ocean	50.0	50.0	50.0	50.0
		Total[a]	71.0	78.8	96.9	120.7
C1	Coastal source = 29 Gg yr^{-1}	Coastal	29.0	29.0	29.0	29.0
		Total[a]	102.6	110.4	128.5	152.3
C2	Coastal source = 7 Gg yr^{-1}	Coastal	7.0	7.0	7.0	7.0
		Total[a]	80.6	88.4	106.5	130.3
S1	τ_{SOIL} = 1.00 yrs, τ_{ATM} = 0.47 yrs	Total[a]	87.6	95.4	113.5	137.3
S2	τ_{SOIL} = 3.54 yrs, τ_{ATM} = 0.70 yrs	Total[a]	87.6	95.4	113.5	137.3
OH1	τ_{OH} = 2.45 yrs, τ_{ATM} = 0.71 yrs	Total[a]	87.6	95.4	113.5	137.3
OH2	τ_{OH} = 1.47 yrs, τ_{ATM} = 0.59 yrs	Total[a]	87.6	95.4	113.5	137.3
L	No soil nor stratospheric sink, and τ_{OH} increased to 2.45 yr, τ_{ATM} = 1.02 yrs	Total[a]	87.6	95.4	113.5	137.3
LF1	F1 + L, τ_{ATM} = 1.02 yrs	Preplanting	0.0	0.0	5.7	45.0
		Postharvest	0.0	0.3	3.4	13.1
		Structural	0.0	0.1	0.6	2.1
		Total[a]	87.6	95.4	116.5	159.2
Ar1E	Artificial source of 92 Gg yr^{-1} tied to pop., even distribution	Artificial Source	31.8	39.2	62.7	87.2
		Total[a]	119.4	134.6	176.2	224.5
Ar1B	Artificial source of 92 Gg yr^{-1} tied to pop., distributed as biomass burning source	Artificial Source	31.8	39.2	62.7	87.2
		Total[a]	119.4	134.6	176.2	224.5
Ar1L	Artificial source of 92 Gg yr^{-1} tied to pop., distributed by land area	Artificial Source	31.8	39.2	62.7	87.2
		Total[a]	119.4	134.6	176.2	224.5
Ar1C	Artificial source of 92 Gg yr^{-1} tied to pop., distributed as coastal source	Artificial Source	31.8	39.2	62.7	87.2
		Total[a]	119.4	134.6	176.2	224.5

Table 2. (continued)

Run	Comment, Changes From Base Case	Source	1920 Gg yr^{-1}	1950 Gg yr^{-1}	1975 Gg yr^{-1}	1995 Gg yr^{-1}
Ar2C	Artificial source of 92 Gg yr^{-1} 80% tied to pop., 20% constant, distributed as coastal source	Artificial Source	43.8	49.8	68.6	88.1
		Total[a]	131.4	145.2	182.1	225.4

[a]Totals are derived from the emission strengths for each source as described for the base case unless specifically given.

[36] The increases in concentration in the southerly most box in both the first half of the century (0.16 ppt with an RMS range of 0.04–0.31 ppt) and the second half of the century (0.98 ppt with an RMS range of 0.50–1.57 ppt) (Table 4) are well below that inferred from the firn air data (0.7 and 2.0–2.5 ppt, respectively), even considering the RMS uncertainty range.

7. Sensitivities to Individual Sources and Sink

7.1. Ocean

[37] Runs O1a and O1b use biological loss rates of 0.00 and 0.10 day^{-1} respectively, both in the actual runs and in the preruns used to determine the oceanic productivity. Since the preruns are constrained by the observed 1990s atmospheric concentrations and saturation anomalies to give a net flux of −15 Gg yr^{-1}, the emission term is reduced to 42 Gg yr^{-1} for O1a and increased to 78 Gg yr^{-1} for O1b to balance the decreased uptake of 57 Gg yr^{-1} for O1a and the increased uptake of 93 Gg yr^{-1} for O1b. Therefore, although the τ_{ATM} for O1a is increased to 0.71 yr with no biological loss, while that for O1b is reduced to 0.62 yr with a doubling of the biological loss, the atmospheric concentrations in the southerly most model box in run O1b are higher than those of O1a by 1–2 ppt (Figure 5b). Thus, if a shorter oceanic lifetime is assumed because of a larger estimate of the in situ loss, then the estimate of the emission rate is larger tending toward better agreement with the absolute atmospheric concentrations inferred from the firn air, but poorer agreement with their rate of increase because of the smaller τ_{ATM}. In reality the oceanic production may well be sensitive to environmental factors that may have changed (e.g., nutrient availability), but without knowledge of the production mechanism it cannot be estimated.

[38] Runs O3a, O2a, O2b and O3b used oceanic productivities that had been calculated in preruns using saturation anomalies which had been altered by +9, +3, −4 and −13% giving net fluxes of −3, −11, −20 and −31 Gg yr^{-1}, respectively. These 4 runs simulate the extreme ranges of the net flux estimates published by *King et al.* [2000] (−11 to −20 Gg yr^{-1}) (O2a and O2b) and *Kurylo et al.* [1999] (−3 to −32 Gg yr^{-1}) (O3a and O3b). Using the range quoted by *King et al.* [2000] only makes a difference of 0.6 ppt to the atmospheric concentrations calculated for the southerly most model box (Figure 5c). The larger range quoted by *Kurylo et al.* [1999], leads to a difference of 2.0 ppt in the atmospheric concentrations calculated for the southerly most model box (Figure 5c). *Kurylo et al.* [1999] state that the range in net fluxes quoted arises from uncertainties in the physical parameters used in the derivation of ocean uptake for regions sampled and that uncertainties due to extrapolation of measurements to the global ocean are more difficult to quantify, and that this should be kept in mind in assessing the uncertainties in the CH_3Br budget. Although *King et al.* [2000] made use of data collected since the *Kurylo et al.* [1999] assessment, and reclassified some coastal supersaturations as seasonal, open-ocean supersaturations, there must still remain considerable additional uncertainty in the global extrapolation. Overall, this suggests that the uncertainty in the observed saturation anomalies leads to an uncertainty in the calculated concentration of CH_3Br over Antarctica of around 1–2 ppt.

7.2. Coastal

[39] Another nonindustrial source of CH_3Br in the model is that from coastal salt marshes, the net flux of which was estimated to be 14 (7–29) Gg yr^{-1} [*Rhew et al.*, 2000]. This source is prescribed in the model as a gross term, so is actually underestimated since the soil sink will effectively

Table 3. The Hemispheric Average Concentrations and IHR for Each Model Run for the Years 1920, 1950, 1975, and 1995

	1920			1950			1975			1995		
Run	NH[a]	SH[b]	IHR[c]	NH[a]	SH[b]	IHR[c]	NH[a]	SH[b]	IHR[c]	NH[a]	SH[b]	IHR[c]
Base	3.8	3.9	0.96	4.2	4.1	1.02	5.2	4.7	1.12	6.6	5.4	1.22
A1	3.8	3.9	0.96	4.7	4.3	1.08	6.5	5.3	1.24	6.8	5.5	1.23
A2	3.8	3.9	0.96	3.9	4.0	0.97	4.4	4.3	1.02	6.5	5.3	1.21
B1	4.1	4.2	0.98	4.6	4.4	1.03	5.8	5.2	1.13	7.4	6.0	1.22
B2	3.6	3.8	0.95	4.0	4.0	1.01	5.0	4.5	1.11	6.2	5.1	1.21
B3	4.3	4.3	0.99	4.6	4.5	1.03	5.5	4.9	1.12	6.6	5.5	1.22
B4	3.5	3.7	0.94	3.9	3.9	1.00	5.1	4.6	1.12	6.6	5.4	1.22
B5	5.1	5.0	1.02	5.4	5.1	1.06	6.3	5.1	1.06	7.4	6.1	1.22
F1	3.8	3.9	0.96	4.2	4.1	1.02	5.4	4.8	1.14	7.9	6.0	1.31
F2	3.8	3.9	0.96	4.2	4.1	1.02	5.2	4.6	1.11	5.9	5.1	1.16
O1a	3.2	3.1	1.03	3.6	3.3	1.10	4.7	4.0	1.20	6.2	4.8	1.29
O1b	4.0	4.3	0.95	4.4	4.4	1.00	5.4	4.9	1.10	6.7	5.6	1.20
O2a	3.9	4.1	0.95	4.3	4.3	1.00	5.4	4.9	1.10	6.7	5.6	1.20
O2b	3.6	3.7	0.98	4.0	3.9	1.03	5.0	4.4	1.14	6.4	5.1	1.24
O3a	4.2	4.6	0.93	4.6	4.7	0.98	5.7	5.3	1.08	7.0	6.0	1.17
O3b	3.1	3.1	1.02	3.5	3.2	1.09	4.6	3.8	1.21	5.9	4.5	1.31
C1	4.5	4.5	1.00	4.9	4.7	1.05	6.0	5.2	1.14	7.3	6.0	1.23
C2	3.4	3.7	0.94	3.8	3.9	1.00	4.9	4.4	1.11	6.2	5.2	1.21
S1	2.7	3.2	0.83	2.9	3.3	0.88	3.6	3.7	0.98	4.6	4.2	1.08
S2	4.2	4.2	1.00	4.6	4.4	1.06	5.8	5.0	1.16	7.3	5.8	1.26
OH1	4.1	4.3	0.96	4.6	4.5	1.01	5.7	5.2	1.11	7.2	6.0	1.20
OH2	3.5	3.6	0.96	3.9	3.8	1.02	4.9	4.3	1.13	6.1	5.0	1.24
L	6.4	5.7	1.12	7.0	6.0	1.17	8.9	7.0	1.26	11.1	8.3	1.34
LF1	6.4	5.7	1.12	7.0	6.0	1.17	9.1	7.1	1.28	13.3	9.4	1.42
Ar1E	5.1	5.4	0.94	5.9	6.0	0.98	7.9	7.6	1.04	10.2	9.5	1.08
Ar1B	5.3	5.2	1.03	6.1	5.6	1.08	8.2	7.1	1.16	10.7	8.7	1.23
Ar1L	5.4	5.0	1.08	6.2	5.5	1.13	8.4	6.8	1.24	11.0	8.4	1.31
Ar1C	5.3	5.1	1.04	6.1	5.6	1.09	8.3	7.0	1.19	10.8	8.6	1.26
Ar2C	5.9	5.6	1.07	6.6	6.0	1.11	8.6	7.2	1.19	10.9	8.7	1.26

[a]Annual average concentration (ppt) in the Northern Hemisphere, calculated from 12 midmonth values.

[b]Annual average concentration (ppt) in the Southern Hemisphere, calculated from 12 midmonth values.

[c]Annual average interhemispheric ratio (N/S), calculated from 12 midmonth values of the ratio.

Table 4. Change in Concentration in the Southerly Most Model Box for Each Model Run

Run	1904–1950 ppt	1950–1995 ppt
Base	0.16	0.98
A1	0.29	0.94
A2	0.07	1.01
B1	0.22	1.19
B2	0.13	0.88
B3	0.11	0.77
B4	0.19	1.10
B5	0.11	0.77
F1	0.16	1.44
F2	0.16	0.73
O1a	0.23	1.27
O1b	0.14	0.86
O2a	0.16	0.98
O2b	0.16	0.98
O3a	0.16	0.98
O3b	0.16	0.98
C1	0.16	0.98
C2	0.16	0.98
S1	0.10	0.67
S2	0.18	1.09
OH1	0.19	1.12
OH2	0.14	0.87
L	0.35	1.79
LF1	0.35	2.66
Ar1E	0.80	3.47
Ar1B	0.50	2.26
Ar1L	0.54	2.19
Ar1C	0.56	2.50
Ar2C	0.48	2.20

be accounted for twice in these regions. However, setting this to the high value of 29 Gg yr^{-1} (C1) increases concentrations in the southerly most box by only 0.5 ppt (Figure 5d).

7.3. Automobiles

[40] Increasing the automobile source by assuming an emission factor of 25% (A1), as opposed to 10% in the base run, leads to a greater rate of increase in concentration between 1925 and 1975, such that by 1975 the concentration in the southerly most box is 0.45 ppt higher than in the base case (Figure 5d). The concentration in this box increases by 0.75 ppt between 1950 and 1975 (0.03 ppt yr^{-1}), but then only by a further 0.19 ppt to 1995, such that the total increase between 1950 and 1995 is 0.94 ppt, slightly lower than in the base case (Table 4). The slow rate of increase during the latter quarter of the century is not consistent with the rate of 0.03 ppt yr^{-1} determined by *Miller* [1998] from air samples collected at Cape Grim. The increase in the first half of the century is nearly doubled to 0.29 ppt. This is still considerably less than the value of 0.7 pptv inferred from the firn air and does not account for any increase prior to 1925. Therefore increasing the automobile source helps to improve the agreement between the modeled concentrations and those derived from the firn air data in the middle part of the century, but still leaves considerable disagreement for the earlier and latter parts.

7.4. Fumigation

[41] The upper limit for the fumigation source was estimated to be that which would occur given the upper ranges of the emissions factors for preplanting (90%), and for durables (88%) and perishables (95%), giving a post-harvesting emission factor of 91% (F1) (Figure 5d). This leads to an increase of 1.44 ppt in the southerly most box between 1950 and 1995, which is still considerably less than the 2.0–2.5 ppt derived from the firn air data. The increase is virtually unchanged from that in the base case between 1950 and 1975 with the majority of the difference occurring between 1975 and 1995. The rate of increase in this latter period (0.048 ppt yr^{-1}) is slightly less than that of the firn air trend for the 1970s and 1980s (0.05–0.06 ppt yr^{-1}) as calculated by *Butler et al.* [1999], but greater than that observed by *Miller* [1998] between 1979 and 1998 at Cape Grim (0.03 ppt yr^{-1}). Overall, the increasing rate of growth in this model run is similar to the trend derived by *Butler et al.* [1999], although the modeled rate of increase between 1950 and 1970 is slower.

7.5. Biomass Burning

[42] There is also considerable uncertainty in the biomass burning source strength. A factor of 2 uncertainty is considered by assuming that the emission ratio of CH_3Br/CH_3Cl is twice that in the base case (i.e., 2% instead of 1%, (B1)) giving a 1999 source strength of 34 Gg yr^{-1}, closer to the higher limit of uncertainty quoted by others (see above). However, this change makes very little difference to the concentrations prior to 1950 (Figure 5e and Table 3), since the emissions are only increased by 7–8 Gg yr^{-1} over this period (Table 2). This is largely because of the assumption that 90% of the biomass burning is a linear function of population, so emissions in the first part of the 20th century are relatively small in the base run. However, it could be argued that the biomass burning source should not show an historical trend if natural fires burnt more material in the absence of anthropogenically induced fires. Run B3 considers this by holding the source strength of CH_3Br from biomass constant at the 1999 value (17 Gg yr^{-1}), but again the increase in concentration is small (Figure 5e and Table 3). However, assuming that the emission ratio of CH_3Br/CH_3Cl is twice that in the base case and assuming no historical trend (B5) gives concentrations in the southerly most box that are higher than in the base case by about 0.7 ppt for the first half of the century, reducing to 0.5 ppt higher toward the end of the century.

[43] The historical trend assumed for biomass burning only accounts for just over a quarter of the calculated increase in CH_3Br prior to 1950 in the southerly most box (i.e., 0.05 ppt). The increase in CH_3Br between 1950 and 1995 due to this historical trend in biomass burning is calculated to be 0.21 ppt. *Yokouchi et al.* [2000] suggested that this increase could be no more than 0.5 ppt, because of the comparable 50 ppt increase in CH_3Cl derived from firn air data [*Butler et al.*, 1999]. This is based on a 1% ratio for CH_3Br:CH_3Cl emissions from biomass burning, as also used in the current study. It should be noted that there is some uncertainty in this value of 0.5 ppt because of the uncertainties in the inferred increase in CH_3Cl [*Butler et al.*, 1999] and the CH_3Br:CH_3Cl ratio [*Manö and Andreae*, 1994; *Andreae et al.*, 1996; *Blake et al.*, 1996]. Run B1 (doubled CH_3Br from biomass burning) gives an increase, between 1950 and 1995, of 1.19 ppt of which 0.42 ppt was due to the biomass burning. This higher rate of increase

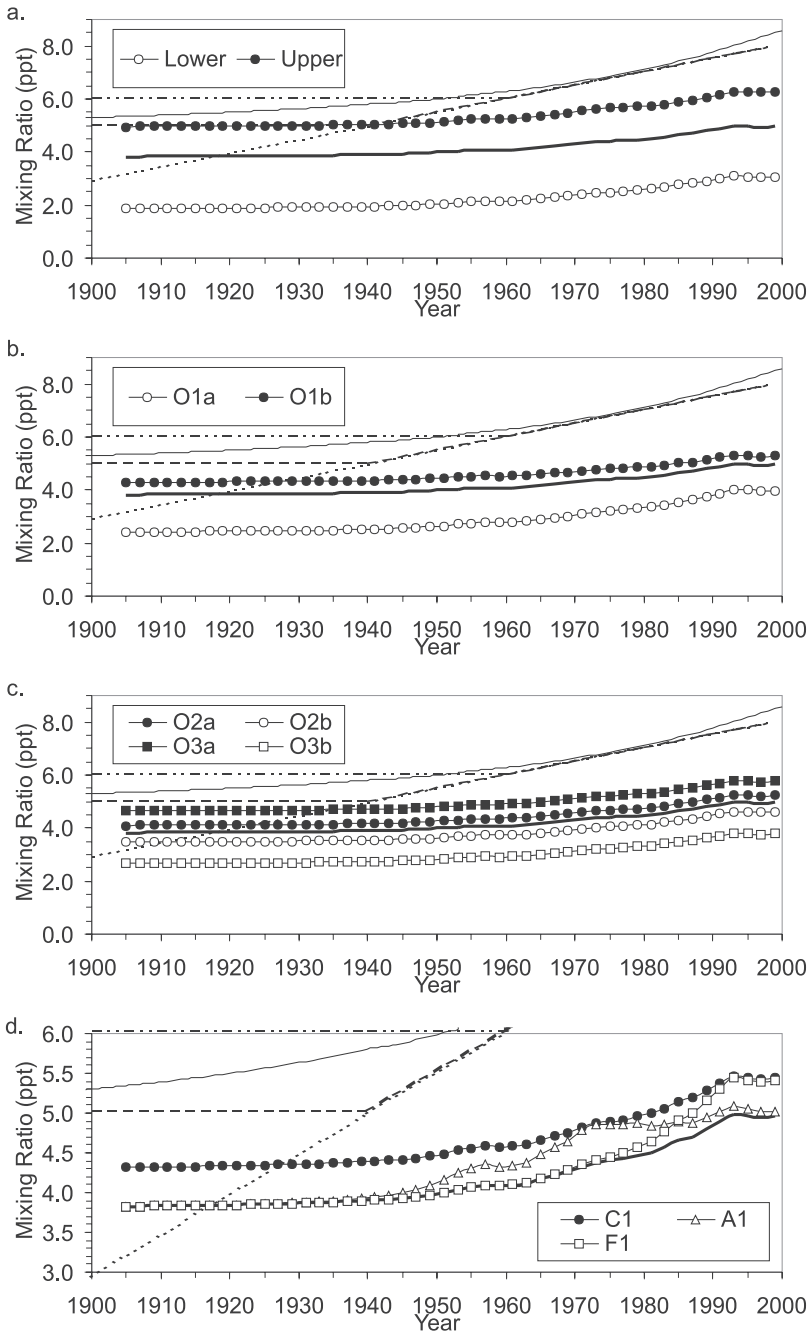

Figure 5. The historical trend in Antarctic atmospheric concentrations of CH_3Br derived from firn air data, *Butler et al.* [1999] (thin solid line) and scenarios 2 (dashed line), 4 (dotted line) and 5 (dash dotted line) from *Sturges et al.* [2001a], and as calculated in the base case run (thick solid line). (a) lower and upper RMS error analysis values, (b) runs O1a (biological loss = 0.0 day^{-1}, τ_{ATM} of 0.71 yr) and O1b (biological loss = 0.1 day^{-1}, τ_{ATM} of 0.62 yr), (c) runs O2a, O2b, O3a and O3b, which used saturation anomalies with a global average of 8%, 15%, 2% and 24%, respectively, to determine the production rates, (d) runs C1 (coastal salt marshes = 29 Gg yr^{-1}), A1 (automobile emission factor = 25%) and F1 (maximum fumigation emission factors), (e) runs B1 (biomass burning strength doubled), B3 (no historical trend in biomass burning) and B5 (no historical trend and biomass burning strength doubled), (f) runs S1 (τ_{SOIL} decreased to 1.00 yr, τ_{ATM} = 0.47 yr), S2 (τ_{SOIL} increased to 3.54 yr, τ_{ATM} = 0.70 yr), L (no soil or stratospheric sinks and τ_{OH} increased to 2.45 yr, τ_{ATM} = 1.02 yr) and LF1 (no soil or stratospheric sinks and τ_{OH} increased to 2.45 yr (τ_{ATM} = 1.02 yr) and maximum fumigation emission factors), and (g) runs with an artificial source tied to population: Ar1E (even distribution), Ar1L (land distribution), Ar1B (biomass burning distribution) and Ar1C (coastal distribution); and an artificial source with 80% tied to population: Ar2C (coastal distribution).

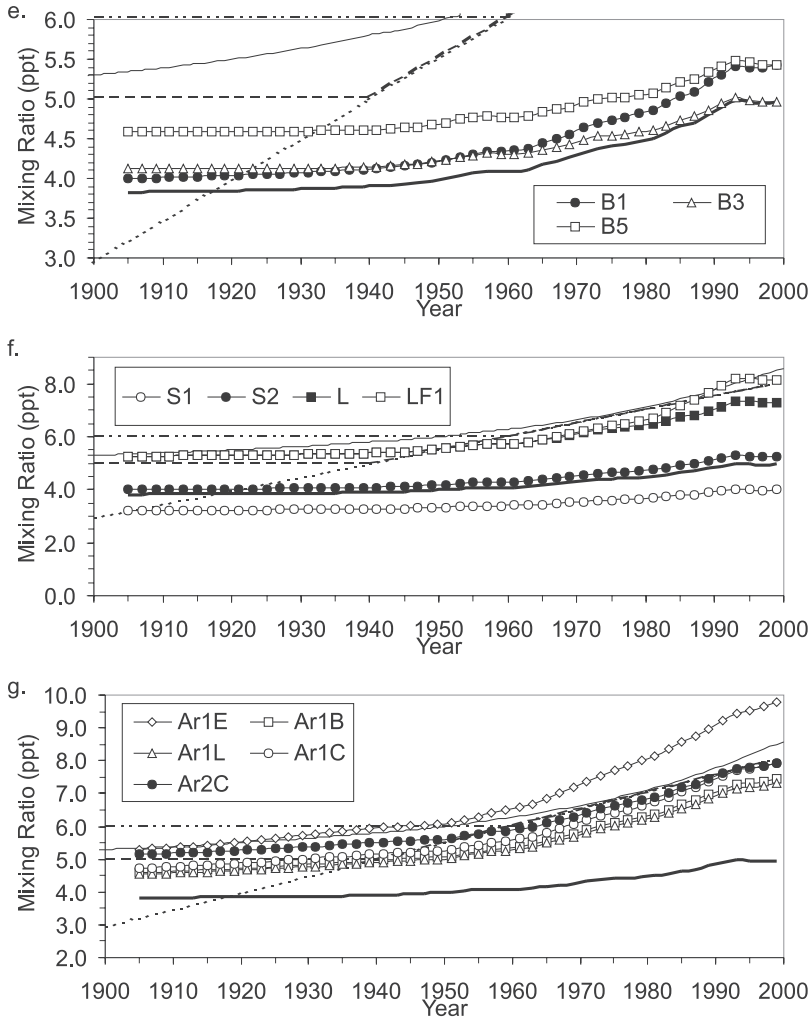

Figure 5. (continued)

due to biomass burning is much closer to the 0.5 ppt derived from the CH_3Cl firn data, but the total rate is still well below that required for agreement with the CH_3Br firn data, which would require this source to be increased by a factor of 6–8 rather than 2.

7.6. Soil

[44] As described above, the range of uncertainty in the soil sink is large. Here it is assumed that the uncertainty is reasonably represented by the range of 94 ± 54 Gg yr^{-1}, the estimate made by *Serca et al.* [1998] using their biome areas and mean deposition velocities (except bog) from their work and the *Shorter et al.* [1995] study. This is equivalent to a τ_{SOIL} range of 0.97–3.54 yr and τ_{ATM} of 0.47–0.70 yr (Runs S1 and S2 in Table 1). The longer lifetime (S2) has the effect of not only increasing the absolute concentrations by 0.2–0.3 ppt (Figure 5f), but also increasing their rate of growth such that between 1904 and 1950 the concentrations in the southerly most box increase by 0.18 ppt and between 1950 and 1995 by 1.09 ppt (Table 4). However, these are still considerably lower than the respective values of 0.7 and 2.0–2.5 ppt derived from the firn air. The shorter lifetime (S1) leads to concentrations and a rate of increase well below those derived from the firn air data (Figure 5f and Table 4) and a very low IHR of 1.08 in 1995 (Table 3).

8. Lifetime of CH_3Br

[45] *Yokouchi et al.* [2000] calculated that the lifetime of CH_3Br must be between 0.7 and 1.2 yr with a best estimate of 1.0 yr to account for the increase in atmospheric concentrations derived from the firn air data, assuming an industrial source of 46 Gg yr^{-1}. The uncertainties in the partial lifetimes quoted by *Kurylo et al.* [1999] lead to an upper RMS value for τ_{ATM} of 1.00 yr. Since the oceanic emission in the model is dependent on the oceanic loss terms (as illustrated by runs O1a and O1b), changing the lifetime of CH_3Br by altering its oceanic removal, does not provide a true illustration of the effect of a different partial lifetime. Removing the soil and stratospheric sinks and increasing the OH lifetime by 25% (L) gives a value for τ_{ATM} of 1.02 yr. This run should be seen purely as an illustration of the effect on atmospheric concentrations of a lifetime similar to the upper limit of its uncertainty and not as a suggestion that the soil sink does not exist.

[46] The longer lifetime has the effect of not only increasing the absolute concentrations, but also increasing

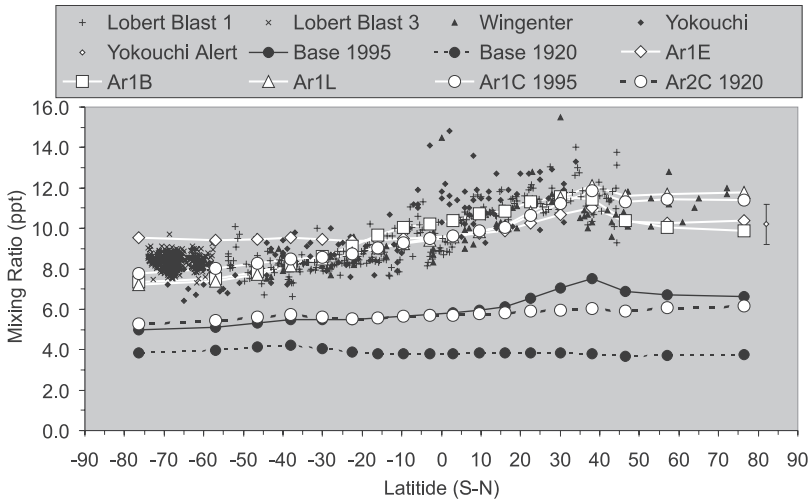

Figure 6. The latitudinal distribution of atmospheric CH_3Br calculated for 1995 (solid lines) and 1920 (dashed lines) in the base run and runs Ar1E (even distribution), Ar1B (biomass burning distribution), Ar1L (land distribution), Ar1C and Ar2C (coastal distribution). Runs Ar1 include an artificial source tied to population and run Ar2 includes an artificial source with 80% tied to population. Atmospheric concentrations are shown as observed by *Lobert et al.* [1995, 1997], *Wingenter et al.* [1998] and *Yokouchi et al.* [2000].

their rate of growth (Figure 5f and Table 4). It gives concentrations that are within the uncertainty of the firn air data prior to 1950, but slightly below those after 1950. The increase of 1.79 ppt between 1950 and 1995 is close to, but still slightly lower than that derived from the firn air (Table 4). If, in addition to the longer lifetime, the maximum emission factors of CH_3Br from fumigation are assumed (LF1), then the concentrations increase by 2.66 ppt from 1950 to 1995, which is actually above that inferred by the firn air trend (Table 4 and Figure 5f). That is, with this longer lifetime, the increase in concentrations between 1950 and 1995 inferred from the firn air can be more than accounted for by fumigation sources, if the upper ranges of their emissions factors are assumed. The IHR of 1.42 in 1995 (Table 3) for this run is too high, but it should be remembered that the complete removal of the soil sink, which is predominantly in the Northern Hemisphere, will tend toward an overprediction of the IHR. It should also be noted that a currently unidentified change in another source is still required to reproduce the increase in the first half of the century.

[47] If the lifetime is shorter than currently estimated, either because of a higher estimate of a known sink (e.g., runs S1 and OH2) or because of an unidentified sink, the budget imbalance would be greater and further beyond the uncertainties in the current source strength estimates implying an unidentified source.

[48] It has recently been suggested that the global average OH concentration rose by 15 ± 22% between 1979 and 1989 and then fell to a value in 2000 about 10 ± 24% below the 1979 level [*Prinn et al.*, 2001]. For a τ_{ATM} of 0.64 yr for CH_3Br this equates to changes of ±6%. These are relatively small changes compared to the overall uncertainty in the lifetime of CH_3Br. If such a change in OH were introduced into the model it would accentuate slightly the pattern in the calculated concentrations, which show an increase in the 1980s and a leveling off in the 1990s.

9. Artificial Runs

[49] In this section, it is assumed that the current best estimates of the individual sources and sinks are correct, and therefore that an additional source is required to balance the budget. An attempt is made to identify the characteristics of this source by including various artificial sources with different characteristics into the model and comparing the results with the observed data. Initially it is assumed that a single additional source is required.

[50] On the basis of the comparison between the base case run and the firn air data, it is clear that any such source must have increased during the century and from comparison with the current atmospheric burden (146 Gg, *Kurylo et al.* [1999]), the strength of this source at the end of the 20th century must have been 92 Gg yr^{-1}. Since the cause of the increase in this source is most likely due to anthropogenic influence, its strength is assumed to be a linear function of world population. Since the population in 1900 was 29% of that in 1999, it is assumed that the strength of the artificial source was 27 Gg yr^{-1} in 1900 and that it increased to 92 Gg yr^{-1} by the year 1999 (Table 2).

[51] Adding this artificial source with an even latitudinal distribution (Ar1E) leads to concentrations that are in good agreement with those from the firn air data for the first half of the century, but with a rate of increase in the second half of the century that is too fast (Table 4 and Figure 5g) such that concentrations in the Southern Hemisphere in 1995 are higher than observed (Figure 6). If this source is distributed in the same way as the biomass burning source (Ar1B) or according to land area (Ar1L), then the rate of increase in the southerly most box is in good agreement with that inferred from the firn air data (Table 4), although the

concentrations are slightly lower (Figure 5g). Since a distribution based on coastal regions includes a significant fraction south of 30°S, model run Ar1C leads to higher concentrations in the southerly most box particularly, in the latter years, which are closer to those predicted by the firn air data (Figure 5g). If it is assumed that only 80% of the source is tied to world population while 20% is constant (Table 2) and assuming the coastal distribution (Ar2C), the concentrations calculated for the southerly most box are in excellent agreement with those inferred from the firn air data (Figure 5g).

[52] The artificial runs with the source distribution based on land area (Ar1L), biomass burning areas (Ar1B) and coastal areas (Ar1C and Ar2C) give IHRs in 1995 of 1.23, 1.31 and 1.26, respectively which are all within the large range of 1.3 ± 0.1 quoted by *Kurylo et al.* [1999] and within or close to the narrower range of 1.21 ± 0.03 given by *Wingenter et al.* [1998]. However, comparison between the model results for the lowest boxes and the observed surface atmospheric concentrations shows two interesting features (Figure 6). First, the model reproduces the decrease in concentrations from midlatitudes to high latitudes as observed by *Yokouchi et al.* [2000]. This is largely because the emissions in the model are mostly emitted into the lower latitude boxes as in Figure 1. The additional source distributed according to coastal regions gave slightly better agreement in the southern high latitudes, with the other runs perhaps giving too much of a decrease toward the South Pole. Second, comparison with the observed data suggests that the model runs with the additional land or coastal source position the gradient between the higher northern hemispheric concentrations and the lower southern hemispheric concentrations too far to the north. That is, concentrations calculated for the northern tropical region tend to be lower than observed. Examination of the seasonal variation in the model suggests that this is not simply a function of the time of year that the observations were made (November to March). When the artificial source is distributed according to biomass burning the calculated concentrations are higher in the tropics in better agreement with the observations. This may suggest that a significant part of the additional source needs to be in the tropical regions. This is in agreement with an earlier model study by *Lee-Taylor et al.* [1998] and might suggest a source similar to the recently found source of CH_3Cl from tropical plants [*Yokouchi et al.*, 2002a]. However, there is much uncertainty in this conclusion given the errors introduced by the transport scheme, as discussed in section 4.

[53] Since historical records of atmospheric concentrations from firn air are only available from the Southern Hemisphere, there is no knowledge of how atmospheric concentrations changed over the last century in the Northern Hemisphere. The base case gave an IHR of around 1.0 during the first half of the century (Table 3 and Figure 6), but this is based on the best estimates of known sources which do not lead to a balanced budget. With the artificial source distributed according to the coastal regions and with 80% tied to population (Ar2C), the IHR in the first half of the century is about 1.1 and the average northern hemispheric concentration increased by 85% between 1920 and 1995 (Table 3 and Figure 6). However, it may be that the concentrations have not changed in the Northern Hemisphere by as much as these runs predict.

[54] If it is assumed that emissions in the Northern Hemisphere have changed by no more than expected from the best estimates of known sources, is it possible to reproduce the concentrations in the Southern Hemisphere, by assuming that the artificial source only changes in the Southern Hemisphere? This was assessed by further runs in which the artificial source equalling 92 Gg yr^{-1} in 1999 was split between the Northern and Southern Hemispheres with that in the Northern Hemisphere held constant and that in the Southern Hemisphere a linear function of world population. Different runs were performed such that for each run the fraction of the additional source emitted into each hemisphere was changed. As the percentage of the source emitted into the Southern Hemisphere in 1999 was increased from 0 to 100%, the modeled IHR in 1995 decreased from 1.45 to 0.82, while the change in concentration between 1950 and 1995 in the southerly most box increased from 0.99 to 4.97 ppt. Both these terms are within the range of the observed values (i.e., IHR of 1.18–1.40 and concentration increase of 2.0–2.5 ppt) when the southern hemispheric fraction, in 1999, is between about 25 to 35%.

10. Seasonal Variation

[55] To assess the effect of the seasonality of the various processes on the atmospheric concentrations, the average hemispheric concentrations and IHR from run Ar2C for the year 1999 were compared with observed data (Figure 7). It should be remembered that the effects of the seasonal variations assumed for each source and sink are dependent on the relative contributions that each of these processes makes to the overall budget of this model run. In this run the seasonally varying sources are as prescribed in the base run while there is the additional seasonally constant artificial source. Plotted along with the results from Ar2C are further runs that used the same source magnitudes, but which switched off the seasonality in various source or sink terms.

[56] The seasonal variation in the northern hemispheric concentrations for run Ar2C is very similar to the observed. This particular run gives absolute values that are higher than the observed, but the phase and amplitude are similar. The phase is similar to that expected from OH oxidation and when the seasonal variation in OH is removed the cycle is dampened. The late summer maximum assumed for the preplanting fumigation source leads to elevated northern hemispheric average concentrations at this time, but has virtually no effect on the southern hemispheric average concentrations. This suggests that the timing of the use of CH_3Br as a fumigant could possibly affect the seasonal variation of concentrations observed in the Northern Hemisphere. However, it should be noted that the samples collected by *Wingenter et al.* [1998] were taken upwind of areas experiencing summertime fumigation and therefore might be expected to be lower than calculated in a 2-D, latitudinally averaged model at this time of year. If it is assumed that CH_3Br is deposited to frozen soil, the northern hemispheric averages are reduced particularly in winter.

[57] The calculated southern hemispheric concentrations show virtually no seasonal variation. The smaller amplitude compared to the Northern Hemisphere is in agreement with

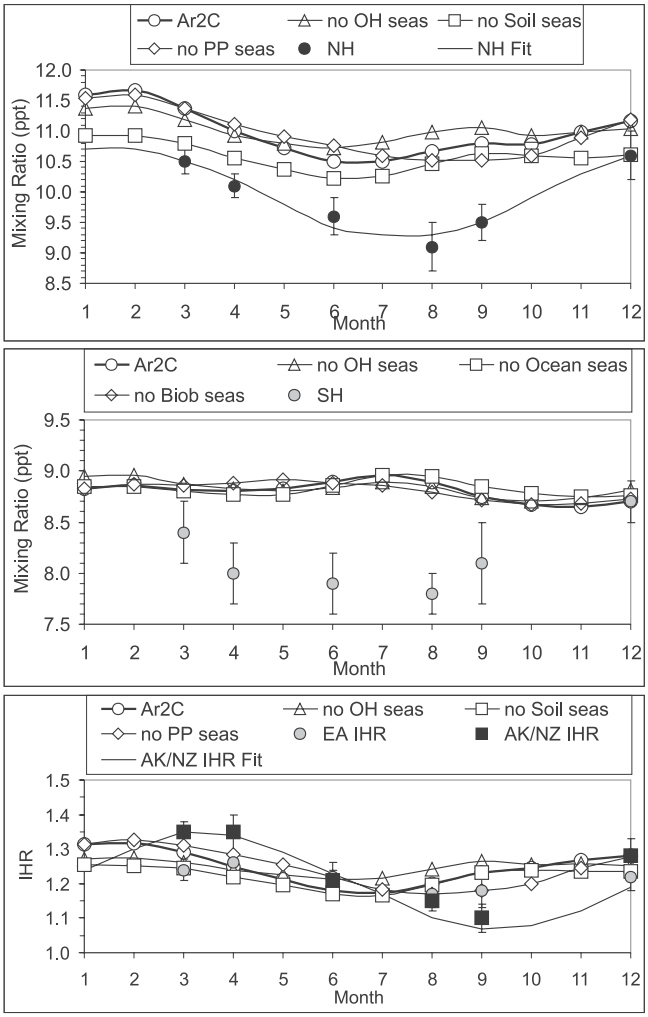

Figure 7. The seasonal variation of atmospheric CH_3Br calculated for 1999 in run Ar2C with seasonally varying emissions as described for the base case run, and run Ar2C with no seasonal variation in OH (no OH seas), soil sink (no Soil seas), preplanting fumigation (no PP seas), oceanic productivity (no Ocean seas) and biomass burning (no Biob seas). The month tick marks represent the middle of the month. Top panel: northern hemispheric average concentrations with observed values (NH) and sinusoidal fit (NH Fit) from *Wingenter et al.* [1998]. Middle panel: southern hemispheric average concentrations with observed values (SH) from *Wingenter et al.* [1998]. Bottom panel: interhemispheric ratio (IHR) with observed equal area IHR (EA IHR), Alaska/New Zealand ratios (AK/NZ IHR) and sinusoidal fit (AK/NZ IHR Fit) from *Wingenter et al.* [1998].

the observations at Cape Grim (41°S), which show no clear seasonal cycle [*Miller*, 1998; *Sturrock et al.*, 2001], although the observed southern hemispheric concentrations from *Wingenter et al.* [1998] suggest lower values in the austral winter. Although the calculated amplitude is small there is still some seasonal variation. If the seasonal variation in the emission terms and OH concentrations are switched off, then the southern hemispheric concentrations show a maximum in summer due to the transport of the higher winter northern hemispheric concentrations. The variation in the OH field counters this by reducing southern hemispheric summer concentrations by more than winter concentrations. The seasonal variation in biomass burning again moderates this by tending toward higher concentrations in winter and lower concentrations in autumn. Similarly the seasonality in the oceanic productivity leads to lower concentrations in spring and autumn. Much of the seasonal variation in the oceanic source comes from the relationship between SST and saturation that was used to define the saturations, which were subsequently used to determine the productivity. As discussed above, the months at which the maximum and minimum occur are not the same for each latitude band. This therefore moderates the effect on the seasonal variation of the hemispheric average.

[58] The modeled IHR are fairly similar in magnitude to the equal area average values (EA IHR) of *Wingenter et al.* [1998], but given the limited number of months for which EA IHR values are available it is difficult to tell if the calculated phase is in agreement. The IHR values derived from the data from Alaska and New Zealand exhibit a phase that is 1–2 months behind the modeled phase. The processes that most affect the seasonal variation of the IHR in the model are those that have the greatest effect on the Northern Hemisphere averages, since the seasonal variation in the southern hemispheric average varies little between runs.

[59] *Miller* [1998] noted that the observed amplitude of the seasonal cycle in atmospheric CH_3Br appears to be largest at high northern latitudes and decreases toward the south. For run Ar2C the model reproduces this general trend. The amplitude is largest in the higher-latitude northern hemispheric bands and decreases southward through the Southern Hemisphere. The observed amplitude of ±0.7 ppt at Trinidad Head (41°N) [*Miller*, 1998] is reproduced well in the northern midlatitude bands (±0.70 to ±0.84 ppt), although the absolute concentrations in run Ar2C are slightly higher than observed. However, the larger amplitudes of greater than ±1 ppt observed at Alert, Canada (83°N) and Barrow, Alaska (71°N) [*Wingenter et al.*, 1998; *Yokouchi et al.*, 2000] are not reproduced in the northern high-latitude band (±0.72 ppt). At these latitudes the seasonality in the soil sink, which is assumed not to be active during the winter months when the ground is expected to be frozen, makes an important contribution to the calculated amplitude, without which the amplitude would be even smaller. To improve the comparison with the observations either the net source term needs to be increased in winter/spring or decreased in summer/autumn. In the northern hemispheric bands south of 19°N biomass burning during the dry winter months acts to increase the amplitude. The calculated seasonal variation in the Southern Hemisphere tropics shows a bimodal pattern with transport of high concentrations from the Northern Hemisphere leading to an austral summer maximum and southern hemispheric biomass burning leading to an austral winter maximum. In the southern extra-tropical bands, a small, broad, austral winter maximum remains, which is consistent with OH oxidation being the main loss process. Although this may appear to be in contrast to observations at Cape Grim (41°S) [*Miller*, 1998; *Sturrock et al.*, 2001], which have shown no clear seasonal cycle, the amplitude of the seasonal cycle in the model results is only ±0.14 to

±0.29 ppt, which is smaller than the variability in the observations.

11. Discussion

[60] The base case illustrates that best estimates of the sources and sinks lead to a budget imbalance throughout the whole of the century, with an underestimation of the sources and/or over estimation of the sinks. Further, this difference cannot be explained by the RMS error in the model results as determined from the uncertainties in the major source and sink terms.

[61] The model results prior to 1925 represent an atmosphere with only natural and biomass burning sources (i.e., "nonindustrial") of CH_3Br. In 1950 emissions from automobiles were beginning to increase rapidly, postharvesting and structural fumigation had begun, but usage amounts were still low. "Nonindustrial" sources are assumed to make up 93% of the emissions in the base case run in 1950. This implies that understanding of the "nonindustrial" budget is out of balance. Either the estimate of the sink strength is too large or there is an underestimate of a known "nonindustrial" source or an unaccounted "nonindustrial" source, or some combination of these. The uncertainty in any individual source (ocean, biomass burning or coastal salt marshes) is not sufficient to account for this discrepancy, although the sensitivity of the results to the uncertainties in the oceanic source is large. However, if all these sources were close to the upper limits of their estimated uncertainty ranges, the budget could be balanced for this period. Alternatively other sources would have to have existed in this period. Possible examples might be that of fungal litter decomposition (0.5–5.2 Gg yr^{-1} [*Lee-Taylor and Holland*, 2000]), wetlands (5 Gg yr^{-1} [*Varner et al.*, 1999b]) or peatlands (0.9 Gg yr^{-1} [*Dimmer et al.*, 2001]), but alone these only make a small contribution. Another possibility may be plants, some of which (e.g., Brassicas and shrubland vegetation) have been shown to be a source of atmospheric CH_3Br [*Saini et al.*, 1995; *Gan et al.*, 1998; *Rhew et al.*, 2001], although the global strength of this source is unknown.

[62] Further, the results imply that the increase in the "anthropogenically influenced" sources during the century is underestimated or that the sink strength is too strong. The increase in atmospheric concentration during the first half of the 20th century as derived from the firn air data by *Butler et al.* [1999] cannot be accounted for by current best estimates for the changes in the strengths of known sources or sinks. Biomass burning, the only source in the model for which an increase prior to 1925 is assumed, is estimated to account for 7% of the increase prior to 1950 inferred from firn air. The automobile source makes the largest contribution in the model to the increase prior to 1950, but it still accounts for only 16% of the increase inferred from the firn air and cannot account for any increase prior to 1925. The uncertainties in the estimates of neither these sources, nor the sinks, are large enough to account for the discrepancy. This implies that some other source (or sink) has changed during this period. It may be a known source, such as the ocean, if, for example, the rate of productivity had changed for some unknown reason. Alternatively other, as yet unidentified, sources would have to have increased during this period. A possible cause of this increase may be changing land use patterns if plants, for example, are a significant source of CH_3Br.

[63] The increase in atmospheric concentration as derived from the firn air data during the second half of the 20th century cannot be accounted for by current best estimates of the changes in the strengths of known "anthropogenically influenced" sources (automobiles, fumigation and biomass burning) assuming sink estimates to be correct. The automobile source increased rapidly from the early 1940s to a peak in the early 1970s. Thereafter emissions rapidly declined to near zero levels by 2000. Just as the automobile source reached its peak in the 1970s, the fumigation source started to increase rapidly before leveling off in the 1990s. Since the automobile source is estimated to be larger in 1950 than in 1995, this source actually contributes a declining amount to concentration over this period. The temporal trend over the period is however sensitive to the automobile source in that it can affect the time at which the increase occurs. Biomass burning is estimated to contribute only 0.21 ppt to the increase between 1950 and 1995 and the uncertainty in this source is not large enough to make up the shortfall. The concentrations after about 1975 are sensitive to the assumed emission factor for fumigation, but even if the maximum emission factor is assumed for fumigation, the increase between 1950 and 1995 is still about 0.5 to 1.0 ppt too small. Alternatively other sources, which must have increased during the second half of the century, would have to have existed. Possible examples might be cultivated plants such as *Brassicas* (7.0 Gg yr^{-1} in 1996 [*Gan et al.*, 1998]) or rice (1 Gg yr^{-1} in the 1990s [*Redeker et al.*, 2000]), but alone these only make a small contribution.

[64] If the lifetime of CH_3Br were longer than best estimates suggest, then the source strength required to balance the budget and the change in it required to reproduce the increase in concentrations would be less. A lifetime of 1 year would allow the pre-1950 budget to balance with the best estimate of "nonindustrial" sources and the increase in the second half of the century could be accounted for by "anthropogenically influenced" emissions within their estimated range of uncertainty.

[65] However, if it is assumed that the best estimates of the sources and sinks are correct then an additional source with the following characteristics could lead to a balanced budget for atmospheric CH_3Br: emissions in 1900 at a level of 30–50% of current day emissions, increasing as a linear function of population; emissions distributed predominantly in the Northern Hemisphere, but including a substantial fraction (30%) in the Southern Hemisphere. Such a source is likely to be terrestrial, but which has been anthropogenically influenced. Alternatively, changes in emissions in the Northern Hemisphere based on current best estimates could be consistent with southern hemispheric concentrations derived from firn air data, providing there is an additional constant northern hemispheric source of around 60–70 Gg yr^{-1} and an additional southern hemispheric source of about 20–30 Gg yr^{-1} in 1999, which increased by about 15–20 Gg yr^{-1} during the last century. One can only postulate what these sources could be, or how probable their existence might be. The constant northern hemispheric source might be a natural terrestrial

source. A source that is mostly confined to the Southern Hemisphere is likely to be associated with the ocean, given its latitudinal distribution. However, it is not known what changes (e.g., environmental factors) might have occurred that could have caused an increase in the oceanic source.

[66] It is also interesting to note that for the base case and all the sensitivity model runs discussed the trends for the 1990s show a leveling off and even signs of a slight decline. This comes about as a result of the assumptions made about the recent CH_3Br emissions from automobiles and fumigation. Such a decline in recent concentrations is in agreement with the observations of *Yokouchi et al.* [2002b]. However, it should be noted that none of these runs, except the one with the lifetime of 1 year and the increased fumigation source (LF1), were able to produce a sufficiently large increase in concentration for the second half of the century. When the increasing artificial source is added to resolve this problem, the increase in the concentrations continues in the 1990s, albeit at a slightly slower rate. This however is at odds with the observations of *Yokouchi et al.* [2002b].

12. Summary

[67] For some time now it has been known that the current understanding of the present-day atmospheric budget of CH_3Br is incomplete, with sinks far out-weighing sources. This modeling study illustrates that not only is this true, but if the atmospheric trends inferred from the firn air data are correct, then our understanding of the nonindustrial budget and anthropogenic changes to it is also incomplete. This difference cannot be explained by the RMS error in the model results as determined from the uncertainties in the major source and sink terms. However, if all the ''non-industrial'' sources (ocean, biomass burning and coastal salt marshes) were close to the upper limits of their estimated uncertainty ranges, the budget prior to 1950 could be balanced. Similarly with a lifetime of 1 year the absolute concentrations prior to 1950 are reasonably well reproduced and only require an increase in emissions from fumigation (within the estimated uncertainty) for the increase in concentrations in the second half of the century to be reproduced. Note, however, that the inferred increase during the early part of the 20th century cannot be reproduced without an, as yet unrecognised, increasing source term (or decreasing sink term). If the current estimates of the known sources and the lifetime of CH_3Br are correct then an additional source or sources are required, which must have existed throughout the whole of the century, in both hemispheres and together have increased over this period. However, such an increasing source would also have to have declined slightly at the end of the 20th century to be consistent with the observed recent decline in atmospheric concentrations of CH_3Br.

[68] **Acknowledgments.** The author acknowledges the help of Matt Gillis (Tri Cal), Bill Thomas (EPA), and Melanie Miller, who provided information on the use of CH_3Br, and to Stuart Penkett, Bill Sturges, and Georgina Sturrock (UEA) for valuable discussions. This work was funded by the Department of the Environment, Transport and the Regions (EPG 1/1/97).

References

Andreae, M. O., et al., Methyl halide emission from savanna fires in southern Africa, *J. Geophys. Res.*, *101*, 23,603–23,613, 1996.

Baker, J. M., C. E. Reeves, S. A. Penkett, L. M. Cardenas, and P. D. Nightingale, An estimate of the global emissions of methyl bromide from automobile exhausts, *Geophys. Res. Lett.*, *25*, 2405–2408, 1998.

Baker, J. M., C. E. Reeves, P. D. Nightingale, S. A. Penkett, S. W. Gibb, and A. D. Hatton, Biological production of methyl bromide in the coastal waters of the North Sea and open ocean of the northeast Atlantic, *Mar. Chem.*, *64*, 267–285, 1999.

Baker, J. M., W. T. Sturges, J. Sugier, G. Sunnenberg, A. A. Lovett, C. E. Reeves, P. D. Nightingale, and S. A. Penkett, Emissions of CH_3Br, organochlorines and organoiodines from temperate macroalgae, *Chemosphere Global Change Sci.*, *3*, 93–106, 2001.

Baumann, H., and K. G. Heumann, Analysis of organobromine compounds and HBr in motor car exhaust gases with a GC/microwave plasma system, *Fresenius Z. Anal. Chem.*, *327*, 186–192, 1987.

Bertram, F. J., and J. B. Kolowich, A study of methyl bromide emissions from automobiles burning leaded gasoline using standardized vehicle testing procedures, *Geophys. Res. Lett.*, *27*, 1423–1426, 2000.

Blake, N. J., D. Blake, B. C. Sive, T. Y. Chen, F. S. Rowland, J. E. Collins Jr., G. W. Sachse, and B. E. Anderson, Biomass burning emissions and vertical distribution of atmospheric methyl halides and other reduced carbon gases in the South Atlantic region, *J. Geophys. Res.*, *101*, 24,151–24,164, 1996.

Butler, J. H., The potential role of the ocean in regulating atmospheric CH_3Br, *Geophys. Res. Lett.*, *21*, 185–188, 1994.

Butler, J. H., M. Battle, M. L. Bender, S. A. Montzka, A. D. Clarke, E. S. Saltzman, C. M. Sucher, J. P. Severinghaus, and J. W. Elkins, A record of atmospheric halocarbons during the twentieth century from polar firn air, *Nature*, *399*, 749–755, 1999.

Chen, T.-Y., D. Blake, and F. S. Rowland, Estimation of global vehicular methyl bromide emission: Extrapolation from a case study in Santiago, Chile, *Geophys. Res. Lett.*, *26*, 283–286, 1999.

Cooke, W. F., B. Koffi, and J.-M. Gregoire, Seasonality of vegetation fires in Africa from remote sensing data and application to a global chemistry model, *J. Geophys. Res.*, *101*, 21,051–21,065, 1996.

De Bruyn, W. J., and E. S. Saltzman, Diffusivity of methyl bromide in water, *Mar. Chem.*, *57*, 55–59, 1997.

Defries, R. S., and J. R. G. Townshend, NDVI-derived land cover classification at a global scale, *Int. J. Remote Sens.*, *15*, 3567–3586, 1994.

DeMore, W. B., S. P. Sander, C. J. Howard, A. R. Ravishankara, D. M. Golden, C. E. Kolb, R. F. Hampson, M. J. Kurylo, and M. J. Molina, Chemical kinetics and photochemical data for use in stratospheric modeling: Evaluation number 12, *JPL Publ.*, *97–4*, 266 pp., 1997.

Derwent, R. G., and A. E. J. Eggleton, Halocarbon lifetimes and concentration distributions calculated using a two-dimensional tropospheric model, *Atmos. Environ.*, *12*, 1261–1269, 1978.

Derwent, R. G., and A. Volz-Thomas, The tropospheric lifetimes of halocarbons and their reactions with OH radicals: An assessment based on the concentration of ^{14}CO, in *Alternative Fluorocarbon Environmental Acceptability Study: Scientific Assessment of Stratospheric Ozone, 1989*, vol. 11, *Appendix, Rep. 20*, pp. 125–146, Global Ozone Res. and Monit. Proj., World Meteorol. Organ., Geneva, 1990.

Dimmer, C. H., R. G. Simmonds, G. Nickless, and M. R. Bassford, Biogenic fluxes of halomethances from Irish peatland ecosystems, *Atmos. Environ.*, *35*, 321–330, 2001.

Elliott, S., and F. S. Rowland, Nucleophilic substitution rates and solubilities for methyl halides in seawater, *Geophys. Res. Lett.*, *20*, 1043–1046, 1993.

Gan, J., S. R. Yates, H. D. Ohr, and J. J. Sims, Production of methyl bromide by terrestrial higher plants, *Geophys. Res. Lett.*, *25*, 3595–3598, 1998.

Gross, M. G., *Oceanography: A View of the Earth*, Prentice-Hall, Old Tappan, N. J., 1972.

Groszko, W., and R. M. Moore, Ocean-atmosphere exchange of methyl bromide: NW Atlantic and Pacific Ocean studies, *J. Geophys. Res.*, *103*, 16,737–16,741, 1998.

Hao, W. M., Industrial sources of atmospheric nitrogen oxide, methyl chloride and methyl bromide, Ph.D. thesis, Harvard Univ., Cambridge, Mass., 1986.

Hao, W. M., M. H. Liu, and P. J. Crutzen, Estimates of annual and regional releases of CO_2 and other trace gases to the atmosphere from fires from the tropics, based on FAO statistics for the period 1975–1980, in *Fire in the Tropical Biota: Ecosytems, Processes and Global Challenges, Ecol. Stud.*, vol. 84, edited by J. G. Goldammer, pp. 440–462, Springer-Verlag, New York, 1991.

Hough, A. M., The development of a two-dimensional global tropospheric model: 1, *The model transport, Atmos. Environ.*, *23*, 1235–1261, 1989.

Hough, A. M., Development of a two-dimensional global tropospheric model: Model chemistry, *J. Geophys. Res.*, *96*, 7325–7362, 1991.

Khalil, M. A. K., R. A. Rasmussen, and R. Gunawardena, Atmospheric methyl bromide: Trends and global mass balance, *J. Geophys. Res.*, *98*, 2887–2896, 1993.

King, D. B., and E. S. Saltzman, Removal of methyl bromide in coastal seawater: Chemical and biological rates, *J. Geophys. Res.*, *102*, 18,715–18,721, 1997.

King, D., B. Butler, J. H. Montzka, S. A. Yvon-Lewis, and S. A. Elkins, Implications of methyl bromide supersaturations in the temperate North Atlantic Ocean, *J. Geophys. Res.*, *105*, 19,763–19,769, 2000.

Ko, M. K. W., C. H. Jackman, B. A. Boville, C. Bruehl, P. Connell, A. Golombek, J. Levy, J. M. Rodriguez, T. Sasaki, and K. K. Tung, Model calculations of atmospheric lifetime, in *Report on Concentrations, Lifetimes and Trends of CFCs, Halons and Related Species*, edited by J. A. Kaye, S. A. Penkett, and F. M. Ormond, pp. 5-1–5-33, Sci. Div., NASA Off. of Mission to Planet Earth, Washington, D. C., 1994.

Korson, L., W. Drost-Hansen, and F. J. Millero, Viscosity of water at various temperatures, *J. Phys. Chem.*, *73*, 34–39, 1969.

Kurylo, M. J., et al., Short-lived ozone related compounds, in *Scientific Assessment of Ozone Depletion: 1998*, *Rep. 44*, chap. 2, pp. 2.1–2.56, Global Ozone Res. and Monit. Proj., World Meteorol. Organ., Geneva, 1999.

Langenfelds, R. J., P. J. Fraser, R. J. Francey, L. P. Steele, L. W. Porter, and C. E. Allison, The Cape Grim air archive: The first seventeen years, in *Baseline 94–95*, edited by R. J. Francey, A. L. Dick, and N. Derek, pp. 53–70, Bur. Meteorol. and CSIRO Atmos. Res., Melbourne, Victoria, Australia, 1996.

Lee-Taylor, J. M., and E. A. Holland, Litter decomposition as a potential natural source of methyl bromide, *J. Geophys. Res.*, *105*, 8857–8864, 2000.

Lee-Taylor, J. M., S. C. Doney, G. P. Brasseur, and J.-F. Müller, A global three-dimensional atmosphere-ocean model of methyl bromide distributions, *J. Geophys. Res.*, *103*, 16,039–16,057, 1998.

Le Goupil, M., Les proprietes insecticides du bromure de methyle, *Rev. Pathol. Végétale Entomol. Agricole Fr.*, *19*, 169–172, 1930.

Li, Y. H., H. Peng, W. S. Broecker, and H. G. Östlund, The average vertical mixing coefficient for the oceanic thermocline, *Tellus, Ser. B*, *36*, 212–217, 1984.

Lobert, J. M., J. H. Butler, S. A. Montzka, L. S. Geller, R. C. Meyers, and J. W. Elkins, A net sink for atmospheric CH_3Br in the East Pacific Ocean, *Science*, *267*, 1002–1005, 1995.

Lobert, J. M., J. H. Butler, L. S. Geller, S. A. Yvon, S. A. Montzka, R. C. Meyers, A. D. Clarke, and J. W. Elkins, BLAST94: Bromine latitudinal air/sea transect 1994, *NOAA Tech. Memo. ERL CMDL-10*, Natl. Oceanic and Atmos. Admin., Boulder, Colo., 1996.

Lobert, J. M., S. A. Yvon-Lewis, J. H. Butler, S. A. Montzka, and R. C. Meyers, Undersaturation of CH_3Br in the Southern Ocean, *Geophys. Res. Lett.*, *24*, 171–172, 1997.

Lobert, J. M., W. C. Keene, J. A. Logan, and R. Yevich, Global chlorine emissions from biomass burning: Reactive Chlorine Emissions Inventory, *J. Geophys. Res.*, *104*, 8373–8389, 1999.

Louis, J. F., Mean meridional circulation, the natural stratosphere of 1974, *CIAP Monogr. 1, DOT-TST-75–51*, Dep. of Transport, Washington, D. C., 1975.

Manö, S., and M. O. Andreae, Emissions of methyl bromide from biomass burning, *Science*, *263*, 1255–1256, 1994.

Methyl Bromide Technical Options Committee (MBTOC), 1998 assessment of alternatives to methyl bromide, U. N. Envrion. Programme, Nairobi, Kenya, 1998.

Miller, B. R., Abundances and trends of atmospheric chlorodifluoromethane and bromomethane, Ph.D. thesis, Univ. of Calif., San Diego, 1998.

Millero, F. J., Seawater as a multicomponent electrolyte solution, in *The Sea*, vol. 5, edited by E. D. Goldberg, pp. 3–80, John Wiley, New York, 1974.

Moelwyn-Hughes, E. A., The hydrolysis of methyl halides, *Proc. R. Soc. London, Ser. A.*, *164*, 294–306, 1938.

Monro, H. A. U., *Manual of Fumigation for Insect Control, FAO Agric. Stud.*, vol. 79, 2nd ed., Food and Agric. Organ., Rome, 1979.

Moore, R. M., and M. Webb, The relationship between methyl bromide and chlorophyll α in high latitude ocean waters, *Geophys. Res. Lett.*, *23*, 2951–2954, 1996.

Moore, R., M. Webb, M. Tokarczyk, and R. Wever, Bromoperoxidase and iodoperoxidase enzymes and production of halogenated methanes in marine diatom cultures, *J. Geophys. Res.*, *101*, 20,899–20,908, 1996.

Newel, R. E., J. W. Kidson, D. G. Vincent, and G. J. Boer, *The General Circulation of the Tropical Atmosphere and Interactions With the Extratropical Latitudes*, vol. 1, MIT Press, Cambridge, Mass., 1972.

Oram, D. E., C. E. Reeves, S. A. Penkett, and P. J. Fraser, Measurements of HCFC-142b and HCFC-141b in the Cape Grim air archive: 1978–1993, *Geophys. Res. Lett.*, *22*, 2741–2744, 1995.

Oram, D. E., C. E. Reeves, W. T. Sturges, S. A. Penkett, P. J. Fraser, and R. L. Langenfelds, Recent tropospheric growth rate and distribution of HFC-134a (CH_2FCF_3), *Geophys. Res. Lett.*, *23*, 1949–1953, 1996.

Prinn, R. G., R. F. Weiss, B. R. Miller, J. Huang, F. N. Alyea, D. M. Cunnold, P. J. Fraser, D. E. Hartley, and P. G. Simmonds, Atmospheric trends and lifetime of trichloroethane and global average hydroxyl radical concentrations based on 1978–1994 ALE/GAGE measurements, *Science*, *269*, 187–192, 1995.

Prinn, R. G., et al., A history of chemically and radiatively important gases in air deduced from ALE/GAGE/AGAGE, *J. Geophys. Res.*, *105*, 17,751–17,792, 2000.

Prinn, R. G., et al., Evidence for substantial variations of atmospheric hydroxyl radicals in the past two decades, *Science*, *292*, 1882–1888, 2001.

Pyle, J. A., et al., Stratospheric ozone 1999, *DETR Ref. 99EP0458,* sixth report, U.K. Stratospheric Ozone Rev. Group, Dep. of the Environ., Transp. and the Reg., Her Majesty's Stn. Off., London, 1999.

Redeker, K. R., N.-Y. Wang, J. C. Low, A. McMillan, S. C. Tyler, and R. J. Cicerone, Emissions of methyl halides and methane from rice paddies, *Science*, *290*, 966–969, 2000.

Reeves, C. E., and S. A. Penkett, The anthropogenic contribution to atmospheric methyl bromide, *Geophys. Res. Lett.*, *20*, 1563–1566, 1993.

Rhew, R. C., B. R. Miller, and R. F. Weiss, Natural methyl bromide and methyl chloride emissions from coastal salt marshes, *Nature*, *403*, 292–295, 2000.

Rhew, R., C. Miller, B. R. Vollmer, and M. K. Weiss, Shrubland fluxes of methyl bromide and methyl chloride, *J. Geophys. Res.*, *106*, 20,875–20,882, 2001.

Sæmundsdóttir, S., and P. A. Matrai, Biological production of methyl bromide by cultures of marine phytoplankton, *Limnol. Oceanogr.*, *43*, 81–87, 1998.

Saini, H. S., J. M. Atteih, and D. Hanson, Biosynthesis of halomethanes and methanethiol higher plants via a novel methyl transferase reaction, *Plant Cell Environ.*, *18*, 1027–1033, 1995.

Scarrat, M. G., and R. M. Moore, Production of methyl bromide and methyl chloride in laboratory cultures of marine phytoplankton II, *Mar. Chem.*, *59*, 311–320, 1998.

Schauffler, S. M., E. L. Atlas, F. Flocke, R. A. Lueb, V. Stroud, and W. Travnicek, Measurements of bromine organic compounds at the tropical tropopause, *Geophys. Res. Lett.*, *25*, 317–320, 1998.

Serca, D., A. Guenther, L. Klinger, D. Helmig, D. Hereid, and P. Zimmerman, Methyl bromide deposition to soils, *Atmos. Environ.*, *32*, 1581–1586, 1998.

Shorter, J. H., C. E. Kolb, P. M. Crill, R. A. Kerwin, R. W. Talbot, M. E. Hines, and R. C. Harriss, Rapid degradation of atmospheric methyl bromide in soils, *Nature*, *377*, 717–719, 1995.

Sturges, W. T., H. P. McIntyre, S. A. Penkett, J. Chappellaz, J.-M. Barnola, R. Mulvaney, E. Atlas, and V. Stroud, Methyl bromide and other brominated methanes and methyl iodide in polar firn air, *J. Geophys. Res.*, *106*, 1595–1606, 2001a.

Sturges, W. T., S. A. Penkett, J. M. Barnola, J. Chappellaz, E. Atlas, and V. Stroud, A long-term record of carbonyl sulfide (COS) in two hemispheres from firn air measurements, *Geophys. Res. Lett.*, *28*, 4095–4098, 2001b.

Sturrock, G. A., L. W. Porter, and P. J. Fraser, In situ measurements of CFC replacement chemicals and other halocarbons at Cape Grim: The AGAGE GC-MS program, in *Baseline 97–98*, edited by N. W. Tindale, N. Derek, and F. J. Francey, pp. 43–49, Bur. Meteorol. and CSIRO Atmos. Res., Melbourne, Victoria, Australia, 2001.

Thomas, V. M., J. A. Bedford, and R. J. Cicerone, Bromine emissions from leaded gasoline, *Geophys. Res. Lett.*, *24*, 1371–1374, 1997.

Thomas, W. B., Methyl bromide use background document, internal document, U.S. Environ. Prot. Agency, Washington, D. C., 1999.

Tokarczyk, R., and E. S. Saltzman, Methyl bromide loss rates in surface waters of the North Atlantic Ocean, Caribbean Sea, and eastern Pacific Ocean (8°–45°N), *J. Geophys. Res.*, *106*, 9843–9851, 2001.

Tokarczyk, R., K. D. Goodwin, and E. S. Saltzman, Methyl bromide loss rate constants in the North Pacific Ocean, *Geophys. Res. Lett.*, *28*, 4429–4432, 2001.

United Nations, World population 1998, *U. N. Publ. ST/ESA/SER. A/176, Sales E.99.XIII.6*, Geneva, 1999.

Varner, R. K., P. M. Crill, R. W. Talbot, and J. H. Shorter, An estimate of the uptake of atmospheric methyl bromide by agricultural soils, *Geophys. Res. Lett.*, *26*, 727–730, 1999a.

Varner, R. K., P. M. Crill, and R. W. Talbot, Wetlands: A potentially significant source of atmospheric methyl bromide and methyl chloride, *Geophys. Res. Lett.*, *26*, 2433–2436, 1999b.

Volz, A., D. H. Ehalt, and R. G. Derwent, Seasonal and latitudinal variation of ^{14}CO and the tropospheric concentration of OH radicals, *J. Geophys. Res.*, *86*, 5163–5171, 1981.

Wanninkhof, R., Relationship between wind speed and gas exchange over the ocean, *J. Geophys. Res.*, *97*, 7373–7382, 1992.

Wilhelm, S., and A. O. Paulus, How soil fumigation benefits the California strawberry industry, *Plant Disease*, *64*, 265–270, 1980.

Wingenter, O. W., C. J.-L. Wang, D. R. Blake, and F. S. Rowland, Seasonal variation of tropospheric methyl bromide concentrations: Constraints on anthropogenic input, *Geophys. Res. Lett.*, *25*, 2797–2800, 1998.

Woodwell, G. M., P. H. Rich, and C. A. S. Hall, Carbon in estuaries, in *Carbon and the Biosphere, Brookhaven Symp. Biol.*, vol. 24, edited by G. M. Woodwell and E. V. Pecan, pp. 221–240, U.S. At. Energy Comm., Washington, D. C., 1973.

Yokouchi, Y., T. Machida, L. A. Barrie, D. Toom-Sauntry, Y. Nojiri, Y. Fujinuma, Y. Inuzuka, H. J. Li, H. Akimoto, and S. Aoki, Latitudinal distribution of atmospheric methyl bromide: Measurements and modeling, *Geophys. Res. Lett.*, *27*, 697–700, 2000.

Yokouchi, Y., M. Ikeda, Y. Inuzuka, and T. Yukawa, Strong emission of methyl chloride from tropical plants, *Nature*, *416*, 163–165, 2002a.

Yokouchi, Y., D. Toom-Sauntry, K. Yazawa, T. Inagaki, and T. Tamura, Recent decline of methyl bromide in the troposphere, *Atmos. Environ.*, *36*, 4985–4989, 2002b.

Yvon-Lewis, S. A., and J. H. Butler, The potential effect of the oceanic biological degradation on the lifetime of atmospheric CH_3Br, *Geophys. Res. Lett.*, *24*, 1227–1230, 1997.

C. E. Reeves, School of Environmental Sciences, University of East Anglia, Norwich, Norfolk NR4 7TJ, UK. (c.reeves@uea.ac.uk)

A three-dimensional global model study of atmospheric methyl chloride budget and distributions

Yasuko Yoshida, Yuhang Wang, and Tao Zeng
School of Earth and Atmospheric Sciences, Georgia Institute of Technology, Atlanta, Georgia, USA

Robert Yantosca
Division of Engineering and Applied Sciences, Harvard University, Cambridge, Massachusetts, USA

Received 23 April 2004; revised 3 September 2004; accepted 12 October 2004; published 29 December 2004.

[1] Global simulations of atmospheric methyl chloride (CH_3Cl) are conducted using the GEOS-CHEM model in order to understand better its sources and sinks. Observations from 7 surface sites and 9 aircraft field experiments are used to evaluate the model simulations with assimilated meteorology fields for 7 years. The model simulates CH_3Cl observations at northern mid and high latitudes reasonably well. The seasonal variation of CH_3Cl at southern mid and high latitudes is severely overestimated, however. Simulated vertical profiles of CH_3Cl are in general agreement with the observations in most regions; the disagreement occurs in the vicinities of major sources, principally reflecting the uncertainties in the estimated distributions of our added pseudobiogenic and the biomass burning sources. Our estimate of known sources (1.5 Tg yr^{-1}) from ocean, biomass burning, incineration/industry, salt marshes, and wetlands accounts for only 34% of the total source (4.4 Tg yr^{-1}). We hypothesize that the missing source of 2.9 Tg yr^{-1} is likely of biogenic origin. On the basis of the observed CH_3Cl seasonality at northern mid and high latitudes, we find that this pseudobiogenic source is located at 30°N–30°S, not at mid and high latitudes. If so, the observed CH_3Cl latitudinal distribution indicates that the annual hemispheric mean OH ratio is within the range of 0.8–1.3. The net uptake regions by ocean are located at high latitudes. A relatively small loss of 150 Gg yr^{-1} over these regions is critical for the model to reproduce the observed annual mean latitudinal gradient of CH_3Cl in the southern hemisphere. The large overestimate of the seasonal variation of CH_3Cl at southern mid and high latitudes likely implies that the seasonality of simulated oceanic uptake is incorrect as a result of defects in the parameterization of this loss in the model. *INDEX TERMS:* 0322 Atmospheric Composition and Structure: Constituent sources and sinks; 0365 Atmospheric Composition and Structure: Troposphere—composition and chemistry; 0312 Atmospheric Composition and Structure: Air/sea constituent fluxes (3339, 4504); *KEYWORDS:* atmospheric methyl chloride, sources and sinks, global model study

Citation: Yoshida, Y., Y. Wang, T. Zeng, and R. Yantosca (2004), A three-dimensional global model study of atmospheric methyl chloride budget and distributions, *J. Geophys. Res.*, *109*, D24309, doi:10.1029/2004JD004951.

1. Introduction

[2] Methyl chloride (CH_3Cl) is one of the most abundant chlorine-containing gas in the atmosphere; it is a major contributor to stratospheric chlorine. The global average mixing ratio of CH_3Cl in the troposphere is measured at about 550 ± 30 parts per trillion per volume (pptv) [*Montzka et al.*, 2003]. It is believed that CH_3Cl originates in large part from natural sources [*Khalil et al.*, 1999]. According to the emission data provided in the Reactive Chlorine Emissions Inventory (RCEI) conducted under the International Global Atmospheric Chemistry (IGAC) Global Emissions Inventory Activity (GEIA) project, known sources such as biomass burning, ocean, incineration/industrial sources are 910 (650–1120), 650 (40–950), and 162 (30–294) Gg (giga gram = 10^9 gram) yr^{-1}, respectively [*Keene et al.*, 1999; *Khalil et al.*, 1999; *Lobert et al.*, 1999; *McCulloch et al.*, 1999]. Emission from certain wood-rotting fungi is estimated at 156 (35–385) Gg yr^{-1}, though no global distribution is currently available [*Watling and Harper*, 1998; *Khalil et al.*, 1999; *Lee-Taylor et al.*, 2001]. In addition, *Rhew et al.* [2000] estimated annual global release of 170 (65–440) Gg of CH_3Cl from salt marshes and *Varner et al.* [1999] calculated a global flux of 48 Gg yr^{-1} from wetlands.

[3] The major removal process of CH_3Cl in the atmosphere is due to oxidation by OH radicals, which accounts for 3.5 (2.8–4.6) Tg (tera gram = 10^{12} gram) loss per year [*Koppmann et al.*, 1993]. It is estimated that about 285 Gg

0148-0227/04/2004JD004951$09.00

of tropospheric CH_3Cl is transported to the stratosphere and lost there by photo dissociation and OH oxidation. Although the ocean is a net source globally, it is a significant net local sink in high-latitude regions. The RCEI estimate for the oceanic sink over the net uptake regions is 150 Gg yr^{-1} [*Moore et al.*, 1996; *Khalil et al.*, 1999; *Keene et al.*, 1999]. Soils are recognized as an additional sink, and *Keene et al.* [1999] estimated that it could be as much as 256 Gg yr^{-1}, but the uncertainty is quite high [*Lee-Taylor et al.*, 2001; *Rhew et al.*, 2001]. The CH_3Cl budget based on the current "best guess" estimates given above leaves a substantial deficit for sources by $\sim$1.8 Tg yr^{-1}. This imbalance might be explained by one or some combination of the following: (1) the emission from one or more sources is underestimated; (2) the CH_3Cl loss by reaction with OH is overestimated; (3) there exists some significant unidentified source(s) of CH_3Cl [*Keene et al.*, 1999].

[4] The overall uncertainties in CH_3Cl emissions from known sources are relatively large and the estimated OH sink has significant uncertainties that come in part from the uncertainties in the temperature dependence of the OH + CH_3Cl reaction rate constant [*Keene et al.*, 1999; *Lee-Taylor et al.*, 2001]. After examining the results of a series of model runs using different OH reaction rates, *Lee-Taylor et al.* [2001] concluded that the budget imbalance is not due to assumption 2 above. Their model results with identified emissions showed a significant interhemispheric gradient, which was not observed. In order to remove the gradient, some unidentified source must exist at high latitudes in the southern hemisphere such as oceanic emissions, which might be unrealistic considering available oceanic observations. Therefore they concluded that the budget discrepancy likely comes from a land-based missing source [*Lee-Taylor et al.*, 2001].

[5] *Yokouchi et al.* [2000] reported that enhanced mixing ratios of CH_3Cl were correlated with α-pinene, a short-lived species emitted by vegetation, in air masses over subtropical Okinawa Island. Strong emissions of CH_3Cl from tropical plants were observed by *Yokouchi et al.* [2002], and they suggested that tropical forests could be the major source. However, emission fluxes and the detailed emission mechanisms from terrestrial vegetation are unknown [*Keene et al.*, 1999; *Yokouchi et al.*, 2000, 2002].

[6] Very few global 3-D simulations of CH_3Cl have been conducted. *Lee-Taylor et al.* [2001] presented a 3-D model study for CH_3Cl distributions, but they evaluated their results using only surface observations and did not interpret the results in terms of contributions of each source to the observed concentrations and seasonal variations. In this paper we present more comprehensive modeling and analyses of CH_3Cl on the basis of surface and aircraft observations using the global GEOS-CHEM model.

2. Model Description

[7] The model used in this study is the GEOS-CHEM (version 5.02) global 3-D chemical transport model of tropospheric chemistry driven by assimilated meteorological fields from the Goddard Earth Observing System (GEOS) of the NASA Global Modeling and Assimilation Office (GMAO) (http://www-as.harvard.edu/chemistry/trop/geos/) [*Bey et al.*, 2001]. We use a horizontal resolution of 4° latitude $\times$ 5° longitude. The vertical layers vary by different model simulation years. In order to compare to atmospheric field experiments, we simulated the CH_3Cl distributions using 7 different meteorological fields for the years of 1991, 1992, 1994, 1995, August 1996–September 1997, 2000, and 2001. For simulation years before December 1995, the model has 20 vertical levels, for December 1995, 1996 and 1997, 26 levels, and for 2000 and 2001, 48 levels. To calculate the chemical loss of CH_3Cl, the tropospheric OH field was taken from the GEOS-CHEM full-chemistry simulation by *Martin et al.* [2003] and the stratospheric OH field taken from a 2-D stratosphere/mesosphere model was used [*Schneider et al.*, 2000]. The tropospheric OH field yields a global mean methyl chloroform (CH_3CCl_3) lifetime of 5.6 years in good agreement with the observations [*Spivakovsky et al.*, 2000; *Prinn et al.*, 2001; *Martin et al.*, 2003]. In this study, CH_3Cl emitted from different sources is transported as separate tracers. In this manner, contributions from each source to the spatial and temporal distributions of CH_3Cl can be evaluated in the model.

3. Sources of CH_3Cl

3.1. Biomass Burning

[8] Biomass burning is the largest known source of CH_3Cl. *Lobert et al.* [1999] estimated 910 (650–1120) Gg yr^{-1} emissions from this source in the RCEI inventory on a 1° $\times$ 1° grid based on the emission ratios of CH_3Cl to CO and CO_2. Hot spots of emission are located in the regions of Southeast Asia, India, tropical Africa and South America. No seasonality was given in the inventory; we scaled their annual biomass burning CH_3Cl flux with seasonal biomass and biofuel burning CO emissions used in GEOS-CHEM. The satellite observation-based biomass burning CO inventory was obtained from *Duncan et al.* [2003] except for the time period of February–April 2001, when the monthly inventory by *Heald et al.* [2003] is used. Model simulations using this inventory show large overestimates over the western Pacific. *Lee-Taylor et al.* [2001] reduced the biomass burning source over Southeast Asia by 50% in the RCEI inventory. In our work, we apply a CH_3Cl/CO molar emission ratio of 5.7 $\times$ 10^{-4} [*Lobert et al.*, 1999] to estimate a new biomass burning CH_3Cl source of 611 $\pm$ 38 Gg yr^{-1}. The range reflects the interannual variability of biomass burning CO by *Duncan et al.* [2003] and *Heald et al.* [2003]. The estimate used in our study is at the lower limit calculated by *Lobert et al.* [1999]. We found that a lower biomass burning source is in better agreement with the observations (section 5).

3.2. Oceanic Emissions

[9] The ocean is the second largest known source of CH_3Cl. In the RCEI inventory, *Khalil et al.* [1999] estimated an annual net oceanic emission of CH_3Cl of 655 Gg yr^{-1} using an empirical relationship between sea surface temperature (SST) and CH_3Cl saturation anomaly. Oceanic emissions are located mainly in the tropics and subtropics. At latitudes higher than 50°, the ocean is a net sink. The estimated uncertainties of the oceanic flux are a factor of 2 to 3, mainly due to measurement uncertainties of several variables used in the transfer velocity calculation [*Khalil et*

al., 1999]. Based on the measured solubility of CH_3Cl in seawater at different temperatures, *Moore* [2000] estimated a net CH_3Cl flux of 300–400 Gg yr^{-1} from the ocean including a global annual ocean uptake of 90–150 Gg. In this study, we recalculated the oceanic flux using the National Oceanic and Atmospheric Administration Climate Monitoring and Diagnostics Laboratory (NOAA-CMDL) empirical relationship between saturation and SST as by *Khalil et al.* [1999] with monthly climatological wind speed distributions. The wind data are taken from the revised monthly mean summaries of the Comprehensive Ocean-Atmosphere Data Set (COADS) produced at University of Wisconsin-Milwaukee in collaboration with NOAA/National Oceanographic Data Center [*daSilva et al.*, 1994]. Sea surface temperature fields are the 10-year averages (1990–1999) of a global extended reconstructed SST (ERSST) produced by *Smith and Reynolds* [2003] based on the COADS data. The sea-air interface transfer velocity of CH_3Cl (k) was calculated following *Wanninkhof* [1992]:

$$k\left(\text{cm h}^{-1}\right) = 0.39\ v^2 (S_c/660)^{-1/2}, \quad (1)$$

$$S_c = 2385 \times \left[1 - 0.065(\text{SST}) + 0.002043(\text{SST})^2 - 2.6 \times 10^{-5}(\text{SST})^3\right], \quad (2)$$

where v is the long-term average wind speed (m s^{-1}) at 10 m above sea level, S_c is the unitless Schmidt number of CH_3Cl, and SST is in °C [*Khalil and Rasmussen*, 1999; *Khalil et al.*, 1999].

[10] In our model calculation, monthly mean sea ice coverage is applied to prevent CH_3Cl loss to the sea ice. The sea ice data are taken from the International Satellite Land-Surface Climatology Project (ISLSCP) Initiative II data archive [*Hall et al.*, 2003]. Our model result of the global annual oceanic flux is about 350 Gg yr^{-1}, which is 20% lower than the value estimated by a direct extrapolation of in situ observations (440 Gg yr^{-1}) by *Khalil et al.* [1999] and 47% lower than the 655 Gg yr^{-1} in the RCEI inventory, but is in the same range given by *Moore* [2000]. A critical issue we found in the comparison of simulated and observed surface CH_3Cl concentrations is the ocean loss over the uptake region at southern high latitudes. Our estimate of 30 Gg yr^{-1} is much lower than that in the RCEI inventory of 150 Gg yr^{-1}. Therefore we use two inventories to account for the difference. The first inventory is as described above. In the second inventory, we increased the sink over ocean uptake regions to 150 Gg yr^{-1}. The emissions over the net source regions are increased to ~500 Gg yr^{-1} (by ~30%) in order to maintain the net ocean source of 350 Gg yr^{-1}.

3.3. Incineration/Industrial Emissions

[11] It is known that CH_3Cl is released into the atmosphere from combustion of fossil fuels with high chlorine contents such as coal. Combustion of domestic and municipal waste containing chlorine also emits CH_3Cl. *McCulloch et al.* [1999] calculated the global emissions from fossil fuel combustion and waste incineration to be 75 ± 70 and 32 ± 23 Gg Cl yr^{-1}, respectively. They also estimated a source of 7 Gg Cl yr^{-1} from other industrial sources. The total CH_3Cl emission from coal combustion, incineration and other industrial activities is then estimated as 162 (114 ± 93) Gg yr^{-1} in the RCEI inventory [*McCulloch et al.*, 1999]. In this study, we applied the nonseasonal RCEI emission inventory for this source.

3.4. Salt Marshes and Wetlands

[12] *Rhew et al.* [2000] estimated the global CH_3Cl emissions from salt marshes as 170 (65–440) Gg yr^{-1} based on field studies from two coastal salt marshes in California. We distribute the flux using a land cover database from the International Satellite Land Surface Climatology Project (ISLSCP) Initiative I data [*Sellers et al.*, 1995]. We confine the emissions to the growing season such as May to September at northern mid to high latitudes and November to March at southern mid to high latitudes.

[13] The global CH_3Cl flux from freshwater wetlands was calculated by *Varner et al.* [1999] as 48 Gg yr^{-1}. In our model, the emissions are distributed using the ISLSCP Initiative I land cover data [*Sellers et al.*, 1995] and are limited to the growing season in the same manner as in the salt marsh emission calculation.

3.5. Biogenic Emissions

[14] Close correlations between enhanced concentrations of CH_3Cl and αpinene, which is emitted by terrestrial plants, have been observed [*Yokouchi et al.*, 2000]. *Yokouchi et al.* [2002] reported that some particular plant families in tropical forests (certain types of ferns and Dipterocarpaceae) emit a significant amount of CH_3Cl. They calculated that the emission from only Dipterocarpaceae species in Asian tropical forests could be 910 Gg yr^{-1} by extrapolating emission rates obtained from CH_3Cl flux measurements in a glasshouse, although the uncertainty is very large. *Hamilton et al.* [2003] estimated a global annual CH_3Cl production of 75–2500 Gg between 30°N and 30°S based on their CH_3Cl flux observation from senescent and dead leaves. *Lee-Taylor et al.* [2001] conducted model studies for CH_3Cl, assuming that terrestrial vegetation plays a significant role in CH_3Cl production. They concluded that the model most successfully reproduced the observed mixing ratios of CH_3Cl when they added 2330–2430 Gg yr^{-1} of a hypothetical biogenic source combined with a 50% reduction of biomass-burning emissions from Southeast Asia in the RCEI biomass burning inventory.

[15] In our study, 2430–2900 Gg yr^{-1} is added as the biogenic source of CH_3Cl. We distributed the biogenic source to all vegetated areas between 30°N and 30°S. The land cover classification is based on the ISLSCP Initiative I data set [*DeFries and Townshend*, 1994]. The uniform distribution over all vegetated areas with the flat annual emission rate is based on model sensitivity analyses (the results are not shown) since currently the dependence of biogenic CH_3Cl emission on vegetation, temperature, and sunlight is unknown. The major constraint is the observed seasonal variation of CH_3Cl at northern mid and high latitudes. Biogenic emissions at mid and high latitudes in summer would lead to overestimates of CH_3Cl in those regions. Furthermore, scaling biogenic CH_3Cl emission to the seasonality of isoprene [e.g., *Lee-Taylor et al.*, 2001] would also lead to a too small seasonal variation in

comparison to the observations because the seasonality of isoprene emissions is opposite to the observed seasonality of CH_3Cl. Our calculated emissions between 30°S–30°N account for 93% of the global CH_3Cl source, which agrees with the estimates by *Khalil and Rasmussen* [1999], who suggested that 85% of the emission of CH_3Cl comes from tropical and subtropical regions based on their inverse modeling results with simplified box models for tropospheric transport and OH oxidation.

4. Sinks of CH_3Cl

4.1. Reaction With OH

[16] The main sink of CH_3Cl in the atmosphere is oxidation by hydroxyl radicals:

$$(R1) \qquad CH_3Cl + OH \rightarrow CH_2Cl + H_2O.$$

In our model calculation, we used two different reaction rate constants for reaction (R1), k_{97}, and k_{03}, reported by *DeMore et al.* [1997] and *Sander et al.* [2003], respectively. The rate constant (k) is represented by the Arrhenius expression $k = A \exp(-E/RT)$, where values for A given by *DeMore et al.* [1997] and *Sander et al.* [2003] are 4.0×10^{-12} and 2.4×10^{-12} cm^3 s^{-1}, and for E/R, 1400 and 1250 K, respectively. T is temperature (K). The rate constant at 298 K is 3.6×10^{-14} cm^3 s^{-1} for both, and the uncertainty (at 298 K) is 1.2 and 1.15, respectively. The k_{03} value is higher than k_{97} by about 9% at T = 250 K. The calculated global losses of CH_3Cl with the "reference" emissions (Table 1) using k_{97} and k_{03} are 4.1 Tg yr^{-1} for both, which agree with literature values [*Koppmann et al.*, 1993; *Khalil and Rasmussen*, 1999]. The model results with the different k value are compared in section 5.1.

[17] The OH field used is taken from the work by *Martin et al.* [2003]. The interhemispheric ratio of mass-weighted OH is 1.03; about 2.6% higher in the northern hemisphere (NH) than in the southern hemisphere (SH). Calculated annual mean global CH_3CCl_3 lifetime to loss by tropospheric OH is 5.6 years, which is consistent with estimates from observations by *Spivakovsky et al.* [2000] (5.7 ± 0.7 years) and *Prinn et al.* [2001] (6.0 + 1.0, −0.7 years). However, the interhemispheric OH ratio calculated from CH_3CCl_3 measurements using the inverse method varies by study. For instance, the NH/SH ratio estimated by *Prinn et al.* [2001] and *Krol and Lelieveld* [2003] is 0.88 and 0.98, respectively. *Krol and Lelieveld* [2003] commented that the differences between their interhemispheric ratio and that given by *Prinn et al.* [2001] could be due to the model resolution difference. They also explained that their slightly higher OH concentrations in the SH than NH might be derived from model or emission errors. Nearly equal hemispheric mean OH was also reported by *Spivakovsky et al.* [2000].

[18] In order to test the sensitivity of the CH_3Cl distribution to reaction with OH in our model, we conducted three test simulations using OH fields with different NH/SH distribution, such as original OH field (the annual mean NH/SH mass ratio is 1.03), OH increased and decreased by 10% (NH/SH ratio of 1.26), and decreased and increased by 10% (NH/SH ratio of 0.84), in the NH and SH, respectively. Figure 1 shows the resulting latitudinal CH_3Cl distributions with different OH distributions compared with observed concentrations. In these simulations, the reaction rate constant was taken from *Sander et al.* [2003]. The result with the original OH concentrations gives almost symmetrical N-S distribution as observed while results with modified OH fields show clear N-S gradients. It is therefore clear that deviation from the current hemispheric mean OH ratio by ±20% could not reproduce the observed CH_3Cl distributions. The additional constraint on the interhemispheric mean OH ratio is valuable because the estimate is not as sensitive to model errors of the interhemispheric transport as that derived from CH_3CCl_3, the source of which is located in the northern industrial regions.

Table 1. Estimated Global Budget of CH_3Cl[a]

Runs	Reference	OC-1	OC-2	Model Mean
Sources (total)	(4525)	(4214)	(4333)	(4399 ± 43)
Ocean	805[b]	380	499	508 ± 5
Biomass burning	910[c]	554	554	611 ± 38
Incineration/industrial	162[d]	162[d]	162[d]	162[d]
Pseudobiogenic	2430[e]	2900	2900	2900
Salt marshes	170[f]	170[f]	170[f]	170[f]
Wetlands	48[g]	48[g]	48[g]	48[g]
Sinks (total)	(4525)	(4214)	(4333)	(4399 ± 43)
OH reaction	4124	3926	3930	3994 ± 42
Ocean	145[b]	32	147	149 ± 1
Soil	256[h]	256[h]	256[h]	256[h]

[a]Units are in Gg yr^{-1}. Emissions and sinks are calculated as explained in the text, except those taken from the following references.
[b]*Khalil et al.* [1999].
[c]*Lobert et al.* [1999].
[d]*McCulloch et al.* [1999].
[e]*Lee-Taylor et al.* [2001].
[f]*Rhew et al.* [2000].
[g]*Varner et al.* [1999].
[h]*Khalil and Rasmussen* [1999] and *Keene et al.* [1999].

4.2. Soil Sink

[19] The global soil sink of CH_3Cl is estimated to be 256 Gg yr^{-1} [*Keene et al.*, 1999; *Khalil and Rasmussen*, 1999]. No global distribution of the soil uptake rates is available. *Rhew et al.* [2001] found that there is a strong correlation in the measured uptake rates of CH_3Br and CH_3Cl in southern California shrubland ecosystems, and concluded there could be a similar mechanism of consumption for both compounds. In our model, we scaled the soil sink of CH_3Cl with that of methyl bromide (CH_3Br), whose global loss rates were estimated by *Shorter et al.* [1995], assuming that the soil uptake of CH_3Cl is proportional to CH_3Br. The soil type was defined using vegetation type data from the ISLSCP Initiative I data [*DeFries and Townshend*, 1994]. Seasonality was applied by assuming growing seasons of 365, 240, and 180 days in tropical, temperate, and boreal regions, respectively [*Shorter et al.*, 1995]. The calculated annual CH_3Cl loss to soil is, 69, 137, 16, and 34 Gg yr^{-1} for tropical forest/savanna, temperate forest/grassland, boreal forest, and cultivated land, respectively.

5. Results

[20] We conducted several model runs with different input data: one of them employs the sources from existing emission inventories such as the RCEI inventories (for oceanic, biomass burning, incineration/industrial sources)

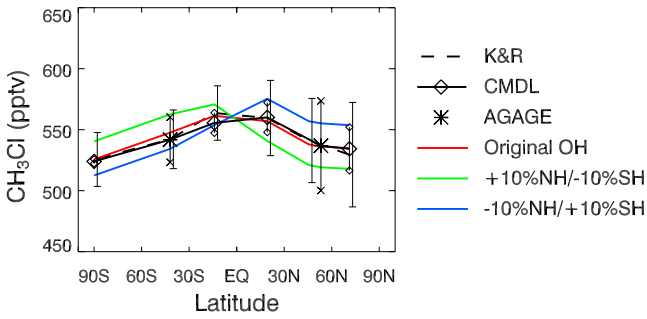

Figure 1. Latitudinal distributions of observed and simulated CH_3Cl at the surface sites. Dashed line indicates data by *Khalil and Rasmussen* [1999] (the data were lowered by 8.3% to account for a calibration difference). The thick black solid line links the CMDL (diamonds) and AGAGE data (asterisks). Thin vertical lines indicate the standard deviations; the end symbols are minus signs, diamonds, and asterisks for K&R, CMDL, and AGAGE data, respectively. Emission inventories for OC-2 (Table 1) are used. Model results are shown with the standard OH concentrations and two perturbation cases, in which the NH and SH hemispheric OH concentrations are either increased or decreased by 10% (see text for more details).

and pseudobiogenic emission of the literature value [i.e., *Lee-Taylor et al.*, 2001], which is referred to as the reference run. Run OC-1 includes the oceanic and biomass burning emissions calculated in our model (section 3). The oceanic sink in run OC-1 is about 80% smaller than that calculated by *Khalil et al.* [1999], and it resulted in higher average surface concentrations in the SH by about 10 pptv (~2%) than in the NH, which is not observed. In run OC-2, oceanic emissions and sinks are increased so that total oceanic sink over net uptake regions becomes the same as that given by RCEI [*Khalil et al.*, 1999] and the net oceanic emissions are the same as in OC-1 run. The runs of reference, OC-1 and OC-2 are simulated with the same meteorological field of September 1996–August 1997. Figure 2 summarizes the latitudinal distributions of the annual-mean emissions and sinks (except the sink via OH oxidation) of CH_3Cl used in those runs. The average values of 7-year model runs (1991, 1992, 1994, 1995, Sep96–Aug97, 2000, 2001) are shown as "model mean." The annual total of the emissions and sinks are listed in Table 1. Figure 3 shows simulated global surface CH_3Cl mixing ratio distributions for January and July. Higher concentrations are simulated over regions where major sources are located. The lower concentrations in the summer hemisphere are due in part to active OH oxidation.

[21] The model results are evaluated with surface and aircraft observations. Seven surface sites and 9 aircraft field experiments are included. Table 2 summarizes these observations used.

5.1. Global Distributions of Atmospheric CH_3Cl Near the Surface

5.1.1. Seasonal Variations

[22] Our model results are compared with three observation data sets measured at 7 surface stations. The locations of these 7 sites are shown in Figure 4. The observed and simulated seasonal variations of CH_3Cl at the stations are compared in Figure 5. The data from *Khalil and Rasmussen* [1999] was lowered by 8.3% in all figures in order to adjust to the calibration difference [*Montzka et al.*, 2003]. We note that the CMDL data may have a systematic error up to 20 pptv due to losses of CH_3Cl in field deployed reference tanks (G. Dutton, personal communication, 2004). There are two observed data sets for Alaska, Hawaii, Samoa, Tasmania and Antarctica, and those two seasonal variations are similar except in Samoa, where the CMDL data show two peaks in February–March and in August, while a single peak in June–July was reported by *Khalil and Rasmussen* [1999].

[23] The model results with a total emission of 4,500 Gg yr^{-1} ("reference" in Table 1) with different OH reaction rate constants (k_{97} and k_{03}, section 4) are shown in Figure 5 as Ref-k97 and Ref-k03, respectively. The other

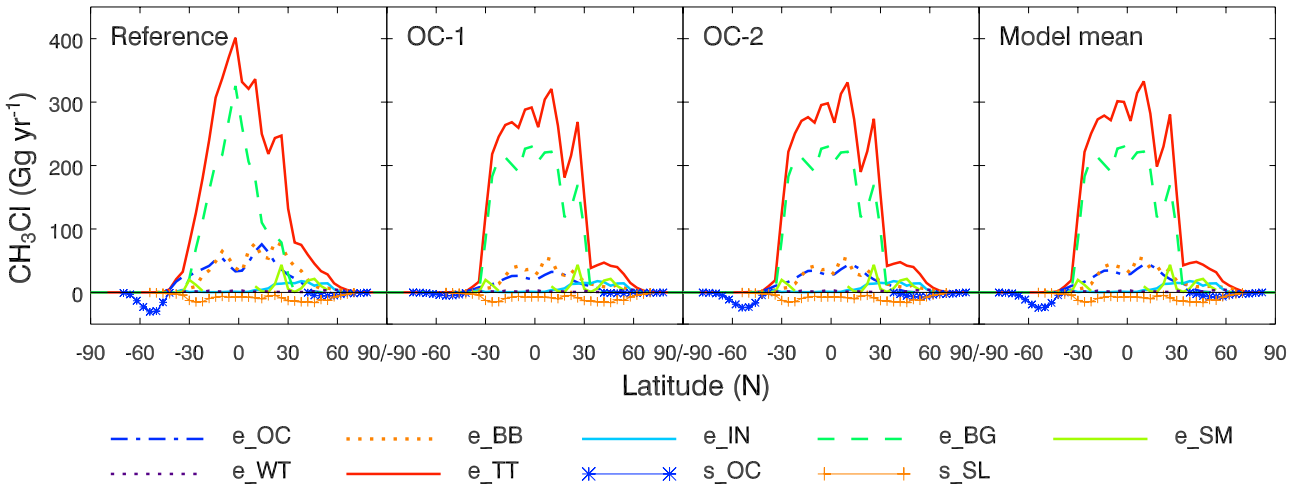

Figure 2. Latitudinal distribution of the known sources and sinks of CH_3Cl. For the legend, "e_" and "s_" denote emission and sink, respectively, and characters OC, BB, IN, BG, SM, WT, TT, SL denote ocean, biomass burning, incineration/industrial, biogenic, salt marshes, wetlands, the total of all emissions, and soil, respectively.

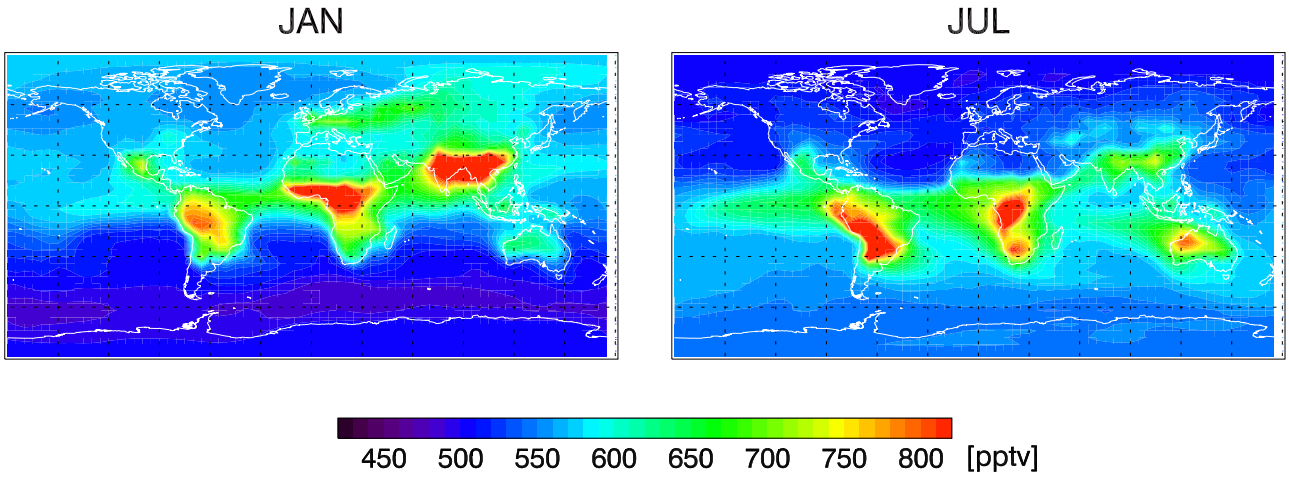

Figure 3. Simulated surface mixing ratio of CH_3Cl for January and July.

model results shown as OC-1, OC-2, and model mean are calculated using k_{03}. The global annual mean surface concentration of Ref-k97 and Ref-k03 is 599 and 579 pptv, respectively, and the difference, about 3%, is solely due to the difference of the reaction rate constants. The reference run with k_{97} (Ref-k97) gives higher concentrations than the observations by 3–18% especially at the tropical and NH sites. Using the rate constant k_{03}, the run Ref-k03 overestimates the observations by up to 14% except for January–June at Tasmania and Antarctica. For these two sites, the OC-2 concentrations are close to the Ref-k03 concentrations except for June–October in Tasmania, where Ref-k03 gives lower concentrations by 3–4%. The overestimates of Ref-k03 indicate that the biomass burning emissions in the RCEI inventory might be overestimated. The wrong seasonality simulated in the Ref-k03 run is due to the scaling of the biogenic source to isoprene emissions, which peak in summer, when observed CH_3Cl shows a minimum.

[24] OC-1 and OC-2 show little difference at all sites except for Tasmania and Antarctica, where the effect of the oceanic uptake of CH_3Cl is significant. OC-2 gives lower concentrations than OC-1 by about 2–5% in better agreement with the observations. The model results with our estimates of biomass burning and oceanic emissions with increased oceanic sink over the uptake regions (OC-2 and model mean) reproduces the general features and the magnitudes of seasonal variations relatively well at northern high latitude stations (Alaska, Ireland, and Oregon), such as maxima in spring to early summer and minima in late summer and fall. At the Hawaii site, the summer overestimate is largest in August in Ref-k97. The peak for the multiyear mean is not as large, but the summer overestimate is apparent, suggesting that the biogenic source upwind

Table 2. Atmospheric Measurements of CH_3Cl

	Region	Time Period	References
Surface Stations			
K&R	Alaska (71.2N, 156.5W) Oregon (45.5N, 124W) Hawaii (19.3N, 154.5W) Samoa (14.1S, 170.6W) Tasmania (42S, 145E) Antarctica (90S)	1981–1997	*Khalil and Rasmussen* [1999]
NOAA-CMDL	Alaska (71.3N, 156.6W) Hawaii (19.5N, 155.6W) Samoa (14.2S, 170.6W) Antarctica (90.0S, 102.0E)	Jan. 1998–March 2002 Dec. 1999–Feb. 2002 Dec. 1998–Feb. 2003 Jan. 2001–Nov. 2003	G. Dutton (personal communication, 2004)
AGAGE	Ireland (53.2N, 9.5W) Tasmania (40.4S, 144.4E)	1998–2001	*Simmonds et al.* [2004]
Aircraft Missions			
PEM-Tropics A	tropical Pacific	Aug.–Oct. 1996	*Blake et al.* [1999a]
PEM-Tropics B	tropical Pacific	March–April 1999	*Blake et al.* [2001]
ACE 1	Pacific/Southern Ocean	Nov.–Dec. 1995	*Blake et al.* [1999b]
TRACE-A	tropical Atlantic	Sept.–Oct. 1992	*Blake et al.* [1996]
INDOEX	Indian Ocean	Feb.–March 1999	*Scheeren et al.* [2002]
PEM-West A	western Pacific	Sept.–Oct. 1991	*Blake et al.* [1997]
PEM-West B	western Pacific	Feb.–March 1994	*Blake et al.* [1997]
TRACE-P	western Pacific	Feb.–April 2001	*Blake et al.* [2003b]
TOPSE	North America	Feb.–May 2000	*Blake et al.* [2003a]

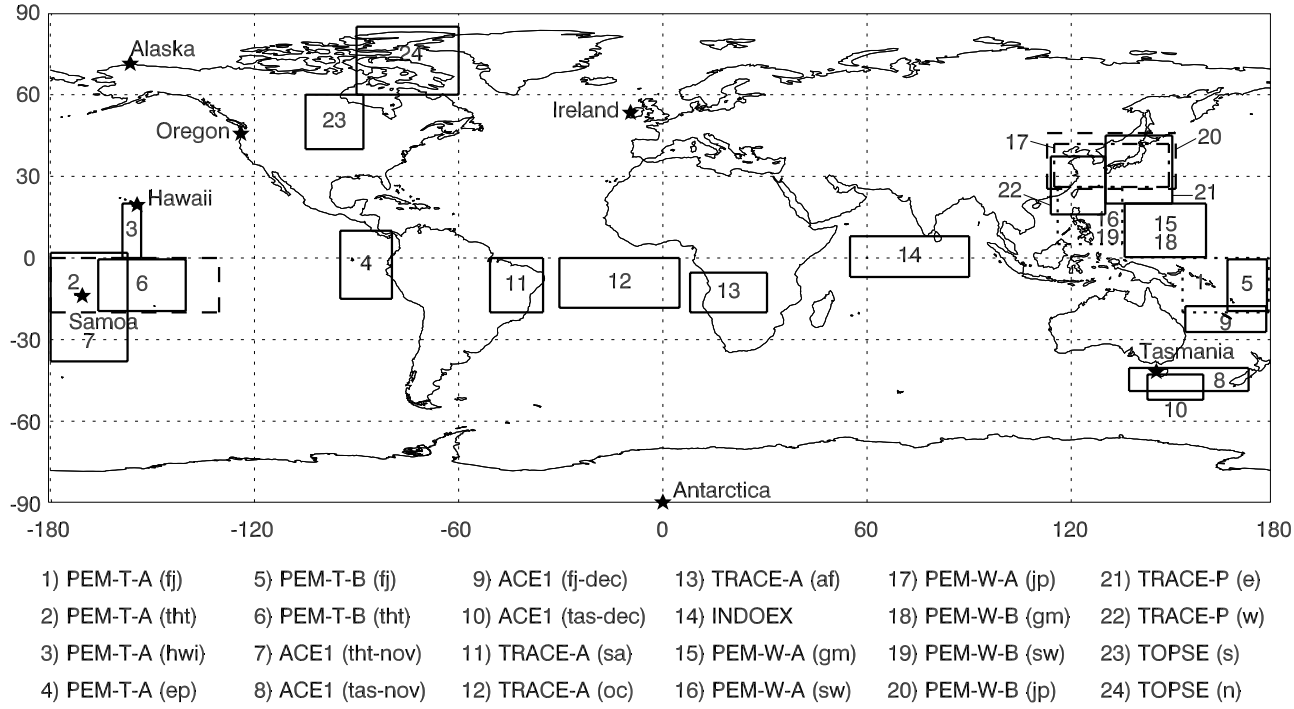

Figure 4. Surface measurement sites (indicated by symbols) and aircraft observation regions used in this study.

from Hawaii is overestimated. The amplitude of the seasonal cycle calculated by the model is too large compared to the observations at southern higher latitudes. The reasons will be discussed further in the next section.

5.1.2. Latitudinal Variations

[25] Figure 6 shows the annual and seasonal latitudinal distributions of CH_3Cl at the same 7 surface stations in Figure 4. The observed annual means of CH_3Cl show little interhemispheric gradient, while there are relatively clear seasonal gradients. Ref-k03 overestimates the observations in the tropics and northern higher latitudes. A possible reason for the higher concentrations in the NH for the run Ref-k03 is that the biomass burning emissions are biased toward the NH. The estimated NH/SH ratio of biomass burning emissions by *Lobert et al.* [1999] is about 2.2; whereas we calculated a ratio of 1.6 based on scaling to the biomass burning CO inventory [*Duncan et al.*, 2003]. *Lee-Taylor et al.* [2001] mentioned that they reduced the biomass burning CH_3Cl flux from southern and eastern Asia by half in order to reduce the interhemispheric gradient in their model results. The overestimates of Ref-k03 at low latitudes could be explained by the distribution of the isoprene-scaled biogenic emissions, which are biased toward equatorial regions (Figure 2).

[26] The difference between OC-1 and OC-2 runs shows the effect of oceanic sink on surface concentrations. These two runs have almost the same net oceanic emissions, but OC-2 has more than four times the oceanic sink over the net uptake regions than OC-1. Since the SH has more oceanic areas than the NH, the concentrations of CH_3Cl are more sensitive to ocean uptake in the SH than the NH. The OC-1 run shows a south-north gradient, while OC-2 shows a symmetrical distribution as observed (Figure 6a). However, the simulated seasonal variations in OC-2 and for other years ("model mean") are much higher than the observations. It largely reflects the small seasonal variation in the ocean uptake at southern high latitudes, which is ± 2 Gg yr^{-1} as compared to ± 100 Gg yr^{-1} driven by the seasonality of the OH chemistry. The physical parameterization is based on wind speed and SST [*Khalil et al.*, 1999]. *Khalil et al.* [1999] mentioned that this proxy calculation represented the flux for warm waters well, but not the uptake in cold waters. *Tokarczyk et al.* [2003] reported that the CH_3Cl degradation rate constants have no clear SST dependence. Further investigation is needed to understand the mechanisms controlling the seasonality of ocean uptake.

5.2. Vertical Profiles of Atmospheric CH_3Cl

[27] Figure 7 shows the vertical distributions of CH_3Cl from aircraft measurements and our model for the regions shown in Figure 4. Model results are taken from simulations with assimilated meteorology for the same period as the observations except for PEM-Tropics B and INDOEX, for which the GMAO assimilated meteorological data for GEOS-CHEM are unavailable. For these two missions, we use the average of 7-year runs for 1991, 1992, 1994, 1995, Sep1996–Aug1997, 2000, and 2001. The OC-2 oceanic sink over the uptake regions is applied. The contribution for individual sources is shown. We discuss the results by geographical region.

5.2.1. Tropical Pacific (PEM-Tropics A and B)

[28] The PEM-Tropics A took place over the remote South Pacific Ocean between August 24 and October 6, 1996. The observations of CH_3Cl show little variation with altitude except over the eastern Pacific region (ep) (Figures 7-1–7-4). Over this region, the observations show elevated concentrations at about 2–4 km, which

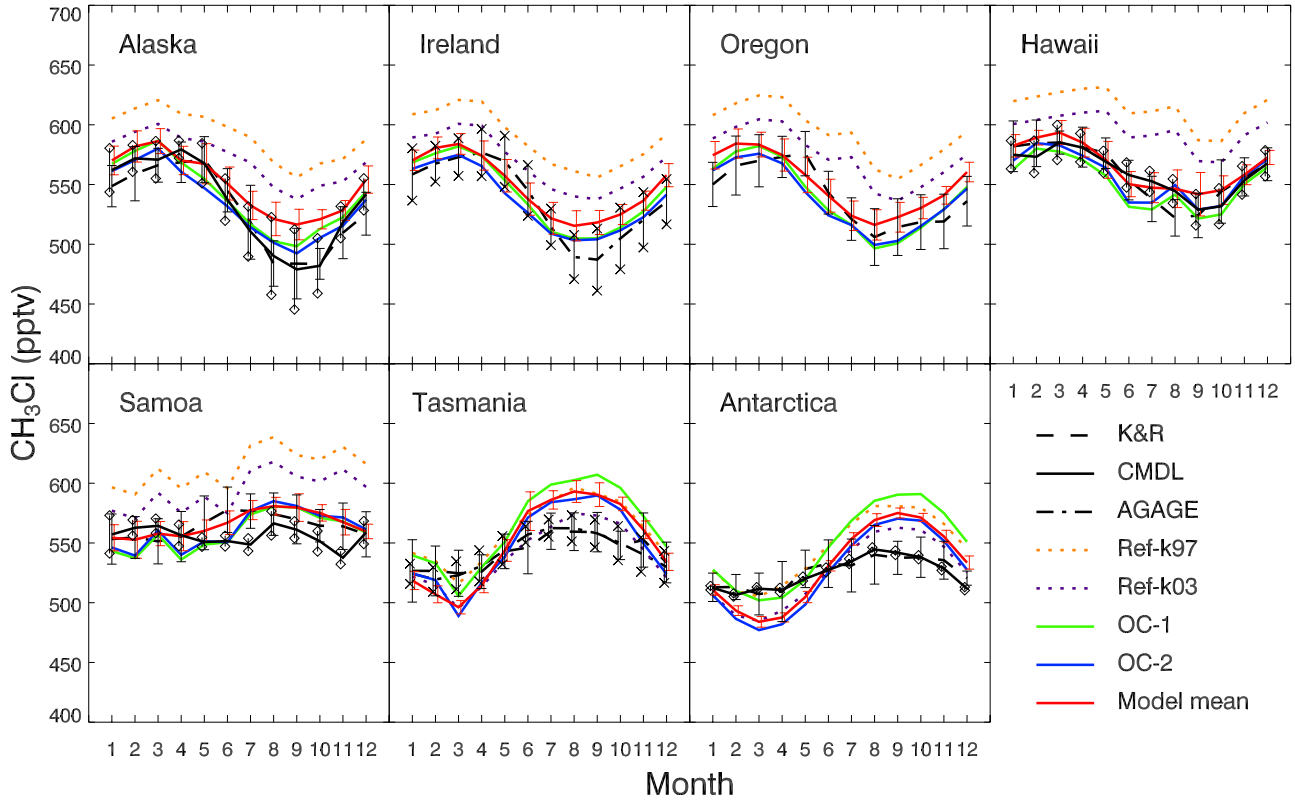

Figure 5. Seasonal variations of observed and simulated CH_3Cl at the surface sites. Dashed lines indicate data by *Khalil and Rasmussen* [1999], black solid lines indicate CMDL data (G. Dutton, personal communications, 2004), and dot-dashed lines indicate AGAGE data [*Simmonds et al.*, 2004]. The K&R data were lowered by 8.3% to account for a calibration difference. Model results are shown in color. The orange dotted lines are the reference run with the OH reaction rate constant by *DeMore et al.* [1997]. The purple dotted lines are the reference run with the OH rate constant by *Sander et al.* [2003]. The green lines are the OC-1 run. The blue lines are the OC-2 run. These four simulations used meteorological data for September 1996 to August 1997. The red solid lines are the mean of 7-year simulations with oceanic sink calculated as in the OC-2 run. The vertical lines represent the standard deviations.

reflects the easterly outflow of air masses from South America that were strongly influenced by biomass burning emissions [*Blake et al.*, 1999a]. The model closely reproduces the observations for Fiji (fj) although it overestimates for the eastern Pacific region (ep) especially near the surface, where concentrations are over-predicted due to biogenic CH_3Cl emissions from tropical rain forests in our model (Figure 7-4). For Hawaii (hwi), the model concentrations are higher than the observations by ~30 pptv for all altitudes.

[29] Measurements during the PEM-Tropics B mission were taken over the tropical Pacific in March and early April 1999. Observed and simulated values are compared for Fiji (fj) and Tahiti (tht) regions (Figures 7-5 and 7-6). The model simulations generally show slight overestimates. *Blake et al.* [2001] reported that CH_3Cl concentrations observed in PEM-Tropics A were higher than observed in PEM-Tropics B south of 10°S because of significant biomass burning emissions during PEM-Tropics A in the tropical dry season. In Figures 7-1–7-6, however, this trend is not obvious in regional profiles because we average the concentrations over larger areas as shown in Figure 4. The latitude-altitude plots discussed in section 5.3 (Figures 8-1, 8-2, 8-5, and 8-6) show this trend.

5.2.2. Tropical Pacific and Southern Oceans (ACE 1)

[30] The ACE 1 mission was conducted over the Pacific and Southern Oceans during November and December 1995. Slight positive vertical gradients of CH_3Cl were observed for samples taken over the four regions shown in Figure 4 (Figures 7-7–7-10). *Blake et al.* [1999b] explained the vertical trend could be derived from the long range transport of air containing high biomass burning CH_3Cl. Our model results overestimate the concentrations for all regions except the Tasmania-December region (tas-dec). Simulated CH_3Cl also shows greater vertical gradients for all regions except for the Tahiti-November region (tht-nov). The overestimates of the vertical gradient in the model are mainly due to our pseudobiogenic CH_3Cl rather than biomass burning CH_3Cl.

5.2.3. Tropical Atlantic (TRACE-A)

[31] The TRACE-A mission, in September–October 1992, focused on investigating the effects of biomass burning over the South Atlantic, South America, and southern Africa. The observed enhancements of CH_3Cl in the boundary layer (at 0–2 km) over Brazil/South America (sa)

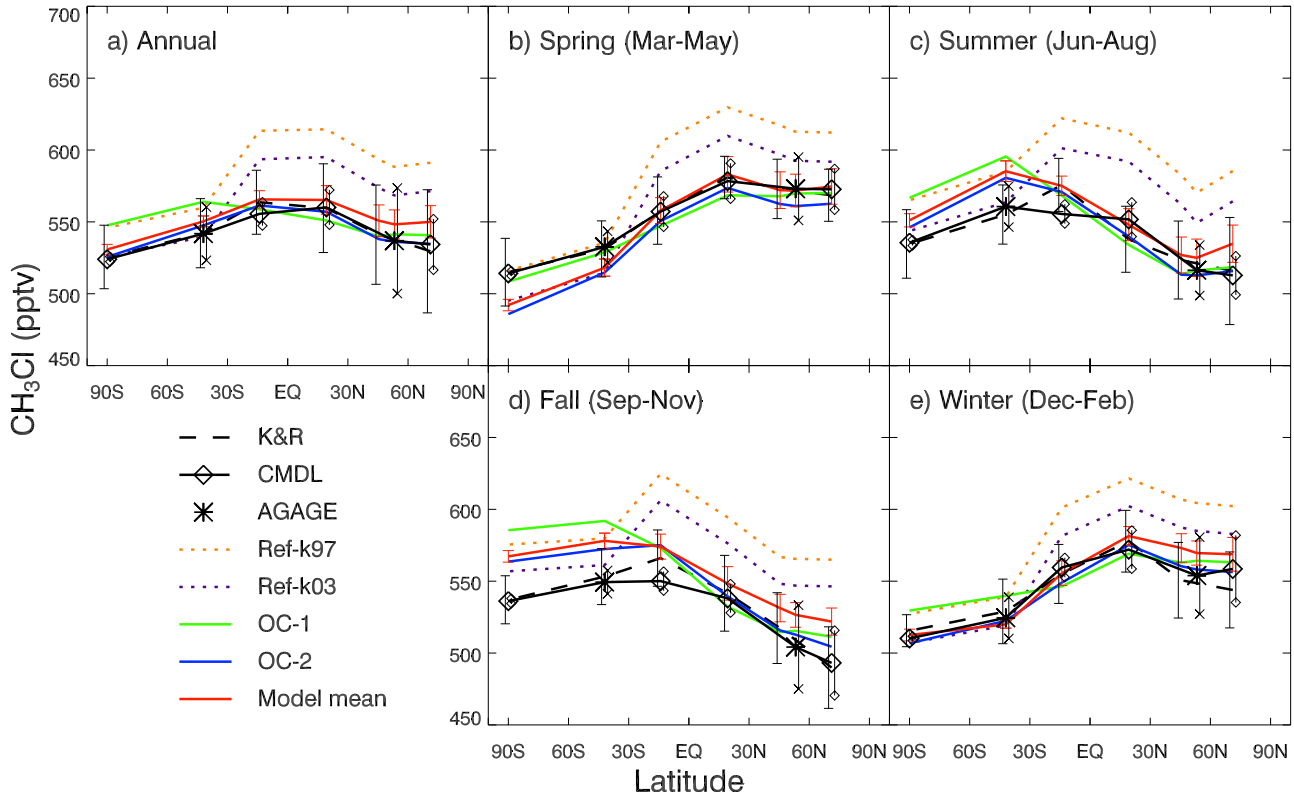

Figure 6. Latitudinal distributions of observed and simulated CH_3Cl at the surface sites. Line symbols are the same as Figure 5.

and southern Africa (af) (Figures 7-11 and 7-13) indicate the regional biomass burning effects [*Blake et al.*, 1996]. Over South America, another maximum was observed above 10 km. Analyzing samples collected at high altitude and the boundary layer, *Blake et al.* [1996] concluded that biomass burning over Brazil and frequent deep convection near and downwind of the fires could explain the enhanced concentrations in the upper troposphere. The model reproduces the maxima in the boundary layer observed over South America and southern Africa, while it underestimates the magnitudes. In addition to the biomass burning source suggested by *Blake et al.* [1996], our model indicates that our added biogenic source contributes significantly to the boundary layer enhancement (Figures 7-11 and 7-13). The biomass burning source of CH_3Cl is often deduced by the enhancement ratio of CH_3Cl to CO on the basis of field measurements. Our model results suggest that such deduced biomass burning source of CH_3Cl could be overestimated if the biogenic contribution to the observed CH_3Cl to CO enhancements ratios is not properly accounted for.

[32] The model does not reproduce the observed high concentrations in the upper troposphere over South America (Figure 7-11). However, no such large enhancement is evident over the tropical South Atlantic (Figure 7-12) or Africa (Figure 7-13). The convective enhancement at 12 km may therefore reflect the biased sampling of specific convective plumes by the DC-8 aircraft, which would not be reflected in the simulated monthly mean concentrations. Over the South Atlantic (oc) (Figure 7-12), the vertical profile of measured CH_3Cl concentrations shows slight increases with altitude and the model matches relatively well with the observations except at 0–2 km, where combined biogenic and biomass burning CH_3Cl concentrations result in a maximum that was not present in the observations.

5.2.4. Indian Ocean (INDOEX)

[33] During the INDOEX campaign air samples were collected over the northern Indian Ocean in February–March 1999. Enhanced concentrations of CH_3Cl and other combustion tracers such as CO, hydrocarbons, and CH_3CN were observed in the outflow from India and Southeast Asia, indicating that extensive biofuel emissions in those areas contributed to the high CH_3Cl levels [*Scheeren et al.*, 2002]. The model underestimates the observations at all altitudes (Figure 7-14). Based on the INDOEX observations, *Scheeren et al.* [2002] reported a CH_3Cl/CO molar emission ratio of 1.74×10^{-3} for the biofuel emissions, which is about three times larger than that of 0.57×10^{-3} [*Lobert et al.*, 1999] used in our model. Increasing the biofuel CH_3Cl/CO molar ratio to 1.74×10^{-3} led to an increase of 50 pptv in India and Southeast Asia, resulting in a better agreement with the observations (not shown).

5.2.5. Western Pacific (PEM-West A and B, TRACE-P)

[34] The PEM-West A mission was conducted in September and October 1991 over the western Pacific. During the PEM-West B mission, air samples were collected from February to March 1994. One major feature in the vertical profiles of CH_3Cl during PEM-West A (Figures 7-15–7-17)

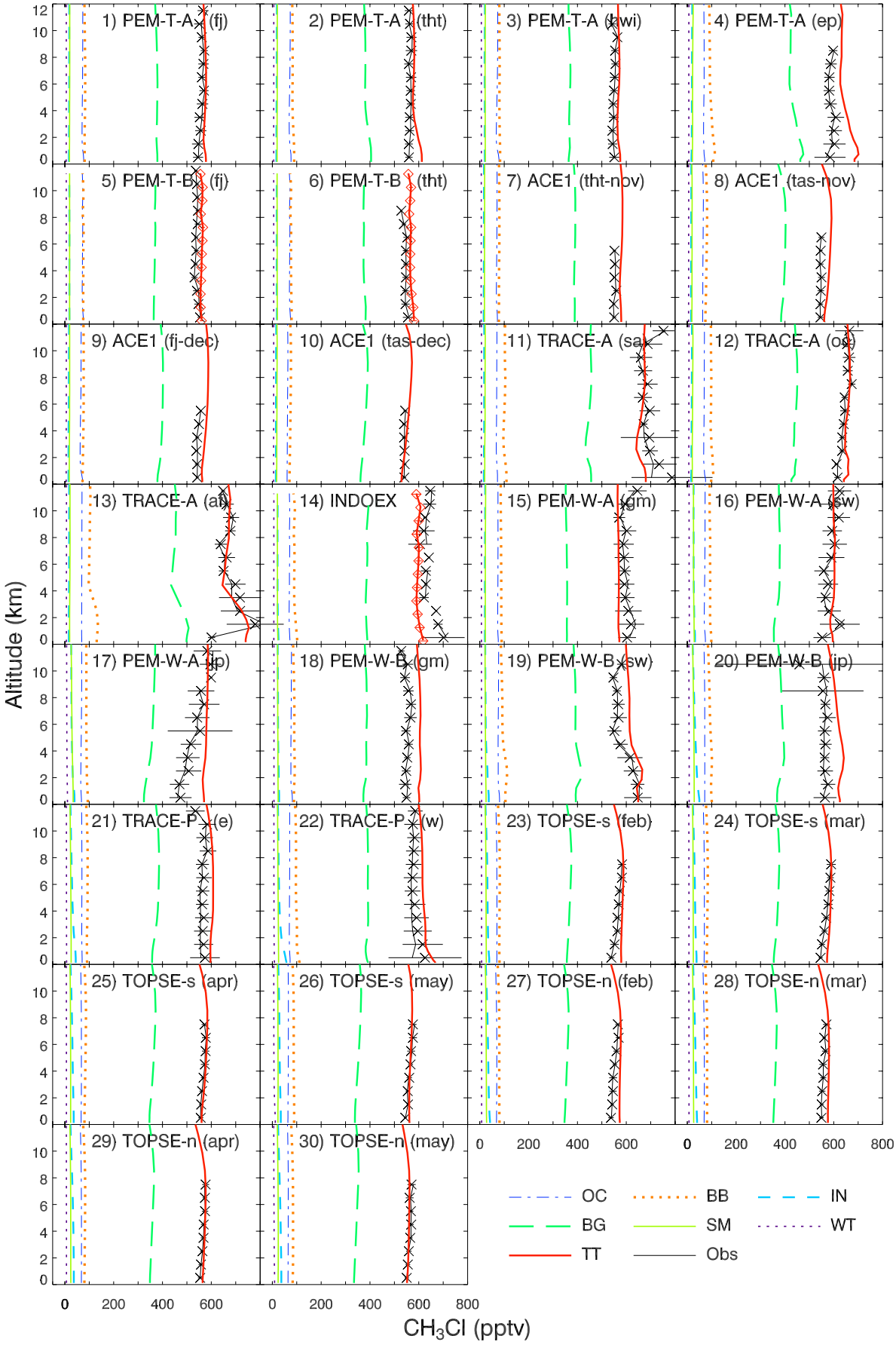
1) PEM-T-A (fj)
2) PEM-T-A (tht)
3) PEM-T-A (hwi)
4) PEM-T-A (ep)
5) PEM-T-B (fj)
6) PEM-T-B (tht)
7) ACE1 (tht-nov)
8) ACE1 (tas-nov)
9) ACE1 (fj-dec)
10) ACE1 (tas-dec)
11) TRACE-A (sa)
12) TRACE-A (os)
13) TRACE-A (af)
14) INDOEX
15) PEM-W-A (gm)
16) PEM-W-A (sw)
17) PEM-W-A (ip)
18) PEM-W-B (gm)
19) PEM-W-B (sw)
20) PEM-W-B (ip)
21) TRACE-P (e)
22) TRACE-P (w)
23) TOPSE-s (feb)
24) TOPSE-s (mar)
25) TOPSE-s (apr)
26) TOPSE-s (may)
27) TOPSE-n (feb)
28) TOPSE-n (mar)
29) TOPSE-n (apr)
30) TOPSE-n (may)
Altitude (km)
CH_3Cl (pptv)
OC
BB
IN
BG
SM
WT
TT
Obs

Figure 7

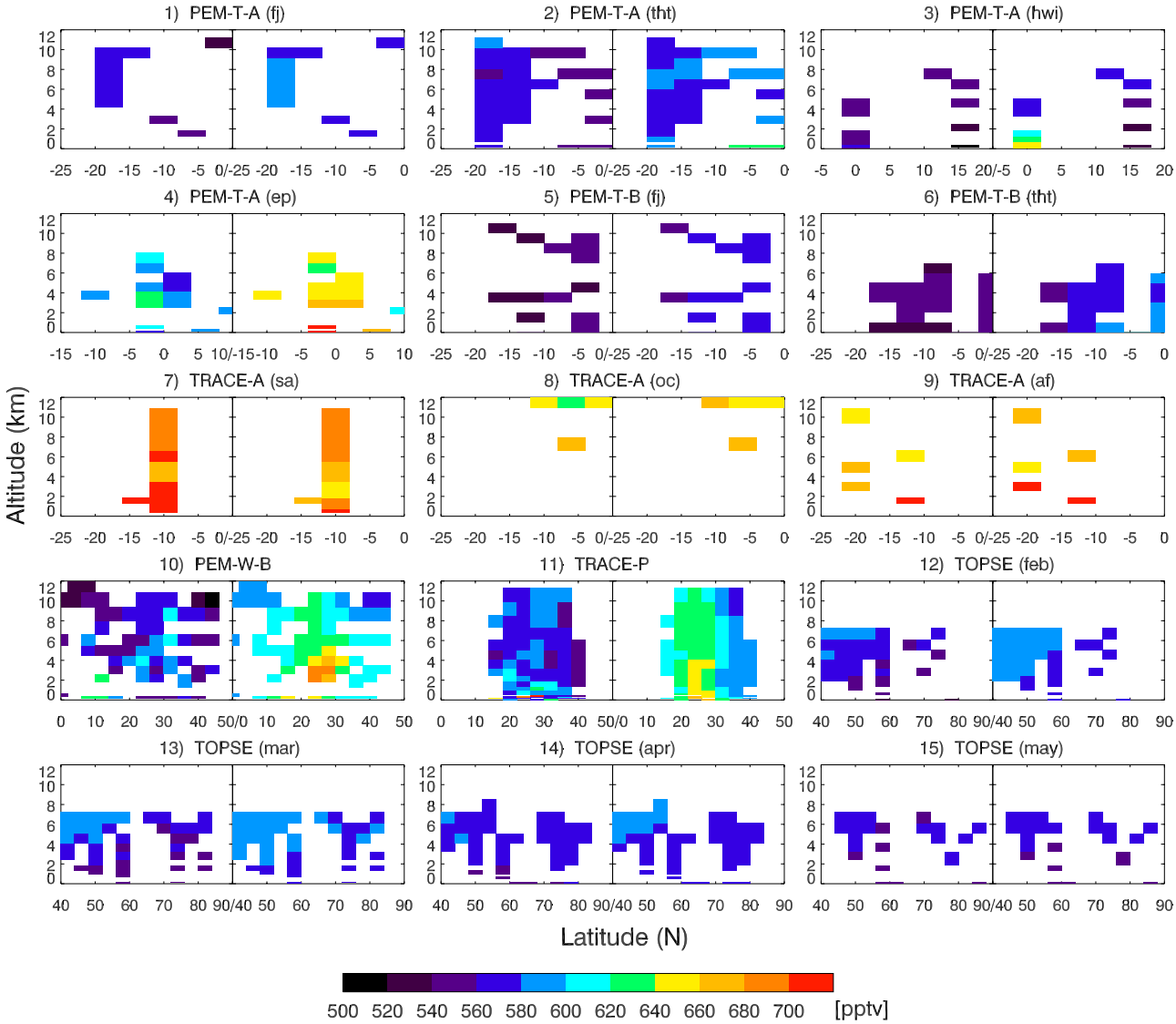

Figure 8. (left) Observed and (right) simulated latitude-altitude distributions for selected aircraft observation regions shown in Figure 4. For TRACE-P and TOPSE, the western/eastern and the northern/southern regions are combined, respectively. Abbreviations are the same as used in Figure 7. Only grid boxes with >10 observation points are shown.

is the enhanced concentrations observed at high altitude (above 10 km), which reflect transport of CH_3Cl by typhoons [*Newell et al.*, 1996; *Blake et al.*, 1997; *Kondo et al.*, 1997]. The model results show little vertical variation and did not reproduce those elevated concentrations. Higher CH_3Cl mixing ratios observed below 6 km during PEM-West B than PEM-West A in the southwest (sw) region (Figures 7-16 and 7-19) could be explained by stronger westerly outflow from the Asian continent in winter than in fall [*Blake et al.*, 1997; *Kondo et al.*, 1997]. During PEM-West B, little vertical variations were observed over Guam (gm) and Japan (jp) (Figures 7-18 and 7-20), reflecting small influence from the continental outflow while over the southwest (sw) region, CH_3Cl concentrations are higher at 0–5 km (Figure 7-19). Our model tends to overestimate the observations possibly as the result of

Figure 7. Vertical profiles of CH_3Cl averaged over the aircraft observation regions shown in Figure 4. For the TOPSE experiment, monthly mean values from February to May are calculated. Please see the text for the abbreviation for each project region. Thin solid lines indicate the medians of observations, crosses indicate the means of observations, and thin horizontal lines indicate the observed standard deviations. Diamonds indicate the means of the seven model runs. For model results, contributions from each source as well as all sources are shown. OC, BB, IN, BG, SM, WT, and TT denote ocean, biomass burning, incineration/industrial, biogenic, salt marshes, wetlands, and total, respectively.

its tendency to transport too much biogenic CH_3Cl from low latitudes. In the southwestern region, simulated concentrations show some enhancements at low altitude (3 km), which are due to biogenic and biomass burning emissions (Figure 7-19).

[35] The measurements during TRACE-P were obtained over the northwestern Pacific between February and April 2001. During this mission, a strong influence of Asian outflow was detected, which also characterized the main feature of the PEM-West B observations [*Jacob et al.*, 2003]. TRACE-P observations indicate significant effects of biomass burning emissions at high altitudes [*Liu et al.*, 2003; *Russo et al.*, 2003]. In the eastern region of TRACE-P (e), our model results show higher concentrations at middle altitudes than observed; the simulated bulge is largely attributed to the biogenic source (Figure 7-21). In the western region (w), both the model and observed (mean) values are higher in the boundary layer and decrease with altitude, reflecting higher concentrations of incineration/industrial and biomass burning sources near the surface (Figure 7-22). The simulated CH_3Cl concentrations from the biosphere appear to be overestimated. We will examine the potential causes of the overestimates in the next section.

5.2.6. North America (TOPSE)

[36] The TOPSE experiment was carried out during February to May 2000 at mid to high latitudes over North America. Figures 7-23–7-30 show monthly mean observed and simulated vertical profiles for northern and southern TOPSE regions in Figure 4. Slight positive vertical gradients were observed throughout the measurement period. The largest vertical gradients were observed at midlatitudes in February and March (Figures 7-23 and 7-24). Our model closely reproduces the observed concentrations in general. However, it does not reproduce the higher vertical gradients in February and March due to the overestimated emissions near the surface. The positive vertical gradients are largely attributed by the model to biogenic CH_3Cl transported from the tropics.

5.3. Latitude-Altitude Distributions of Atmospheric CH_3Cl

[37] Latitude-altitude cross sections of observed and simulated CH_3Cl concentrations for selected aircraft field experiments are compared in Figure 8. Figure 9 illustrates the relative difference between observed and simulated values. During PEM-Tropics A, a slight north-south gradient was observed over the Tahiti region; the concentrations south of 10°S are higher by about 20 pptv than in the northern section. Our model simulates the observations well for the southern section, where the difference is within ±5%, but overestimates by 5 to 15% in the northern section (Figures 8-2 and 9-2). Simulated surface concentrations are too high due to the westward transport of model biogenic and biomass burning CH_3Cl from Central and South America. Unfortunately, there are not enough data points to see the latitudinal variability for the other three PEM-Tropics A regions, although Figures 9-2–9-4 show that the model tends to overestimate the concentrations close to the equator near the surface, resulting mainly from the strong outflow of biogenic CH_3Cl mentioned above.

[38] During PEM-Tropics B, the concentration gradient observed over the Fiji region is opposite to that during PEM-Tropics A (Figure 8-5). The model captures the trend although it overestimates the concentrations by 10% for some locations (Figure 9-5). The simulated latitudinal gradient is due to the combination of biomass burning and biogenic CH_3Cl gradients in the model. There are not enough data points to investigate the spatial variability for TRACE-A.

[39] During PEM-West B, the model overestimates the observations by 5 to 20% in most regions (Figure 9-10). A few "hot spots" (670–750 pptv) were observed in the lower troposphere around 10°N that could be attributed to biomass burning plumes [*Blake et al.*, 1997]; they are shifted to the northern latitudes in the model results (Figure 8-10). After investigating the correlation of CH_3Cl with CO during PEM-West B, *Blake et al.* [1997] concluded that at latitudes north of 25°N, no significant amount of CH_3Cl is emitted from urban/industrial sources or from other high-latitude continental sources and that the enhanced concentrations observed at low latitudes (<25°N) could result from the continental biomass burning outflow. The high concentrations simulated in the model near 25°N are due to biomass burning and biogenic emissions.

[40] Figure 8-11 shows a comparison of observed and simulated spatial variability for the TRACE-P experiment. The enhanced concentrations observed in the boundary layer north of 25°N were due to fossil fuel/biofuel combustion effluent from China. During TRACE-P, transport of biomass burning effluents from Southeast Asia was limited to high altitudes south of 35°N [*Blake et al.*, 2003b; *Liu et al.*, 2003]. The model reproduces the general trend, but shows a more distinct latitudinal gradient. The model overestimates the observations at 20°–30°N by 5–15% as a result of strong model transport of biogenic CH_3Cl descending from the upper troposphere (Figure 9-11). This strong subsidence persists at the same location, even when the biogenic emissions are restricted to 10°S to 10°N in the model (results not shown), indicating stronger influence of transport from the tropics on midlatitude CH_3Cl concentrations in the model than is apparent from the observations. Simulated concentrations at 0–2 km north of 30°N are lower by <5% than the observed values. Considering the strong boundary layer Asian outflow at 30°–45°N during TRACE-P [*Liu et al.*, 2003], incineration/industrial and/or biofuel emissions in our model could be underestimated.

[41] Figures 9-12–9-15 show the difference between the observations and model simulations for the TOPSE experiment. The model closely reproduces the observations. Spatial variations and their seasonal evolutions of CH_3Cl concentrations are shown in Figures 8-12–8-15. Higher concentrations were observed in the middle troposphere at lower latitudes (<60°N). The latitudinal/altitudinal concentration gradient decreases with season reflecting the reduction of CH_3Cl transport from the tropical regions. The model reproduces the seasonal trend properly. The higher concentrations in the middle troposphere might be explained by CH_3Cl transport from biomass burning and biogenic sources from the tropics and Southeast Asia.

6. Conclusions

[42] We apply a 3-D chemical transport model, GEOS-CHEM, to simulate the global distributions of CH_3Cl. The

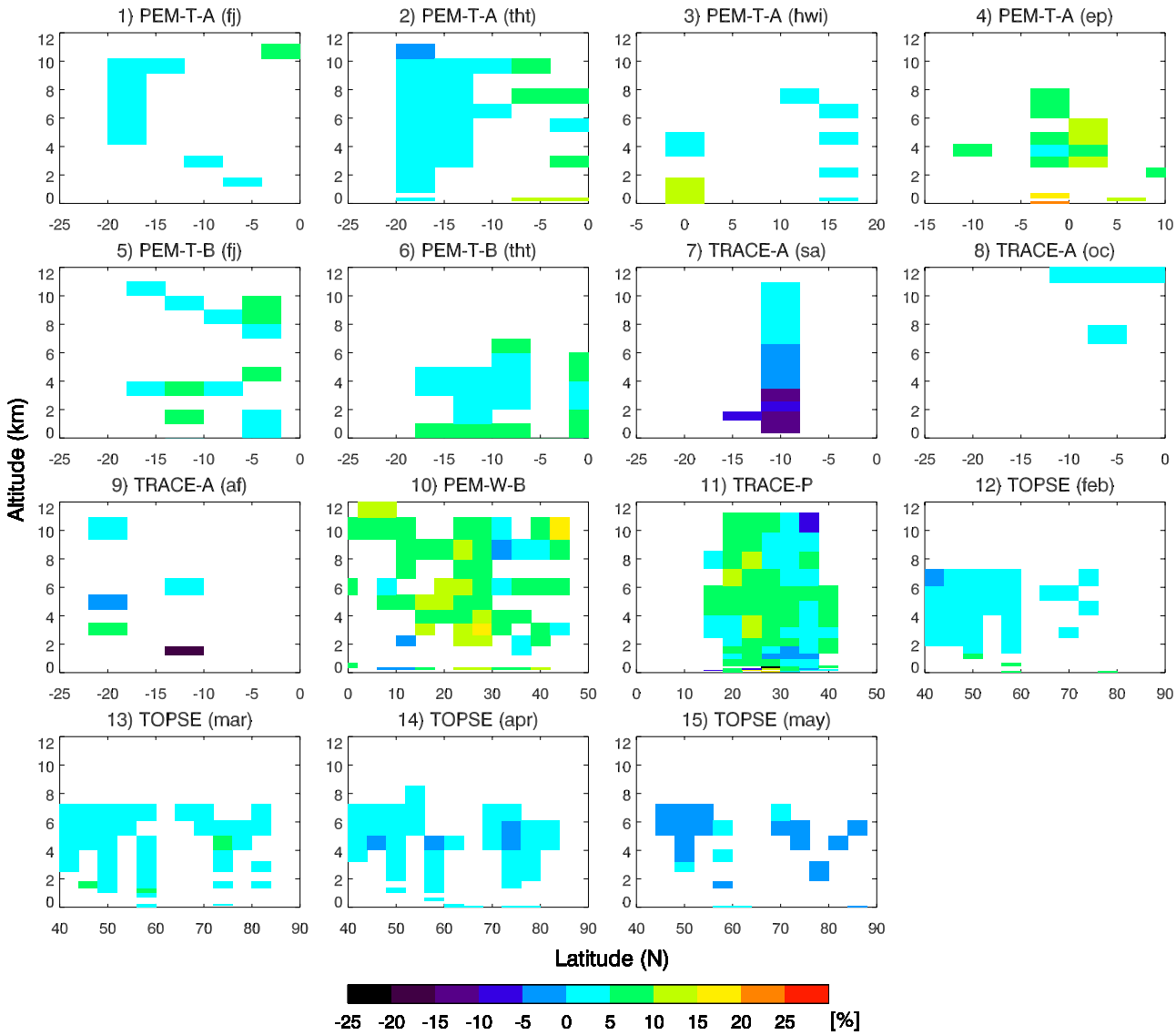

Figure 9. Same as Figure 8, but for the relative difference computed as (model-observation)/model.

model simulations are constrained by surface and aircraft observations to define better the characteristics of the required pseudobiogenic source of atmospheric CH_3Cl that we added to the model and to examine the observational constraints on the other better-known sources. Contributions from the pseudobiogenic, oceanic, biomass burning, incineration/industrial, salt marsh and wetland sources are quantified through tagged-tracer simulations. Their effects on seasonal variations, latitudinal trends, and regional vertical profiles of CH_3Cl are investigated.

[43] We find that a pseudobiogenic source of 2.9 Tg yr^{-1} (66% of the total source) is necessary to explain the observed CH_3Cl concentrations. The large decrease of CH_3Cl from summer to winter at northern midlatitudes implies a negligible biogenic source of CH_3Cl at midlatitudes. We therefore constrain the pseudobiogenic emissions to 30°S–30°N. Furthermore, we find that scaling the pseudobiogenic emission to that of isoprene [e.g., *Lee-Taylor et al.*, 2001] leads to an underestimate of the seasonal CH_3Cl variation at northern midlatitudes and tends to concentrate CH_3Cl to a few tropical and subtropical ecosystems resulting in overestimates of aircraft observations downwind from these regions. We assume that tropical and subtropical ecosystems have the same aseasonal emission rate, which gives better simulations of the observations than scaling the emissions to those of isoprene.

[44] Our model mean annual CH_3Cl oceanic flux over the net emission regions is 510 Gg yr^{-1}, 37% smaller than the RCEI inventory [*Khalil et al.*, 1999]. The calculated total oceanic sink over the uptake regions is about 30 Gg yr^{-1}, which is about one fifth of the RCEI inventory [*Khalil et al.*, 1999]. We find that the ocean uptake plays an important role in reproducing the observed annual-mean latitudinal gradient of CH_3Cl at southern high latitudes, where the uptake is significant. Increasing the oceanic sink over the uptake regions to 150 Gg yr^{-1}, which is the same as in the RCEI inventory, results in the model reproducing well the observed annual-mean latitudinal gradient of CH_3Cl. Our

model overestimates the seasonal variation of CH_3Cl at southern mid and high latitudes, implying an underestimate of the seasonal variation of ocean uptake calculated based on SST and wind speed.

[45] Our calculated CH_3Cl emission from the biomass/biofuel burning source using a molar CH_3Cl/CO emission ratio of 5.7×10^{-4} is 610 Gg yr^{-1}, which is about two thirds of that given in RCEI inventory [*Lobert et al.*, 1999]. Our lower biomass burning CH_3Cl emissions yield better agreement with the observed symmetrical annual-mean latitudinal CH_3Cl gradient, while the model results using biomass burning source data from the RCEI inventory show a clear bias toward overestimates in the northern hemisphere.

[46] Our estimated total emission of CH_3Cl from six sources including our 2.9 Tg yr^{-1} pseudobiogenic source and the other identified sources such as biomass/biofuel burning, ocean, incineration/industry, salt marshes, and wetlands in the model is approximately 4.4 Tg yr^{-1}. The calculated atmospheric burden of CH_3Cl is about 5.0 Tg and the estimated tropospheric lifetime of CH_3Cl against OH oxidation is about 1.2 years. The interhemispheric symmetry in the observed latitudinal distribution of CH_3Cl and a dominant tropical/subtropical pseudobiogenic source imply that the annual hemispheric mean OH ratio is constrained to the range of 0.8–1.3.

[47] A major shortfall in our current understanding of CH_3Cl emissions is the geographical distributions of the biogenic and biomass burning sources. This uncertainty is reflected clearly in the model comparison with aircraft observations. The model simulates generally well vertical profiles of CH_3Cl in most regions especially for high latitudes, where there is little local emission, while the model tends to overestimate or underestimate the observations near biogenic and biomass burning sources, reflecting the uncertainties in those source distributions. The model overestimates the observations over the western Pacific due to the simulated influx of biogenic CH_3Cl associated with the strong subsidence at 20°–30°N. It is noteworthy that the model suggests the dominant source of CH_3Cl in the region is biogenic, while previous studies focused mostly on biomass burning emissions [e.g., *Blake et al.*, 1997; *Liu et al.*, 2003; *Russo et al.*, 2003]. Biomass burning emission sources are likely overestimated in those studies although large uncertainty of the estimated biogenic CH_3Cl source needs to be considered. The comparison over the tropical regions suggests that the model biogenic sources in Central and South America might be overestimated. The estimates of CH_3Cl over the Indian Ocean suggest that the CH_3Cl/CO molar emission ratio in this region is higher than the value we used in the model. Applying a single CH_3Cl/CO emission ratio to the globe is too simplistic since the CH_3Cl emission rate depends on the fuel type and the burning conditions [*Lobert et al.*, 1999]. The estimated incineration/industrial or biofuel emissions near the coast of China might be underestimated.

[48] **Acknowledgments.** We thank David Erickson and Jose L. Hernandez for providing us the UWM-COADS data and helpful comments. We thank Donald Blake for his suggestions. We thank Derek Cunnold for providing us the AGAGE data. We are grateful to CMDL and Geoff Dutton for providing us their unpublished data. We also thank Daniel Jacob and Colette Heald for their help. The GEOS-CHEM model is managed at Harvard University with support from the NASA Atmospheric Chemistry Modeling and Analysis Program. This work was supported by the NASA ACMAP program.

References

Bey, I., D. J. Jacob, R. M. Yantosca, J. A. Logan, B. Field, A. M. Fiore, Q. Li, H. Liu, L. J. Mickley, and M. Schultz (2001), Global modeling of tropospheric chemistry with assimilated meteorology: Model description and evaluation, *J. Geophys. Res.*, *106*, 23,073–23,096.

Blake, N. J., D. R. Blake, O. B. C. Sive, T.-Y. Chen, F. S. Rowland, J. E. Collins Jr., G. W. Sachse, and B. E. Anderson (1996), Biomass burning emissions and vertical distribution of atmospheric methyl halides and other reduced carbon gases in the South Atlantic region, *J. Geophys. Res.*, *101*, 24,151–24,164.

Blake, N. J., D. R. Blake, O. T.-Y. Chen, J. E. Collins Jr., G. W. Sachse, B. E. Anderson, and F. S. Rowland (1997), Distribution and seasonality of selected hydrocarbons and halocarbons over the western Pacific basin during PEM-West A and PEM-West B, *J. Geophys. Res.*, *102*, 28,315–38,331.

Blake, N. J., et al. (1999a), Influence of southern hemispheric biomass burning on midtropospheric distributions of nonmethane hydrocarbons and selected halocarbons over the remote South Pacific, *J. Geophys. Res.*, *104*, 16,213–16,232.

Blake, N. J., et al. (1999b), Aircraft measurements of the latitudinal, vertical, and seasonal variations of NMHCs, methyl nitrate, methyl halides, and DMS during the First Aerosol Characterization Experiment (ACE 1), *J. Geophys. Res.*, *104*, 21,803–21,817.

Blake, N. J., et al. (2001), Large-scale latitudinal and vertical distributions of NMHCs and selected halocarbons in the troposphere over the Pacific Ocean during the March–April 1999 Pacific Exploratory Mission (PEM-Tropics B), *J. Geophys. Res.*, *106*, 32,627–32,644.

Blake, N. J., D. R. Blake, B. C. Sive, A. S. Katzenstein, S. Meinardi, O. W. Wingenter, E. L. Atlas, F. Flocke, B. A. Ridley, and F. S. Rowland (2003a), The seasonal evolution of NMHCs and light alkyl nitrates at middle to high northern latitudes during TOPSE, *J. Geophys. Res.*, *108*(D4), 8359, doi:10.1029/2001JD001467.

Blake, N. J., et al. (2003b), NMHCs and halocarbons in Asian continental outflow during the Transport and Chemical Evolution Over the Pacific (TRACE-P) field campaign: Comparison with PEM-West B, *J. Geophys. Res.*, *108*(D20), 8806, doi:10.1029/2002JD003367.

daSilva, A., A. C. Young, and S. Levitus (1994), Atlas of surface marine data 1994, vol. 1, Algorithms and procedures, *Tech. Rep. 6*, Natl. Environ. Satell., Data, and Inf. Serv., Natl. Oceanic and Atmos. Admin., Silver Spring, Md.

DeFries, R. S., and J. R. G. Townshend (1994), NDVI-derived land cover classification at global scales, *Int. J. Remote Sens.*, *15*, 3567–3586.

DeMore, W. B., S. P. Sander, D. M. Golden, R. F. Hampson, M. J. Kurylo, C. J. Howard, A. R. Ravishankara, C. E. Kolb, and M. J. Molina (1997), Chemical kinetics and photochemical data for use in stratospheric modeling, Evaluation 12, *JPL Publ.*, *97-4*.

Duncan, B. N., R. V. Martin, A. C. Staudt, R. Yevich, and J. A. Logan (2003), Interannual and seasonal variability of biomass burning emissions constrained by satellite observations, *J. Geophys. Res.*, *108*(D2), 4100, doi:10.1029/2002JD002378.

Hall, F. G., B. Meeson, S. Los, L. Steyaert, E. Brown de Colstoun, and D. Landis (Eds.) (2003), *ISLSCP Initiative II* [DVD/CD-ROM], NASA, Greenbelt, Md.

Hamilton, J. T. G., W. C. McRoberts, F. Keppler, R. M. Kalin, and D. B. Harper (2003), Chloride methylation by plant pectin: An efficient environmentally significant process, *Science*, *301*, 206–209.

Heald, C. L., D. J. Jacob, P. I. Palmer, M. J. Evans, G. W. Sachse, H. B. Singh, and D. R. Blake (2003), Biomass burning emission inventory with daily resolution: Application to aircraft observation of Asian outflow, *J. Geophys. Res.*, *108*(D21), 8811, doi:10.1029/2002JD003082.

Jacob, D. J., J. H. Crawford, M. M. Kleb, V. S. Connors, R. J. Bendura, J. L. Raper, G. W. Sachse, J. C. Gille, L. Emmons, and C. L. Heald (2003), Transport and Chemical Evolution Over the Pacific (TRACE-P) aircraft mission: Design, execution, and first results, *J. Geophys. Res.*, *108*(D20), 9000, doi:10.1029/2002JD003276.

Keene, W. C., et al. (1999), Composite global emissions of reactive chlorine from anthropogenic and natural sources: Reactive Chlorine Emissions Inventory, *J. Geophys. Res.*, *104*, 8429–8440.

Khalil, M. A. K., and R. A. Rasmussen (1999), Atmospheric methyl chloride, *Atmos. Environ.*, *33*, 1305–1321.

Khalil, M. A. K., R. M. Moore, D. B. Harper, J. M. Lobert, D. J. Erickson, V. Koropalov, W. T. Sturges, and W. C. Keene (1999), Natural emissions of chlorine-containing gases: Reactive Chlorine Emissions Inventory, *J. Geophys. Res.*, *104*, 8333–8346.

Kondo, Y., M. Koike, S. Kawakami, H. B. Singh, H. Nakajima, G. L. Gregory, D. R. Blake, G. W. Sachse, J. T. Merrill, and R. E. Newell

(1997), Profiles and partitioning of reactive nitrogen over the Pacific Ocean in winter and early spring, *J. Geophys. Res.*, *102*, 28,405–28,424.

Koppmann, R., F. J. Johnen, D. Plass-Dülmer, and J. Rudolph (1993), Distribution of methyl chloride, dichloromethane, trichloroethene, and tetrachloroethene over the North and South Atlantic, *J. Geophys. Res.*, *98*, 20,517–20,526.

Krol, M., and J. Lelieveld (2003), Can the variability in tropospheric OH be deduced from measurements of 1, 1, 1-trichloroethane (methyl chloroform)?, *J. Geophys. Res.*, *108*(D3), 4125, doi:10.1029/2002JD002423.

Lee-Taylor, J. M., G. P. Brasseur, and Y. Yokouchi (2001), A preliminary three-dimensional global model study of atmospheric methyl chloride distributions, *J. Geophys. Res.*, *106*, 34,221–34,233.

Liu, H., D. J. Jacob, I. Bey, R. M. Yantosca, B. N. Duncan, and G. W. Sachse (2003), Transport pathways for Asian pollution outflow over the Pacific: Interannual and seasonal variations, *J. Geophys. Res.*, *108*(D20), 8786, doi:10.1029/2002JD003102.

Lobert, J. M., W. C. Keene, J. A. Logan, and R. Yevich (1999), Global chlorine emissions from biomass burning: Reactive Chlorine Emissions Inventory, *J. Geophys. Res.*, *104*, 8373–8389.

Martin, R. V., D. J. Jacob, R. M. Yantosca, M. Chin, and P. Ginoux (2003), Global and regional decreases in tropospheric oxidants from photochemical effects of aerosols, *J. Geophys. Res.*, *108*(D3), 4097, doi:10.1029/2002JD002622.

McCulloch, A., M. L. Aucott, C. M. Benkovitz, T. E. Graedel, G. Kleiman, P. M. Midgley, and Y. F. Li (1999), Global emissions of hydrogen chloride and chloromethane from coal combustion, incineration, and industrial activities: Reactive Chlorine Emissions Inventory, *J. Geophys. Res.*, *104*, 8391–8403.

Montzka, S. A., et al. (2003), Controlled substances and other source gases, in *Scientific Assessment of Ozone Depletion: 2002*, chap. 1, *Rep. 47*, Global Ozone Res. and Monit. Proj., World Meteorol. Org., Geneva.

Moore, R. M. (2000), The solubility of a suite of low molecular weight organochlorine compounds in seawater and implications for estimating the marine source of methyl chloride to the atmosphere, *Chemosphere Global Change Sci.*, *2*, 95–99.

Moore, R. M., W. Groszko, and S. J. Niven (1996), Ocean-atmosphere exchange of methyl chloride: Results from NW Atlantic and Pacific Ocean studies, *J. Geophys. Res.*, *101*, 28,529–28,538.

Newell, R. E., et al. (1996), Atmospheric sampling of Supertyphoon Mireille with NASA DC-8 aircraft on September 27, 1991, during PEM-West A, *J. Geophys. Res.*, *101*, 1853–1871.

Prinn, R. G., et al. (2001), Evidence for substantial variations of atmospheric hydroxyl radicals in the past two decades, *Science*, *292*, 1882–1888.

Rhew, R. C., B. R. Miller, and R. F. Weiss (2000), Natural methyl bromide and methyl chloride emissions from coastal salt marshes, *Nature*, *403*, 292–295.

Rhew, R. C., B. R. Miller, M. K. Vollmer, and R. F. Weiss (2001), Shrubland fluxes of methyl bromide and methyl chloride, *J. Geophys. Res.*, *106*, 20,875–20,882.

Russo, R. S., et al. (2003), Chemical composition of Asian continental outflow over the western Pacific: Results from Transport and Chemical Evolution Over the Pacific (TRACE-P), *J. Geophys. Res.*, *108*(D20), 8804, doi:10.1029/2002JD003184.

Sander, S. P., A. R. Ravishankara, D. M. Golden, C. E. Kolb, M. J. Kurylo, M. J. Molina, G. K. Moortgat, and B. J. Finlayson-Pitts (2003), Chemical kinetics and photochemical data for use in stratospheric modeling, Evaluation 14, *JPL Publ.*, *02-25*.

Scheeren, H. A., J. Lelieveld, J. A. de Gouw, C. van der Veen, and H. Fischer (2002), Methyl chloride and other chlorocarbons in polluted air during INDOEX, *J. Geophys. Res.*, *107*(D19), 8015, doi:10.1029/2001JD001121.

Schneider, H. R., D. B. A. Jones, M. B. McElroy, and G.-Y. Shi (2000), Analysis of residual mean transport in the stratosphere: 1. Model description and comparison with satellite data, *J. Geophys. Res.*, *105*, 19,991–20,011.

Sellers, P. J., et al. (1995), Remote sensing of the land surface for studies of global change: Models–algorithms–experiments, *Remote Sens. Environ.*, *51*(1), 3–26.

Shorter, J. H., C. E. Kolb, P. M. Crill, R. A. Kerwin, R. W. Talbot, M. E. Hines, and R. C. Harriss (1995), Rapid degradation of atmospheric methyl bromide in soils, *Nature*, *377*, 717–719.

Simmonds, P. G., et al. (2004), In-situ AGAGE observations by GC-MS of methyl bromide and methyl chloride at the Mace Head, Ireland and Cape Grim, Tasmania (1998–2001) and their interpretation, *J. Atmos. Chem.*, in press.

Smith, T. M., and R. W. Reynolds (2003), Extended reconstruction of global sea surface temperature based on COADS data (1854–1997), *J. Clim.*, *16*, 1495–1510.

Spivakovsky, C. M., et al. (2000), Three-dimensional climatological distribution of tropospheric OH: Update and evaluation, *J. Geophys. Res.*, *105*, 8391–8980.

Tokarczyk, R., K. D. Goodwin, and E. S. Saltzman (2003), Methyl chloride and methyl bromide degradation in the Southern Ocean, *Geophys. Res. Lett.*, *30*(15), 1808, doi:10.1029/2003GL017459.

Varner, R. K., P. M. Crill, and R. W. Talbot (1999), Wetlands: A potentially significant source of atmospheric methyl bromide and methyl chloride, *Geophys. Res. Lett.*, *26*, 2433–2436.

Wanninkhof, R. (1992), Relationship between wind speed and gas exchange over the ocean, *J. Geophys. Res.*, *97*, 7373–7382.

Watling, R., and D. B. Harper (1998), Chloromethane production by wood-rotting fungi and an estimate of the global flux to the atmosphere, *Mycol. Res.*, *102*, 769–787.

Yokouchi, Y., Y. Noijiri, L. A. Barrie, D. Toom-Sauntry, T. Machida, Y. Inuzuka, H. Akimoto, H.-J. Li, Y. Fujinuma, and S. Aoki (2000), A strong source of methyl chloride to the atmosphere from tropical coastal land, *Nature*, *403*, 295–298.

Yokouchi, Y., M. Ikeda, Y. Inuzuka, and T. Yukawa (2002), Strong emission of methyl chloride from tropical plants, *Nature*, *416*, 163–165.

Y. Wang, Y. Yoshida, and T. Zeng, School of Earth and Atmospheric Sciences, Georgia Institute of Technology, Atlanta, GA 30332-0340, USA. (yyoshida@eas.gatech.edu)

R. Yantosca, Division of Engineering and Applied Sciences, Harvard University, Cambridge, MA 02138, USA.

REVIEW COMMENTS OF

Steven Hanna, Ph.D.
President, Hanna Consultants
7 Crescent Avenue
Kennebunkport, ME 04046-7235
207-967-4478
hannaconsult@adelphia.net

Steven Hanna

P083 Review

July 4, 2005

Review of EPA document "**Model Development for Assessing California Methyl Bromide Ambient Concentration"** and supporting documents.

Review comments are provided in two sections below. The first section contains general responses to six questions posed by the EPA. The second section contains specific comments referring to specific pages and lines in the document.

Section 1 – Responses to Six Questions Posed by EPA

1. *Does the document, "Model Development for Assessing California Methyl Bromide Ambient Concentrations", provide a clear and adequate description of the goals and methods EPA used to develop and review alternative exposure models? What additional information, if any, is critically needed to complete the documentation?*

Response to Question 1 – The document mainly describes the regression model approach that the EPA decided to use instead of the more traditional, scientific-based models used for most air quality modeling applications. This approach may ultimately prove to be useful, but at the moment, the justifications are weak for using a regression equation in place of a traditional model. As an example of the lack of an adequate review, the well-known and widely-used regression model known as the OBDG (Ocean Breeze – Dry Gulch) regression model described by Nou (1963) is not mentioned:

Nou, V, 1963: Development of the diffusion prediction equation – The Ocean Breeze Dry Gulch Diffusion Program. Vol. II (eds., D.A. Haugen and J.H. Taylor) AFCRL-63-791 (II) DOC Technical Services, Washington DC, pp 1-21.

The OBDG model is an example of how an equation should be formulated using basic physics assumptions and using unknown power law coefficients which are then best-fit by the regression process. This method would have been more appropriate than the current EPA method where the

powers are prescribed before hand rather than being solved. The OBDG equation has the following format:

$$C - C_b = aZ_1^{p1}Z_2^{p2}Z_3^{p3}\ldots Z_i^{pi}\ \ldots\ Z_n^{pn}$$

Where C is concentration, C_b is background concentration, a is a proportionality "constant", Z_i for i = 1 through n are independent input parameters, and p_i for i = 1 through n are power law coefficients applied to the input parameters. For the OBDG equation, the Z_i include basic scientific measures such as wind speed, downwind distance, and vertical temperature gradient.

Also, the rationale for eliminating the ISC model from consideration is weak, and the authors did not survey the literature to identify simpler but scientifically correct area source models. For example, the ATDL area-source dispersion model was specifically designed for adjacent grids of area sources, which is the problem of interest in the current document. That reference is:

Hanna, Briggs, and Hosker, 1982: Handbook of Atmospheric Diffusion. DOE/TIC-11223, pp 59-60.

One reason stated for not using ISC is that the source terms are not known. Yet the authors then proceed to develop measures of the source terms from available usage data for use in the regression equations. This same procedure could have been used in ISC, and then the source magnitude calibrated using the observed concentrations.

2. *What are the overall strengths and weaknesses of the model development process as described?*

Response to Question 2 – See the response to Question 1 for comments on the general scientific approach and the review process. The main strength of the report is that observations of methyl bromide concentration and emissions were used to develop the regression equation. The main weaknesses are that the regression model formulation does not allow for solution of the power law coefficients associated with the independent inputs, does not employ knowledge of standard scientific formulations, does not adequately justify eliminating the logarithmic formulation, and the use of thousands of "models" is irrational. In this reviewer's experience, the regression equation can be solved so that a best fit is obtained for multiple inputs and parameters, without having to independently list and test each combination of inputs.

A weakness of any regression approach is that it implicitly assumes that the basic scientific phenomena are linear. However, most atmospheric phenomena are non linear and sometimes even switch signs as the independent variable increases.

An additional weakness is that there is no indication that the developers discussed the "model" with the air modeling experts at RTP, either in the Air Modeling Division of NERL or in OAQPS.

3. *What are the strengths and weaknesses of the data quality assurance activities conducted during the model development process?*

Response to Question 3 – The observed concentrations and source usage term are fairly well-defined and have been measured over many weeks during two years. However, it would help to have error bars on these observations clearly explained in the text. For example, what is the uncertainty in the magnitude, the location, and the timing of the source information. Also, the rationale for air sampler site placement could be more clearly given (e.g., are the samplers placed in expected "hot spots", or near sensitive locations such as schools, etc.?).

4. *What are the strengths and weaknesses of the model ranking elements, and the model ranking process? Can you identify alternative ranking measures that would be likely to present significantly different information about model performance that should be considered in model selection? Would these alternative measures be likely to change the selection process outcomes as described?*

Response to Question 4 – The ranking methodology is the most confusing aspect of the report. As mentioned above, this reviewer thought that one of the purposes of a multiple regression approach was to have the statistical procedure and software identify the best performing set of parameters and coefficients. Instead, the EPA authors seem to have included a convoluted intermediate step where thousands of possible combinations of parameters and coefficients are selected and denoted as "models", which are subsequently ranked. I can see possibly picking five to ten alternate basic model groupings that fall within a rationale set of criteria, but not thousands of them.

5. *Are one or more of the identified models capable of characterizing the ambient exposure from multiple fumigant sources to receptors in California for the exposure averaging periods of interest?*

Response to Question 5 – Despite the arbitrary nature of the regression "models", it is possible that one or more of them may be useful. However, the data used to develop the regression models are still quite limited and one is not sure that a complete range of conditions has been sampled. For example, are there scenarios anticipated that are outside of the range of the data used for development?

A critical test would be to compare the regression model concentration outputs with the standard (e.g., ISC) model outputs for some well-defined standard scenarios.

6. *Provide any additional comments or recommendations you feel are important to improve the quality of this document.*

Response to Question 6 – Additional comments are given below in Section 2, for specific pages and lines in the EPA document.

Section 2 – Specific Comments on Document

P 5, line 7 of Section 1 – Describe the required accuracies of the exposure estimates. For example, is it satisfactory for the predictions to be within a factor of 10? Factor of 2? 10 %?

P 5, line 8 from bottom – It is stated that a "simpler" method is preferred. But simpler than what?

P 5, lines 6-7 from bottom – The statement about the accuracy of air model predictions refers to deterministic, scientific models such as AERMOD, not to regression equations fit to data. It is well-known that if a regression equation is fit so the best-fit line passes through the middle of the data, then the agreement should be much better.

P 6, top par – A good knowledge of the basic physics is essential, in order to properly choose the important inputs and how they should be combined (e.g., by addition, by multiplication with power laws, etc.).

P 6, line 15 – It is stated that "After reviewing … models such as ISC, …we determined to pursue development of an enhanced version of a regression model …". However, the rationale given to back up this statement is relatively weak. A much stronger case is needed. If a permit application came to the EPA from an industry, the applicant would not be allowed to proceed without providing extensive justifications and back-up data.

P 6, lines 9-11 from bottom – Explain why the AMBI monitoring data were not used.

P 7, top 3 lines – It is stated that met data was obtained from either CIMIS sites or NWS sites. There could be a large difference in wind speeds since the NWS sites are usually at airports with small surface roughness and hence larger wind speeds. Were the two types of data compared for nearby sites?

P 7, line 11 of Section B – Explain why the linear equation format (Y = a + bX) was chosen instead of the multiplicative format (which is linear in logarithms):
$C - C_b = aZ_1^{p1}Z_2^{p2}Z_3^{p3}\ldots Z_i^{pi} \ldots Z_n^{pn}$, such as used in the Nou (1963) formula and in many other similarity formulas for atmospheric boundary layer processes.

P 9, top par – The simple regression equation should be discussed in the context of basic physics. For example, there is a fundamental reason why a certain spatial domain average is most appropriate, and it could be derived from several alternate basic dispersion models. For example, the ATDL area-source dispersion model (Hanna, Briggs, and Hosker, 1982: Handbook of Atmospheric Diffusion. DOE/TIC-11223, pp 59-60) was specifically designed for adjacent grids of area sources, which is the problem of interest in the current study.

P 10, line 7 from bottom – Here again, the words "The authors concluded that …" are used without providing adequate justification.

PP 12-14, Section C on "Evaluation of the Possible Use of ISC Dispersion Model" is very weak, since most of the rationale is faulty. For example, it is stated that "Application of the ISC model requires specification of the pollutant emission rate from each source …. , the actual emission rates are uncertain."

Yet the same problem occurs for the regression model, and the authors went ahead with the model anyway and calibrated the area source strength. A similar calibration procedure could have been used for the ISC model, which is indeed appropriate for the multiple source emissions scenarios and receptors. Also, other science-based simplified area source dispersion models exist (e.g., the ATDL area-source model) and would have been revealed by a thorough literature review.

P 13, par 4 from bottom – The multiple source-receptor scenario described is not a reason for not using ISC. This scenario is exactly what ISC is intended for and many examples exist of this type of application (e.g., the current Houston modeling exercise being carried out by EPA/OAQPS).

P 13, last line of par 4 from bottom – The rationale concerning the uncertainties does not make sense. Are you saying that if there are uncertainties in input data, then there is no need to run ISC and you might as well run a regression model?

P 14, last par – This reviewer is not convinced by the series of weak justifications for not using ISC. If the authors are going to argue "too many sources and too many receptors", then they should back up their qualitative statements with specific quantitative numbers concerning ISC model run times. For example, they should show that it takes t_1 minutes to carry out an ISC run for a single source and n receptors, etc. If the total run time for all sources and receptors exceeds, say, one week, then I might buy their argument. But I have been involved in many ISC projects where there have been thousands of sources and receptors and ISC run times of 1 or 2 weeks are acceptable.

P 15, Technical Overview Section, above Subsection A – Why are so many regression models being considered and discussed? I thought that the purpose of a multiple regression analysis was to best fit a single model? There is no need to pose thousands of alternate models and then test each one. The software should automatically pick the best coefficients and parameters.

Also, it would help the reader if the entire problem could be clearly and briefly posed here. What are the desired averaging times and distances for the concentration outputs? What exactly is going to be done with which data?

PP 15-17 – Again to help the reader, three tables should be inserted summarizing the ambient monitoring data, the pesticide usage data, and the weather data.

P 15, section on ambient monitoring data – List the concentration thresholds and the accuracy of the concentration monitors. Discuss backgrounds.

P 16, par above section 2 – I hope that there will be more discussion of the "monitoring data that were adjusted to account for the influence of a nearby commodity fumigation chamber". Generally it is not a good idea to modify data, especially when developing statistical relations that assume independence.

P 16 – First sentence of Section 2 – How can the regression equation be used in the future if it is not based on basic input data but instead is based on a data set made up of the basic data plus "enhancements"? These enhanced data will not be available at other sites and times.

P 17, last par – Summarize the similarities and differences between the CIMIS met monitoring stations and the NWS stations. This is important because often NWS airport winds are much larger than winds at more sheltered sites or near trees and agricultural fields.

P 18, 1st sentence of Section B on "Alternate Model Formulations" – From the title of this section, I was expecting that more basic scientific models would be discussed. However, apparently the word "alternate" refers only to slight changes in the regression equation. As stated above, I do not see why so many regression models are included, since the authors could have let the statistical analysis best fit the equation by itself.

P 18, line 11 from bottom – There is a precise mathematical equation relating R2 and MSE and it should be given instead of making this vague subjective conclusion. Also, since R2 is dimensionless and MSE has dimensions and is affected by a mean bias, it is not true that R2 and MSE "track closely". The equation would allow this to be seen.

P 19 – It should be stated that a true regression model test would involve independent data. The degree of independence of the cross-validation data should be discussed. Also, the effects of the "enhancements" to the emissions data should be discussed.

P 20, 1st full par – The arbitrary 1 ppb line drawn between "High" and "Low" should be justified. Relate 1 ppb to background.

P 20, Section 2 – Model Ranking System – As stated before, I do not understand why there are so many regression "models". For example, Nou's (1963) OBDG regression model was derived in a simpler manner.

P 21, top par – In the air modeling and monitoring studies that I have done, the rule is used that "all data is innocent until proven guilty". That is, you should not throw out data just because they are outliers. A specific reason based on facts and reviewed by an advisory team is needed.

P 22 FF – Section on Evaluation Process – A better justification is needed for considering tens of thousands of "models" (regression equations). At the most, five to ten alternate formulations are appropriate, and only if fully justified.

P 24, middle – The information on detection limits and other details is very important and should receive more discussion here and in previous sections. A summary table is needed.

P 25, top half – There seems to be too much "fiddling" with data (e.g., correcting some data, tossing out other data, eliminating data due to "flow rate deviations" (whatever that means). A statistical regression process relies on independent data. Subsequent estimates of R2, MSE, and evaluations also rely on independence. The authors should discuss the effects of this "data fiddling" on the conclusions.

P 25, par after Table 1 – Justify the arbitrary choice of 1 ppb for separating "high" and "low".

P 26 bottom and 27 top – Several options for determining background concentration are described. Which method was eventually chosen and why?

P 27, Section 3 – Correction for Commodity Fumigation Effect – More than the current ten lines should be devoted to this discussion.

P 28, Figure 3 – The hard copy of this document that was provided to me has no color.

PP 28-33 – Discussion of Usage Data – Several methods of "improving" the pesticide usage data are discussed. Some are more justified than others. However, more importantly, there is a need for a quantitative estimate of the final uncertainty in the usage data magnitudes and spatial location. Also, the

arbitrary corrections compromise the statistical independence assumptions needed for the regression analysis.

P 33, Section C – Discuss possibly biases between the NWS and CIMIS Met data. For example, the NWS wind speeds are likely to be higher. At the top of p 34, justify the "75% completeness criterion".

P 34, equations for "adjusted usage" – Several arbitrary and unjustified "adjusted usage" factors are listed. For example, why should the usage be multiplied by the inverse of the wind direction standard deviation? What is the effect of these assumptions on the regression equations?

P 35 Section D on "Model Formulations" – As stated earlier, most of this modeling exercise could be handled by an efficient application of the ISC model. ISC is a physics-based "model" rather than the regression equation "models" used in this report.

P 36 – Regression equation formulation – Despite the statement after the bullets that "the basic model underlying the many alternative models examined is formulated based on known physical principles of air dispersion", the authors have missed several important physical principles. For example, it is well known that the power on the distance (x) term varies with distance from an area source (the power is less near the edge of the area source and approaches about 1.5 at large distances). Also, the wind direction term should be related to the expected plume width

In my answer to question 1 above, I mentioned the Ocean Breeze Dry Gulch (OBDG) regression equation developed by the US Air Force (Nou, 1963). The OBDG model is a good example of how an equation should be formulated using unknown power law coefficients which are then best-fit by the regression process. This method would have been more appropriate than the current EPA method where the powers are prescribed before hand rather than being solved. The OBDG equation has the following format:

$$C - C_b = aZ_1^{p1}Z_2^{p2}Z_3^{p3} \ldots Z_i^{pi} \ldots Z_n^{pn}$$

Where C is concentration, C_b is background concentration, a is a proportionality "constant", Z_i for i = 1 through n are independent input parameters, and p_i for i = 1 through n are power law coefficients applied to the input parameters. For the OBDG equation, the Z_i include basic scientific measures such as wind speed, downwind distance, and vertical temperature gradient. This can be written in logarithmic form by taking log of both sides:

$$\log(C-C_b) = \log(a) + p1\log(Z_1) + p2\log(Z_2) + \ldots + pn\log(Z_n)$$

By first calculating correlations between $(C-C_b)$ and the various proposed Z_1, the less important independent variables can be eliminated.

PP 36-37, section 3 on the logarithmic equation – I do not follow the rationale for eliminating this equation. The statement "However, this is a very different formulation to the physically-based equations 1, 2, and 3" is incorrect, since all that has been done is the logarithm taken of the same equation. And if there is "zero reported usage", the correct result is obtained, since log $(C-C_b)$ would be minus infinity, implying correctly that $C = C_b$.

P 37, line above section 5 – Specific rationale should be listed rather than saying "makes sense".

P 38 (bottom) and P 38 (top 2 pars) – Arbitrary constants are chosen (757.53 feet and 459.57 feet) with no justification. Please show the calculations that led to these numbers. Why are five significant figures needed for an arbitrary constant?

P 42 – line 2 of d. (Wind Speed) - Provide the justification for the arbitrary choice of 0.5 m/s as the "minimum daily average wind speed".

P 42, bottom section (e) on wind direction – The wind direction coefficient ignores the physics-based knowledge of lateral dispersion from area sources. The term should be a function of (distance/area source size) and (plume width/distance).

P 44 (and other pages concerning section f on timing of emissions) – There are many assumptions concerning emissions timing that are not backed up by references or discussions. The authors do say, in line 12 of p 44, that "This approach is subject to several large uncertainties". Can the magnitudes of these uncertainties be listed by the authors, based on their extensive work with the data?

P 46, section g on "Empirical time adjustments" – If the Nou (1963) approach were used, these coefficients could have been best-fit by the regression method, rather than using them to suggest yet another layer of "models".

P 48 – Section E on iterative improvements – At some point in the tuning process, the assumption of independence of data no longer holds.

PP 50-51 – Model notation – This reviewer finds the notation impenetrable. It would be better to simply use the mathematical format. Not to mention that there are far too many (by a few thousand) "models".

P 52, section 2 on number of explanatory variables – Many of the variables could have been weeded out by doing a correlation analysis or a sensitivity analysis initially. Also, how do the authors know that a different formulation (e.g., the Nou approach with power laws) would not perform better?

PP 53-76 – Section IV on Model Calibration Regression and Evaluation - I have commented on the process many times already so will not repeat myself here. It would seem that the statistical package would automatically produce a best-fit equation rather than requiring thousands of "models" to be tested.

P 54, line 1 of section 1 – Where is the line drawn between an "error that is so extreme …" and an error that is not? What is the justification?

P 57 – Model performance evaluation – The statistical model performance package was intended for application to field data sets that are independent. If a regression equation has been best fit to a data set, then it is hardly an independent test. For example, I once fit a similarity formula to the Prairie Grass field data, and it then agreed much better with those same data than a Gaussian plume model such as the ISC model, which had not been tuned to those data.

P 65 – If a physics-based power law had been proposed such as $1/d^p$ or $1/w^q$, and then the powers p and q best fit by a regression package, then the agreement would be better. Also, I thought that the sigma-theta method for estimating stability had been discarded long ago, since many groups have shown that large sigma-thetas can occur during both light wind unstable or light wind stable conditions, and hence the relation is not monotonic.

P 69 – Line 1 of third full par - It seems inconsistent that the EPA would endorse a "model" that underestimates concentrations. Couldn't the regression equation be constrained to provide a better fit to the higher concentrations?

P 70, Fig 9 containing observed vs "predicted" concentrations – A threshold (say 0.01 ppb) should be applied to both observed and predicted concentrations to avoid the large collection of points at predicted C = 0.0.
I made a rough calculation on the unpaired "highest 5" observed and predicted concentrations and find that the predicted highest concentrations are about 50 to 60 % of the observed.

Often a "Q-Q" plot is useful, where the ranked observed and predicted concentrations are plotted (e.g., the 13^{th} highest observed C is plotted versus the 13^{th} highest predicted C).

P 77 line 4 – As mentioned earlier, I suspect that a $1/d^{1.5}$ relation would work best at all distances.

PP 79-80 – The 1 1/5 page Observations and Conclusions section is too brief and appears to have been written as an afterthought.

P 79, line 2 above bullets – The words "significantly improve the model performance" are used. Does this imply that a statistical significance test was applied? In that case, what is the confidence level?

P 116 – Attachment 7 on Gaussian Equation – This equation is for a point source. The area source equation should be used for the current application. The u_s term cannot be the "wind speed at release height", since this is a ground level area source. Actually u_s is usually taken to be the speed at the NWS standard anemometer height (sometimes 3 m and sometimes 10 m). These s_y and s_z formulas do not appear to be from the ISC equation. What is the reference?

End of review comments

REVIEW COMMENTS OF

Dong Wang, Ph.D.
Associate Professor
University of Minnesota
Department of Soil, Water, and Climate
1991 Upper Buford Circle
St. Paul, MN 55108
612-625-5779
wangd@umn.edu

1. Does the document, *Model Development for Assessing California Methyl Bromide Ambient Concentrations,* provide a clear and adequate description of the goals and methods EPA used to develop and review alternative exposure models? What additional information, if any, is critically needed to complete the documentation?

This document describes the development and testing of regression models that are intended for use in predicting ambient air concentrations of methyl bromide based on methyl bromide usage information and some environmental variables. The models are based on farm-scale air concentration measurements covering a spatial range of ¼ mile to 15 mile to a maximum of a county level. The temporal applicability extends from one day to one week and to a maximum of nine weeks after soil fumigation with methyl bromide. Some of the environmental variables appearing to be sensitive in the regression model include distance from the fumigated fields, elapsed time after methyl bromide application, and wind speed and direction. This reviewer believes that overall the document provides a good start in describing the process of model development. However, the presentation is not very well organized and requires considerable revision to more clearly separate and describe what has been done prior to this work, what is actually accomplished in this effort, how it improves the accuracy of predicted methyl bromide air concentrations from previous models or existing EPA models, and how it will be used for what?

In a general sense, exposure models require a more definitive description of the receptors including their physical characteristics. The current regression model focused only on predicting ambient air concentrations of methyl bromide at some unknown sites referring to the center of each grid cell as the developer defined. Whereas this approach may provide a systematic assessment of fumigant concentrations for all locales, it lacks specific descriptions for potential physical characteristics where human exposure would most likely occur. The presence of build environment alters physical variables that can lead to higher or lower fumigant concentrations, which is not discussed in the report.

Parameters in the regression models are estimated based on measured air concentrations of methyl bromide. It is paramount important to know exactly how the measurements were made and if the same protocol was followed at different locations over time. The report provided some description on the duration of methyl bromide concentration measurements (e.g. page 6 4th paragraph, page 15

last paragraph, page 24 last two sections), but there is no description on procedures for sample collection or analytical methods for sample analysis. The information is also not available in the supplemental reference materials. This reviewer strongly recommends adding descriptions for sample collection and analytical methods for sample analysis. The height of sampling and rate of air flow would have implications to help relate the concentration measurements to potential receptor characteristics. If there are discrepancies in the data, what steps would be taken to re-interpret them in the regression models?

The other important factor required for exposure models is the determination of duration of exposure at known concentrations. The regression models are designed to run for discrete time steps (e.g. one day, two weeks, or eight weeks) as average concentrations. Because changes in ambient concentrations over time are non-linear, a simple time average would not provide a true representation of actual exposure history at a receptor site. For shorter time increment, such as one day, this may not be a problem. For longer time averages, such as the 7/8 week averages that the model appears to perform the best, the meaning of predicted concentrations would require careful interpretation before making conclusions on exposure risks. Assessment of sub chronic exposure depends not only on the average concentrations but also the history (peaks and their duration) and many other environmental and physiological variables. If detail discussions on this topic are beyond the scope of this report, it at least deserves some explanation of how the predicted concentrations may be used for such purposes and the limitations of the models.

Because methyl bromide is applied in the soil, the soil is variable over different areas, and different surface covers may be used after application, the emission process can be highly variable in terms of total emission loss and the temporal characteristics of the emission flux density. The report recognizes these properties in methyl bromide emissions (page 13 and page 46), however, it is not clear how the emission characteristics are considered in the regression models and how their inclusion improves model predictions. If model type (i.e. “24-hour”, “day”, or “day, night”) and the day-specific time adjustment factor (i.e. “k”) would account for these effects, comparisons with other models or measured data would be needed to determine the improvements on model predictions.

2. What are the overall strengths and weaknesses of the model development process as described?

The overall strength of the regression model approach is its relative simplicity in predicting fumigant air concentrations by taking into account of multiple emission sources over large areas. The approach has a potential for running predictions on a GIS framework that can cover large geographic areas with different degrees of detail on fumigant use in relation to distribution of human population and their characteristics. The potential coupling with GIS software also provides a means of generating outputs in a format that can easily be used for management purposes.

The main weakness of the regression models is its empirical nature. This would limit its usage beyond the areas from where the data was collected for model development. Although the model parameters include the effect of distance, time, and wind, many other environmental variables (such as soil, landscape, and atmospheric properties) are lumped in the parameters lacking specificity from place to place.

3. What are the strengths and weaknesses of the data quality assurance activities conducted during the model development process?

It appears that specific efforts were made to determine the consistency and relevancy of the daily monitored 24-hour average concentrations before they are used for model development (page 24-27 in the report). The inclusion and discussion on background methyl bromide concentrations are also important in helping interpret the intercept term in an empirical regression approach used in this report. Exclusion of the commodity fumigation site is also justified, although it contributes to the overall ambient methyl bromide concentrations. In a more complete assessment of methyl bromide air concentrations for human protection, these point sources should be included (may be supplemented with the ISCST3 model) to provide an overall exposure assessment.

A main weakness in the data quality assurance activities is the lack of description of how the ambient concentrations of methyl bromide were measured, including procedures for sample collection or analytical methods for sample analysis from various monitoring activities. Consistency in measurement protocol is essential.

4. What are the strengths and weaknesses of the model ranking elements, and the model ranking process? Can you identify alternative ranking measures that would be likely to present significantly different information about model performance that should be considered in model selection? Would these alternative measures be likely to change the selection process outcomes as described?

For model evaluation, the report used the mean square error, the R-squared statistic, the 5th and 95th percentile of errors, and the 9th percentile of percentage errors. The choice of these criteria appears to be appropriate and provides a measure of model performance and ranking while reducing the weight of the "outlier" data points.

A normalized ranking scheme such as indices based on the fractional biases used by USEPA may be considered for model evaluation. The advantage of using a normalized system provides an opportunity to compare model performance for different monitoring events or localities where the absolute mean concentrations may be very different. However, it is not clear an alternative ranking system would or would not change the selection or final ranking of model performance.

5. Are one or more of the identified models capable of characterizing the ambient exposure from multiple fumigant sources to receptors in California for the exposure averaging periods of interest?

The two tier distance model with "day, night" option appears to have an advantage over previous models in predicting ambient air concentrations from multiple fumigant sources. It is impossible for this reviewer to conclusively determine which (if any of these) models are actually capable of accurately characterizing the ambient exposure from multiple fumigant sources to receptors in California because of concerns on the empirical nature of the regression models, the lack of description on concentration measurement and analysis, the ambiguity on the treatment of emission flux patterns, and other issues detailed in the following question.

6. Provide any additional comments or recommendations you fell are important to improve the quality of this document.

A main argument for taking the empirical regression model approach is the limitation on or lack of computational capabilities of using more process-based simulation models such as the USEPA ISC or similar models. The rapid and continuous advances in processor speed and upcoming release of 64-bit processors for PCs make the usage of regression models verses process-based models a hardly justifiable choice. A more acceptable justification for choosing the regression model approach is to demonstrate its accuracy and applicability to be comparable to the process-based models. A separate section may be added to compare in a case study where both the regression model and a process-based model are used for predicting air concentrations.

Another main recommendation for improving the quality of this document is to make the writing more structured and organized so it would be easier to follow. The document contains large amount of information and the model development relied on data from difference sources and studies over a time span of many years. Presentation of the data source, model development, and model evaluation should be carefully and concisely described in a logical sequence for any potential readers or users with some scientific background.

Some minor comments and questions are listed below:

- Page 5 second last paragraph, theoretically model predictions should neither under- nor over-predict the concentrations. Why "in the context of this decision, avoiding overestimates which could lead to mistaken conclusion of adverse impacts in support of a finding is desirable"? How about underestimates? Wouldn't this lead to higher exposure risks for the bystanders?
- Page 9 last paragraph, questionable assumptions: (1) all usage distributed somewhere throughout the MTRS is located at the section center, (2) the receptor is located at the section center where the monitoring site is located, and (3) 0.5 mile minimum distance. There is a conflict because assumptions (1) and (2) would put the receptor right on top of the fumigant source while assumption (3) separates the two by > 0.5 miles. Why?

- Page 15 last paragraph, how 24-hour methyl bromide concentration is averaged? Or is it a cumulative measurement of methyl bromide over 24-hr period?
- Page 34 middle section, the temperature effect is accounted for using degree-hours. How is time entered in the formulations for ambient and soil temperatures? Why subtracting 4 from the temperature?
- Page 36 Eq. [3], based on Eq. [2], the log (Conc) on the left side of Eq. [3] is actually log (Conc-Intercept)?